HOKKAIDO UNIVERSITY

Title	Study on quinolones-resistant bacteria and novel drugs for them
Author(s)	Suwanthada, Pondpan
Degree Grantor	北海道大学
Degree Name	博士(感染症学)
Dissertation Number	甲第16163号
Issue Date	2024-09-25
DOI	https://doi.org/10.14943/doctoral.k16163
Doc URL	https://hdl.handle.net/2115/93830
Type	doctoral thesis
File Information	Pondpan_Suwanthada.pdf

Hokkaido University Collection of Scholarly and Academic Papers : HUSCAP

Study on quinolones-resistant bacteria and novel drugs for them

キノロン剤耐性細菌と

それらに対する新規薬剤に関する研究

Pondpan Suwanthada

CONTENTS

CONTENTS 1
ABBREVIATIONS 4
LIST OF PAPER 6
PREFACE 7
CHAPTER I Additive effect of plasmid-encoded quinolone resistance protein QnrB19 with amino acid substitution in *Salmonella* Typhimurium DNA gyrase 20
Introduction 20
Materials and Methods 21
Reagents 21
Construction of WT and mutant DNA gyrase expression vectors 21
Expression and purification of recombinant *S.* Typhimurium DNA gyrase subunits 22
QnrB19 expression vectors 22
Expression and purification of QnrB19 22
Protective activity of QnrB19 to *S.* Typhimurium DNA gyrase inhibited by quinolones. 23
Quinolone-mediated DNA cleavage assay 24
Statistical Analysis 24
Results 24
Expression and purification of recombinant proteins in this study 24
Protective activity of QnrB19 to *S.* Typhimurium DNA gyrase inhibited by quinolones. 24
Quinolone-mediated DNA cleavage assay 25
Discussion 25
Conclusions 28
CHAPTER II Impact of substitutions at positions 1 and 8 of fluoroquinolones on their activity against mutant DNA gyrase in *Salmonella* Typhimurium 44
Introduction 44
Materials and Methods 45
Reagents 45

Expression and purification of recombinant *S.* Typhimurium DNA gyrase subunits ... 45
Inhibition of *S.* Typhimurium DNA gyrase by quinolones ... 45
Induction of quinolone resistance in *S.* Typhimurium ... 45
Confirmation of nucleotide sequence alterations ... 46
Antimicrobial susceptibility testing ... 46
Statistical Analysis ... 46
Results ... 47
Expression and purification of recombinant *S.* Typhimurium DNA gyrase ... 47
Influence of amino acid substitution on DNA gyrase activity of *S.* Typhimurium in response to quinolone ... 47
Mutant *S.* Typhimurium strains ... 47
MICs for *S.* Typhimurium and *S.* Enteritidis ... 48
Discussion ... 48
Conclusion ... 51
CHAPTER III Effect of WQ-3334 on *C. jejuni* carrying a DNA gyrase with dominant amino acid substitutions conferring quinolone resistance. ... 64
Introduction ... 64
Materials and Methods ... 65
Reagents ... 65
Construction of WT and mutant *C. jejuni* DNA gyrases expression vectors ... 65
Expression and purification of recombinant *C. jejuni* DNA gyrase subunits ... 65
Inhibition of *C. jejuni* DNA gyrase by quinolones ... 65
In silico docking simulation ... 65
Induction of quinolone resistance in *C. jejuni* ... 66
MICs for WT and mutant *C. jejuni* strains ... 66
Results ... 67
Recombinant DNA gyrases ... 67
Induction of mutant *C. jejuni* strains ... 67
Inhibitory activities of WQ-3334, WQ-4064 and WQ-4065 against *C. jejuni* recombinant DNA Gyrases ... 67
Docking simulations of WQ-3334 and DNA gyrases ... 67

MICs for WT and mutant *C. jejuni* 68
Discussion 68
Conclusion 71
GENERAL CONCLUSION 80
ACKNOWLEDGEMENTS 82
REFERENCES 82

ABBREVIATIONS

AMR	Antimicrobial Resistance
SDG	Sustainable Development Goals
NTS	Non-Typhoidal Salmonella
WHO	World Health Organization
S83F	Serine at position 83 substituted with Phenylalanine
S83Y	Serine at position 83 substituted with Tyrosine
S83I	Serine at position 83 substituted with Isoleucine
D87N	Aspartic acid at position 87 substituted with Asparagine
D87G	Aspartic acid at position 87 substituted with Glycine
D87Y	Aspartic acid at position 87 substituted with Tyrosine
S83FD87N	Double mutation of Serine at position 83 to Phenylalanine and Aspartic acid at position 87 to Asparagine
PRP	Pentapeptide Repeat Protein
DNA	Deoxyribonucleic Acid
SOS	SOS Response
PMQR	Plasmid-Mediated Quinolone Resistance
T86I	Threonine at position 86 substituted with Isoleucine
D90N	Aspartic acid at position 90 substituted with Asparagine
CIP	Ciprofloxacin
NAL	Nalidixic acid
ENR	Enrofloxacin
LEV	Levofloxacin
NOR	Norfloxacin
R	Resistant
I	Intermediate
S	Susceptible
n/i	No information
A873V	Alanine at position 873 substituted with Valine
R413L	Arginine at position 413 substituted with Leucine
D87GA119E	Double mutation of Aspartic acid at position 87 to Glycine and Alanine at position 119 to Glutamic acid
S83T	Serine at position 83 substituted with Threonine
LB	Luria Bertani
IPTG	Isopropyl β-D-1-thiogalactopyranoside
SDS	Sodium Dodecyl Sulfate

PAGE	Polyacrylamide Gel Electrophoresis
MHB	Mueller-Hinton Broth
EDTA	Ethylenediaminetetraacetic Acid
AMP	Ampicillin
PCR	Polymerase Chain Reaction
Ni-NTA	Ni-nitrilotriacetic Acid
$(NH_4)_2SO_4$	Ammonium sulfate
DTT	Dithiothreitol
BSA	Bovine Serum Albumin
ATP	Adenosine Triphosphate
TAE	Tris-Acetate-EDTA (buffer for electrophoresis)
IC_{80}	Inhibitory Concentration for 80% of organisms
MOX	Moxifloxacin
UV	Ultraviolet
MH	Mueller-Hinton
OD	Optical Density
CLSI	Clinical and Laboratory Standards Institute
ANOVA	Analysis of Variance
LSD	Least Significant Difference
MDR	Multi-Drug Resistant
LEV	Levofloxacin
TOPRIM	Topoisomerase/Primase domain
IC_{50}	Inhibitory Concentration for 50% of organisms
SIT	Sitafloxacin
WT	Wild Type
G81C	Glycine at position 81 substituted with Cysteine
MIC	Minimum Inhibitory Concentration

LIST OF PAPER

Suwanthada P, Kongsoi S, Jayaweera S, Akapelwa ML, Thapa J, Nakajima C, Suzuki Y. Interplay Between Amino Acid Substitution in GyrA and QnrB19: Elevating Fluoroquinolone Resistance in *Salmonella* Typhimurium, ACS infect 2024. https://doi.org/10.1021/acsinfecdis.4c00150. *Online ahead of print.*

Suwanthada P, Kongsoi S, Miura N, Belotindos L, Piantham C, Toyting J, *et al*. Impact of substitutions at 1 and 8 position of fluoroquinolones on the activity against mutant DNA gyrases of *Salmonella* Typhimurium. Microb Drug Resist 2023;29:552–60. https://doi.org/10.1089/mdr.2023.0014.

Miura-Ajima N*, **Suwanthada P***, Kongsoi S, Kim H, Pachanon R, Koide K, *et al*. Effect of WQ-3334 on *Campylobacter jejuni* carrying a DNA gyrase with dominant amino acid substitutions conferring quinolone resistance. J Infect Chemother 2024. https://doi.org/10.1016/j.jiac.2024.04.002. *Online ahead of print.*

*Authors contributed equally to this work

PREFACE

Antimicrobial resistance (AMR) poses a significant global challenge, driven by the widespread use of antimicrobials and their rapid dissemination. The estimations indicate that AMR could result in over 10 million deaths annually by 2050 without any countermeasures, making it the leading cause of death [1]. This resistance emerges naturally over time due to genetic mutations in pathogens, but human activities, such as the misuse and overuse of antimicrobials in humans, animals, and plants, have accelerated its spread [2]. AMR in foodborne pathogens, in particular, raises major concerns for the food production system. Despite not being the focus of the current pandemic, AMR can severely impact serious illnesses, contribute to deaths [3]. Therefore, combating antimicrobial-resistant pathogens is crucial for achieving the Sustainable Development Goals (SDGs), underscoring the global community's urgent need for action. In 2017, the World Health Organization (WHO) published its first ever list of antibiotic-resistant "priority pathogens" to promote research and development (R&D) of new antimicrobial drugs. The list included quinolone-resistant *Salmonella* and *Campylobacter* spp., the most frequent causes of foodborne illness. [4,5] As of 2024, quinolone-resistant *Salmonella* continues to be shown on this list, indicating the persistent challenges [6].

Non-Typhoidal *Salmonella* (NTS) with over 2,600 serovars identified significantly contributes to foodborne illnesses worldwide [7]. Of these, *Salmonella enterica* serovar Typhimurium and serovar Enteritidis are primarily associated with foodborne infections [8,9]. Typically, antimicrobial drugs are not necessary for the treatment of gastroenteritis caused by NTS, however, in children and immunocompromised patients, invasive complications require antimicrobial therapy, specifically with quinolones [10,11]. Figure 1, modified from the systemic analysis study [11], presents a map illustrating for invasive NTS cases across different countries in 2017, as indicated in underscoring the significance of NTS[11].

NTS can acquire resistance to quinolone antibiotics through several mechanisms. Key among these are amino acid substitutions in the DNA gyrase and topoisomerase IV subunits GyrA, GyrB, ParC, and ParE, which result from point mutations. Quinolone resistance-determining region (QRDR) is a crucial area located in the GyrA and GyrB of DNA gyrase, as well as the ParC and ParE of topoisomerase IV. The location of QRDR for those proteins were described in the Table 1 [12,13]. Notably, amino acid substitutions at codons 83 and/or 87 within the quinolone QRDR of GyrA have been linked to a high prevalence of quinolone-resistant NTS strains [12]. This emergence complicates the management of NTS infections using existing antimicrobial drugs [12,14].

In *Salmonella*, mutations at QRDR are frequently observed as shown in Table 2 [12]. Several *Salmonella* strains have been identified with amino acid substitutions at codon 83 in GyrA involving serine to phenylalanine ($GyrA^{S83F}$) and tyrosine ($GyrA^{S83Y}$). In addition, the GyrA substitution at Ser83 to isoleucine ($GyrA^{S83I}$) has been associated with high-level quinolone resistance [12,15,16]. The substitutions in GyrA at codon 87, aspartic acid to asparagine ($GyrA^{D87N}$), glycine ($GyrA^{D87G}$), and tyrosine ($GyrA^{D87Y}$) have also been frequently reported [12]. Additionally clinical *Salmonella* isolates with the double mutation ($GyrA^{S83FD87N}$) in DNA gyrase have been associated with a high level resistance against quinolones [12,15].

Recent studies have identified the contribution of plasmid-mediated quinolone resistance (PMQR) genes to the development of quinolone resistance [12]. These genes, widespread among Enterobacteriaceae, transmit through horizontal gene transfer. The PMQR genes encode proteins, particularly Qnr proteins which can protect DNA gyrase from the inhibition of quinolones and potentially confer to quinolone resistance [17]. Qnr proteins belong to the pentapeptide repeat protein (PRP) family, characterized by a sequence of tandem five-amino-acid motifs. Variants of *qnr* are categorized into families based on less than 10% sequence divergence, including *qnrA*, *qnrB*, *qnrVC*, and *qnrS* families [18]. Previous study showed the Qnr prevalence in 692 studies published between 2008 and 2017 [18]. The investigation revealed a total of 4,459 Enterobacteriaceae isolates containing *qnr* genes: 1,917 *qnrB*, 1,545 *qnrS*, 498 *qnrA*, 459 *qnrD*, 27 *qnrVC*, 12 *qnrC*, and 1 *qnrE*. Notably, QnrB19 accounted for over 80% of Qnr occurrences in *Salmonella* species [19]. I extended the research to investigate the trends in this issue using data published between 2018 and 2020. Figure 2 illustrates the findings, which indicate that *qnrB* is the most prevalent among the *qnr* genes. I further explored the data to confirm *qnrB*'s dominance and *qnrB19* is shown to be dominant among *qnrB* as illustrated in Figure 3.

Despite progress in understanding these mechanisms, the precise function of Qnr in resistance remains partially elucidated. A proposed model suggests that Qnr could mimic T-segment DNA and be trapped by the enzyme-DNA complex [20–22]. Among *Salmonella* species, the QnrB, encoded by the *qnrB*, is notably prevalent according to its regulatory mechanism [17,18]. Specifically, when quinolones induce a DNA break, it could trigger the expression of QnrB via the SOS response system. This occurs through the attachment of *lexA* to a regulatory protein located upstream of the *qnrB*. As a result, the QnrB were expressed [18]. Among the various types of QnrB, QnrB19 stands out as the most frequently identified, highlighting its significant presence among the reported QnrB proteins [23]. Furthermore, their presence can facilitate the acquisition of more potent resistance mechanisms, such as the point mutation in QRDR of DNA gyrase, leading to the emergence

of high-level of quinolone-resistant strains as shown in the clinical isolates in Table 3 [23]. However, the mechanism of resistance induced by Qnr is still not well understood, and there are currently no available drugs to inhibit this protein.

Campylobacteriosis, primarily caused by *Campylobacter* spp. with *C. jejuni* being the predominant species, has emerged as one of the leading cause of global bacterial gastroenteritis [24]. Over the past decade, its incidence and prevalence have surged in both developed and developing countries with significant public health implications [25,26]. In 2019, previous studies highlighted the high prevalence of campylobacteriosis across Europe as shown in Figure 4 [25]. Campylobacteriosis typically causes symptoms such as diarrhea, fever, stomach cramps and vomiting, and often recovering without antibiotic treatment. However, in cases where the immune system is compromised and severe infections may persist, the treatment with antimicrobial drugs such as quinolones and macrolides are necessary [27]. Quinolone resistance in bacteria often results from amino acid substitutions in DNA gyrase or topoisomerase IV, which are the primary and secondary targets of quinolones, respectively [28–30]. However, it is necessary to note that *Campylobacter* lacks the secondary target for quinolones, topoisomerase IV, [30]. Therefore, in *Campylobacter*, resistance predominantly arises from point mutations in the *gyrA* within QRDR. In *C. jejuni*, a prevalent mutation involves the substitution of the 86th amino acid from threonine to isoleucine ($GyrA^{T86I}$), which significantly contributes to quinolone resistance [29–31]. Other mutation in GyrA, such as the substitution of aspartic acid at position 90 with asparagine ($GyrA^{D90N}$), are less commonly observed [31].

Ciprofloxacin (CIP), a second-generation quinolone, is a drug for treating salmonellosis and campylobacteriosis [30–32]. Quinolones target type II topoisomerases including DNA gyrase and topoisomerase IV, essential enzymes for DNA replication and transcription [33]. The mechanism of action for quinolones involves binding to the DNA gyrase/topoisomerase IV-DNA complex, leading to the stabilization of the complex This interaction disrupts the normal function of these enzymes, resulting in the inhibition of DNA replication and transcription and the induction of double-strand breaks [15,34]. Over the years, the evolution of quinolones has been marked by systematic structural modifications aimed to enhancing their antimicrobial potency, pharmacokinetic profiles, and safety margins [15]. These modifications have facilitated the classification of quinolones into four generations, each defined by a broader spectrum of activity against both gram-negative and gram-positive bacteria, as well as improved drug properties such as tissue penetration, half-life, and reduced toxicity optimizing quinolones' ability to penetrate bacterial cell membranes and exert their therapeutic effects [15]. Despite the development of quinolones, the emergence of quinolone-resistant strains of *Salmonella* and

Campylobacter spp. has become major public health concerns, and an increasing rate of resistance to quinolones in these bacteria has been reported in many countries for the last two decades [11,35].

In Chapter I, I deepen the understanding of resistant mechanisms, particularly PMQR. Despite two decades of research and numerous global reports highlighting the prevalence of these genes, there remains a lack of solid knowledge, hindering the development of effective control strategies and the creation of new drugs. This gap has slowed the implementation of prevention and control measures, consequently contributing to the spread of quinolone-resistant bacteria. Notably, the coexistence of amino acid substitutions in DNA gyrase and PMQR genes accelerates resistance to quinolones. Through the use of recombinant mutant DNA gyrase and QnrB19, this study showed the resistance mechanisms of *S.* Typhimurium in the presence of QnrB19.

Chapter II, I explored the efficacy of WQ-compounds which represent a novel series of quinolones, designed to offer improvements over commercial quinolones by targeting bacterial DNA gyrase and topoisomerase IV with potentially enhanced efficacy and reduced resistance [36]. Notably, the WQ-compound with a 6-amino-3,5-difluoropyridine-2-yl group at the R1 position has been demonstrated the significant inhibitory effects on a variety of bacteria, including *Acinetobacter baumannii* (*A. baumannii*), *Escherichia coli* (*E. coli*), *Streptococcus pneumoniae* (*S. pneumoniae*), methicillin-resistant *Staphylococcus aureus* (*S. aureus*), and *Neisseria gonorrhoeae* (*N. gonorrhoeae*) in the drug susceptibility test results [36]. However, their efficacy against mutant DNA gyrases of *S.* Typhimurium has not yet been investigated. This study, therefore, seeks to investigate the effectiveness of these novel quinolones against both wild-type (WT) and quinolones-resistant mutant strains of *Salmonella* DNA gyrases. I aimed to examine the antibacterial properties of these compounds by analyzing how their unique structural characteristics influence their ability to inhibit DNA gyrase activity.

In Chapter III, I conducted the study of WQ-compounds' inhibitory effects on quinolone-resistant *Campylobacter* spp. This analysis included an investigation of the structure-activity relationships of WQ-3334, WQ-4064, and WQ-4065, using *in vitro* assay including supercoiling assays, Minimum Inhibitory Concentration (MIC) tests, and *in silico* docking simulations. This chapter aimed to enhance the understanding and assess the potential of these compounds in treating campylobacteriosis. This study not only provided insights into the compounds' effectiveness but also helped in exploring their inhibitory potential against resistant strains of quinolone resistant *Campylobacter* spp.

Table 1. Location of QRDR in GyrA, GyrB, ParC and ParE

Enzyme	Codon position
DNA gyrase	
GyrA	Ala67 - Gln106
GyrB	Asp426 - Lys447
Topoisomerase IV	
ParC	Als64 - Gln103
ParE	Asp420 - Lys441

Table 2. Amino acid substitution found in QRDR of DNA gyrase in *Salmonella* species.

Codon position	Substitution	Reference
Ala67	Pro	[12]
Asp72	Gly	[12]
Val73	Ile	[12]
Gly81	Cys	[12]
	Ser	[12]
	His	[12]
	Asp	[12]
Asp82	Gly	[12]
	Asn	[12]
Ser83	Tyr	[12]
	Phe	[12]
	Ala	[12]
	Ile	[13]
Asp87	Asn	[12]
	Gly	[12]
	Tyr	[12]
	Lys	[12]
Leu98	Val	[12]

Table 3. The MICs of quinolones including CIP, nalidixic acid (NAL), enrofloxacin (ENR), levofloxacin (LEV), norfloxacin (NOR) and ofloxacin (OFL) for clinical *S.* Typhimurium isolates with amino acid substitutions in DNA gyrase and QnrB presence, using different methods: A for the broth microdilution method and B for the disk diffusion method. The results categorized the isolates as R (resistant), I (intermediate), S (susceptible) and no information (n/i). The specific MIC values were provided in parentheses.

No	Serotype	Source	Method	GyrA	*qnr*	CIP (mg/L)	NAL (mg/L)	ENR (mg/L)	LEV (mg/L)	NOR (mg/L)	OFL (mg/L)	References
1	Derby	Chicken	A	D87N	*qnrB*	R (n/i)	R (n/i)	R (n/i)	R (n/i)	n/i	R (n/i)	[37]
2	Typhimurium	Chicken	A	S83FD87N	*qnrB*	R (n/i)	R (n/i)	R (n/i)	R (n/i)	n/i	R (n/i)	[37]
3	Enteritidis	Chicken	A	D87N	*qnrB*	R (n/i)	R (n/i)	R (n/i)	R (n/i)	n/i	R (n/i)	[37]
4	Derby	Chicken	A	D87N	*qnrB*	R (n/i)	R (n/i)	R (n/i)	R (n/i)	n/i	R (n/i)	[37]
5	Enteritidis	Egg	A	S83FD87N	*qnrB*	R (n/i)	R (n/i)	R (n/i)	R (n/i)	n/i	R (n/i)	[37]
6	Alachua	Porcine	B	D87G	*qnrB15 NDlike*	n/i	n/i	R (≥1)	n/i	n/i	n/i	[38]
7	Alachua	Porcine	B	S83F	*qnrB19*	n/i	n/i	R (≥1)	n/i	n/i	n/i	[38]
8	Typhimurium var 5ND	Porcine	B	D87N	*qnrB19*	n/i	n/i	R (≥1)	n/i	n/i	n/i	[38]
9	Typhimurium var 5ND	Porcine	B	D87N	*qnrB19*	n/i	n/i	R (≥1)	n/i	n/i	n/i	[38]
10	Agona	Porcine	B	S83Y	*qnrB19*	n/i	n/i	R (≥1)	n/i	n/i	n/i	[38]
11	Typhimurium var 5ND	Porcine	B	D87N	*qnrB19*	n/i	n/i	R (≥1)	n/i	n/i	n/i	[38]
12	Muenchen	Porcine	B	A873V	*qnrB19*	n/i	n/i	R (≥1)	n/i	n/i	n/i	[38]
13	Braenderup	Porcine	B	R413L	*qnrB2*	n/i	n/i	R (≥1)	n/i	n/i	n/i	[38]
14	4,[5],12:i:ND	Porcine	B	S83F	*qnrB2*	n/i	n/i	R (≥1)	n/i	n/i	n/i	[38]
15	Heidelberg	Poultry	B	D87G A119E	*qnrB19*	I (0.125–0.75)	R (≥32)	n/i	n/i	n/i	n/i	[39]
16	Heidelberg	Poultry	B	S83F	*qnrB19*	I (0.125–0.75)	R (≥32)	n/i	n/i	n/i	n/i	[39]
17	Heidelberg	Poultry	B	S83F	*qnrB19*	I (0.125–0.75)	R (≥32)	n/i	n/i	n/i	n/i	[39]
18	Heidelberg	Poultry	B	S83F	*qnrB19*	I (0.125–0.75)	R (≥32)	n/i	n/i	n/i	n/i	[39]
19	Heidelberg	Poultry	B	S83F	*qnrB19*	I (0.125–0.75)	R (≥32)	n/i	n/i	n/i	n/i	[39]
20	Heidelberg	Poultry	B	S83F	*qnrB19*	I (0.125–0.75)	R (≥32)	n/i	n/i	n/i	n/i	[39]
21	Brandenburg	Chicken meat	B	D87G	*qnrB19*	R (≥32)	R (0.5-8)	n/i	n/i	n/i	n/i	[40]

Table 3. Continued

No	Serotype	Source	Method	GyrA	*qnr*	CIP (mg/L)	NAL (mg/L)	ENR (mg/L)	LEV (mg/L)	NOR (mg/L)	OFL (mg/L)	References
22	Brandenburg	Chicken meat	B	D87G	*qnrB19*	R (≥32)	R (0.5-8)	n/i	n/i	n/i	n/i	[40]
23	Heidelberg	Environment	B	S83F	*qnrB19*	R (≥32)	R (0.5-8)	n/i	n/i	n/i	n/i	[40]
24	Heidelberg	Chicken meat	B	S83F	*qnrB19*	R (≥32)	R (0.5-8)	n/i	n/i	n/i	n/i	[40]
25	Indiana	Broiler carcass	B	S83FD87N	*qnrB1*	R (≥4)	R (≥256)	n/i	n/i	n/i	n/i	[41]
26	Indiana	Broiler carcass	B	S83FD87N	*qnrB1*	R (≥4)	R (≥256)	n/i	n/i	n/i	n/i	[41]
27	Indiana	Broiler carcass	B	S83FD87N	*qnrB1*	R (≥4)	R (≥256)	n/i	n/i	n/i	n/i	[41]
28	Indiana	Broiler carcass	B	S83FD87N	*qnrB1*	R (≥4)	R (≥256)	n/i	n/i	n/i	n/i	[41]
29	Indiana	Broiler carcass	B	S83FD87N	*qnrB1*	R (≥4)	R (≥256)	n/i	n/i	n/i	n/i	[41]
30	Schwarzengrund	Broiler carcass	B	S83FD87N	*qnrB1*	R (≥4)	S (8)	n/i	n/i	n/i	n/i	[41]
31	Stanleyville	Broiler carcass	B	S83FD87N	*qnrB1*	R (≥4)	R (≥256)	n/i	n/i	n/i	n/i	[41]
32	Indiana	Broiler carcass	B	S83FD87N	*qnrB1*	R (≥4)	R (≥256)	n/i	n/i	n/i	n/i	[41]
33	Indiana	Broiler carcass	B	S83FD87N	*qnrB1*	R (≥4)	R (≥256)	n/i	n/i	n/i	n/i	[41]
34	Indiana	Broiler carcass	B	S83FD87N	*qnrB1*	R (≥4)	R (≥256)	n/i	n/i	n/i	n/i	[41]
35	Schwarzengrund	Broiler carcass	B	S83FD87N	*qnrB1*	R (≥4)	R (≥256)	n/i	n/i	n/i	n/i	[41]
36	Schwarzengrund	Broiler carcass	B	S83FD87N	*qnrB1*	R (≥4)	R (≥256)	n/i	n/i	n/i	n/i	[41]
37	Schwarzengrund	Broiler carcass	B	S83FD87N	*qnrB1*	R (≥4)	R (≥256)	n/i	n/i	n/i	n/i	[41]
38	Schwarzengrund	Broiler carcass	B	S83FD87N	*qnrB1*	R (≥4)	R (≥256)	n/i	n/i	n/i	n/i	[41]
39	Schwarzengrund	Broiler carcass	B	S83FD87N	*qnrB1*	R (≥4)	R (≥256)	n/i	n/i	n/i	n/i	[41]
40	Schwarzengrund	Broiler carcass	B	S83FD87N	*qnrB1*	R (≥4)	R (≥256)	n/i	n/i	n/i	n/i	[41]
41	Indiana	Retail Chicken	B	S83FD87N	*qnrB1*	S (0.125)	R (≥256)	n/i	n/i	n/i	n/i	[41]
42	Schwarzengrund	Retail Chicken	B	S83FD87N	*qnrB1*	R (≥4)	R (≥256)	n/i	n/i	n/i	n/i	[41]
43	Indiana	Retail Chicken	B	S83FD87N	*qnrB1*	R (≥4)	R (≥256)	n/i	n/i	n/i	n/i	[41]
44	Indiana	Chicken	B	S83FD87N	*qnrB1*	R (≥4)	R (≥256)	n/i	n/i	n/i	n/i	[41]

Table 3. Continued

No	Serotype	Source	Method	GyrA	*qnr*	CIP (mg/L)	NAL (mg/L)	ENR (mg/L)	LEV (mg/L)	NOR (mg/L)	OFL (mg/L)	References
45	Schwarzengrund	Chicken	B	S83FD87N	*qnrB1*	R (≥4)	R (≥256)	n/i	n/i	n/i	n/i	[41]
46	Indiana	Chicken	B	S83FD87N	*qnrB1*	R (≥4)	R (≥256)	n/i	n/i	n/i	n/i	[41]
47	Newport	Pork	*	S83T	*qnrB19*	R (2)	R (1024)	n/i	n/i	n/i	n/i	[42]
48	Infantis	Chicken meat	*	S83T	*qnrB19*	S (0.5)	R (1024)	n/i	n/i	n/i	n/i	[42]
49	Thompson	Human	B	S83FD87N	*qnrB*	R (4)	n/i	n/i	n/i	n/i	n/i	[43]

* The isolates were tested using disk diffusion method for Ciprofloxacin and dilution method for Nalidixic acid.

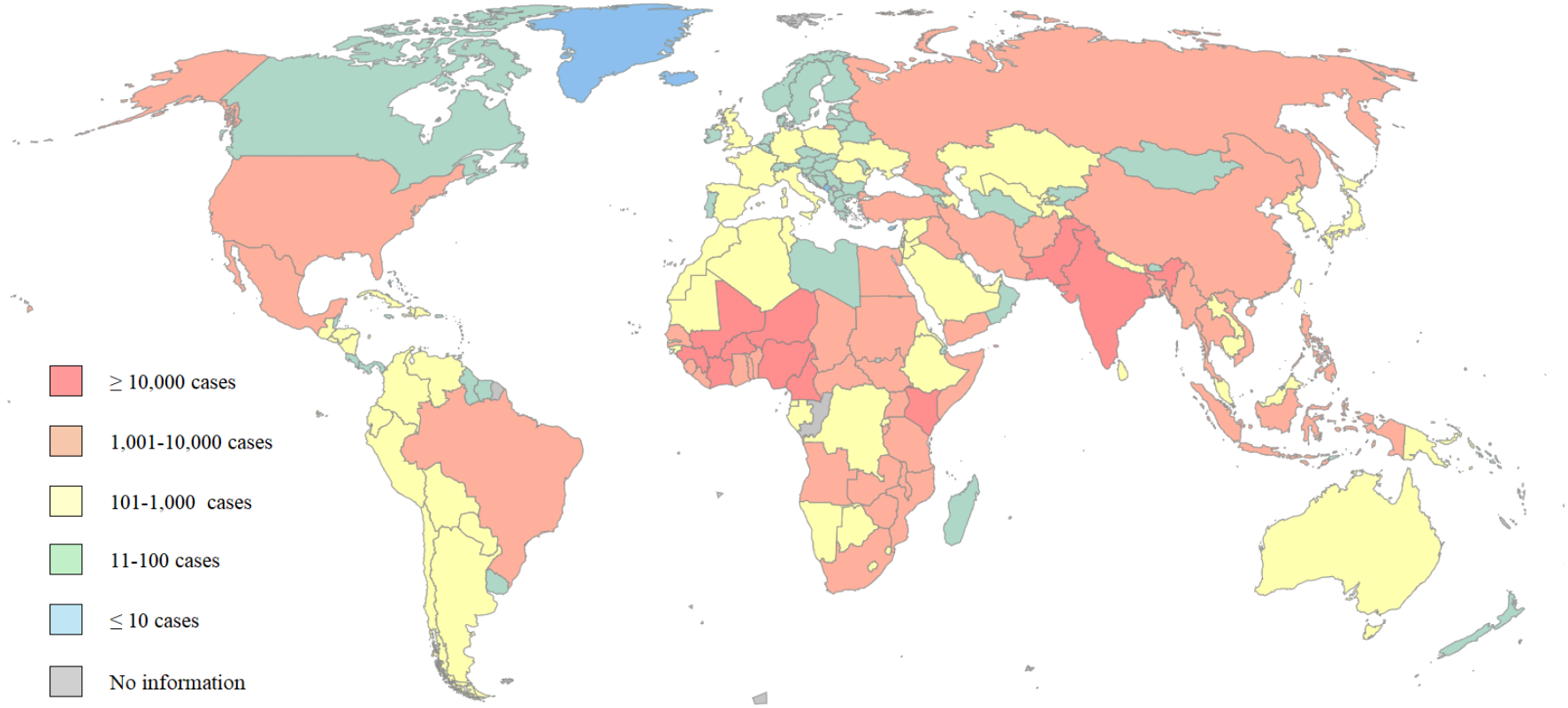

Figure 1. Estimated numbers of iNTS cases, by country, in 2017. Adapted from [11].

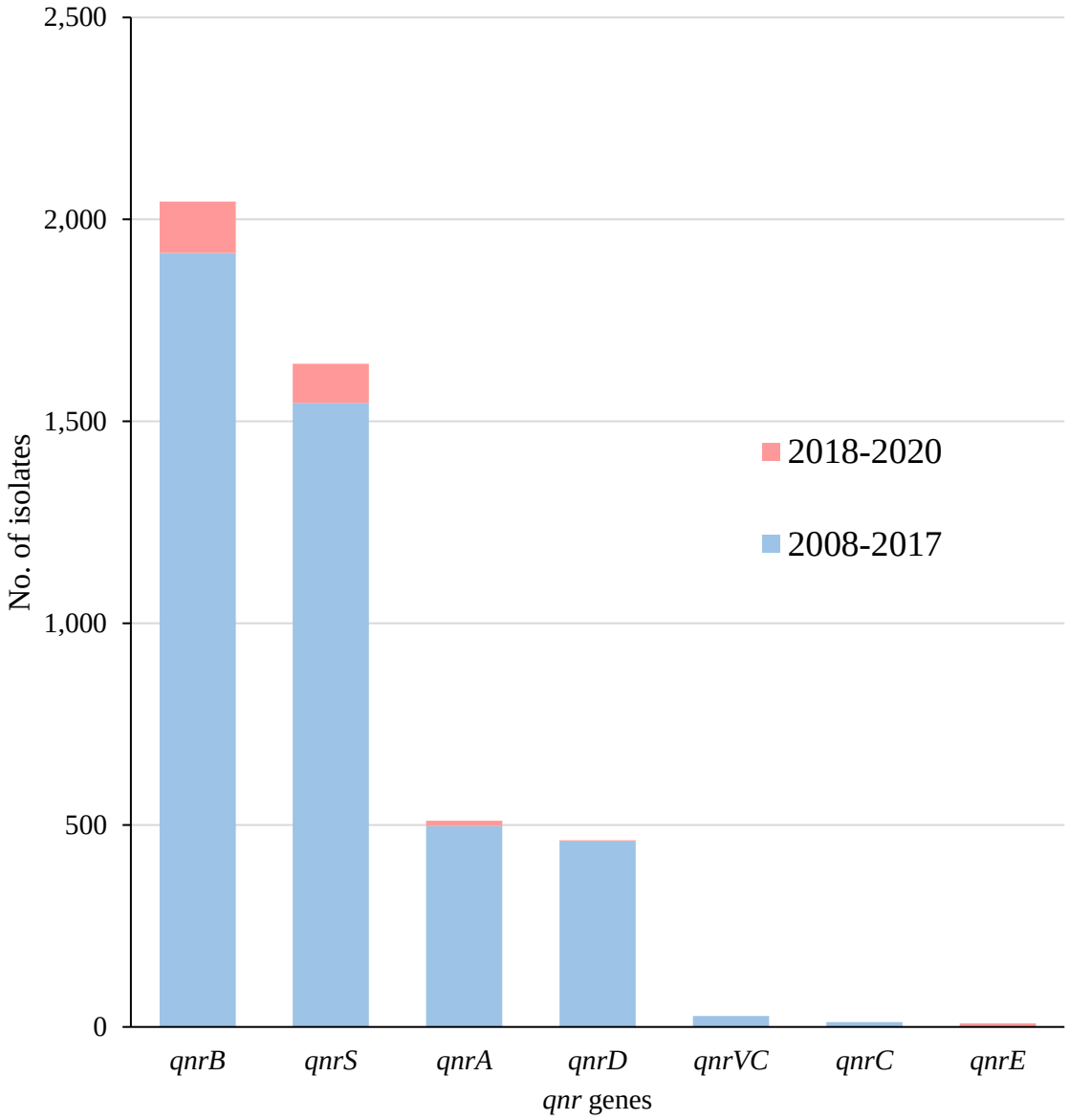

Figure 2. Qnr families identified from 2008 to 2020.

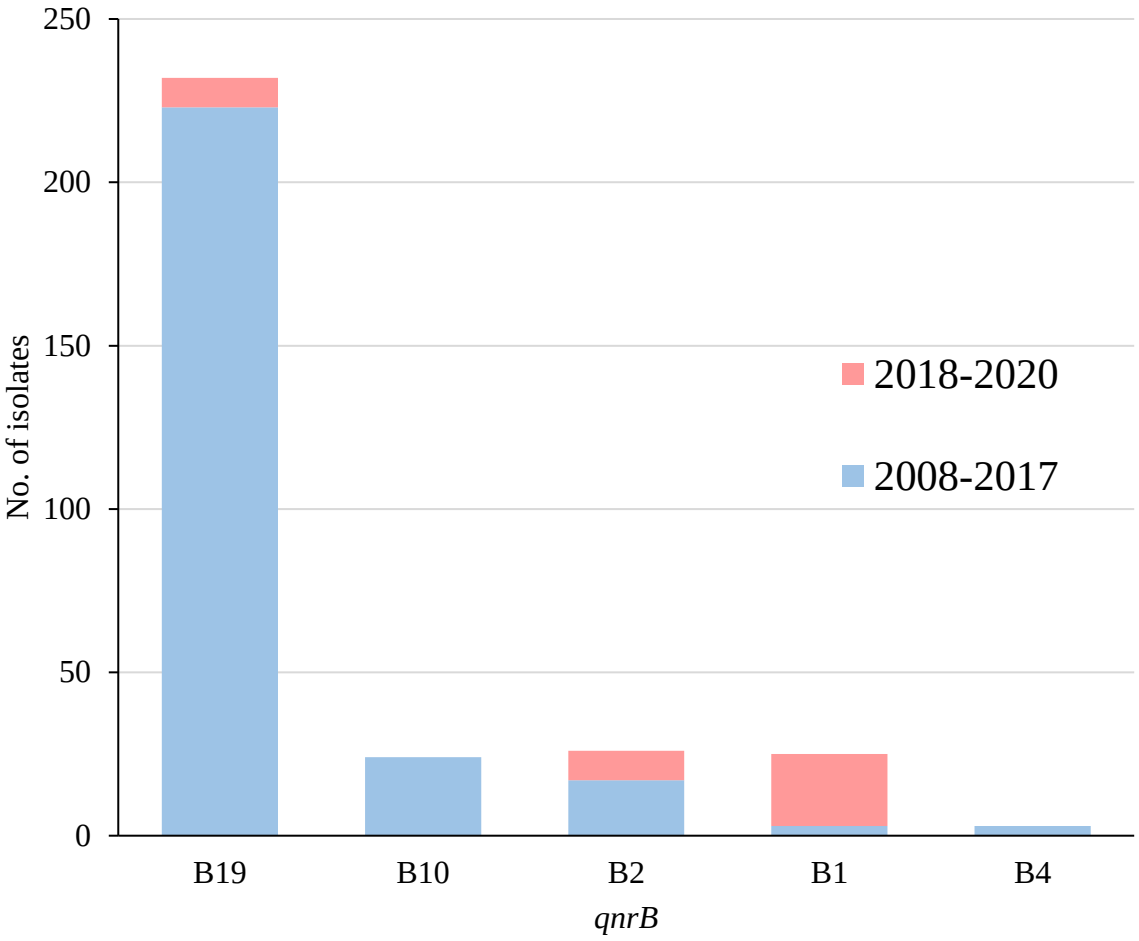

Figure 3. QnrB variants in *Salmonella* spp.

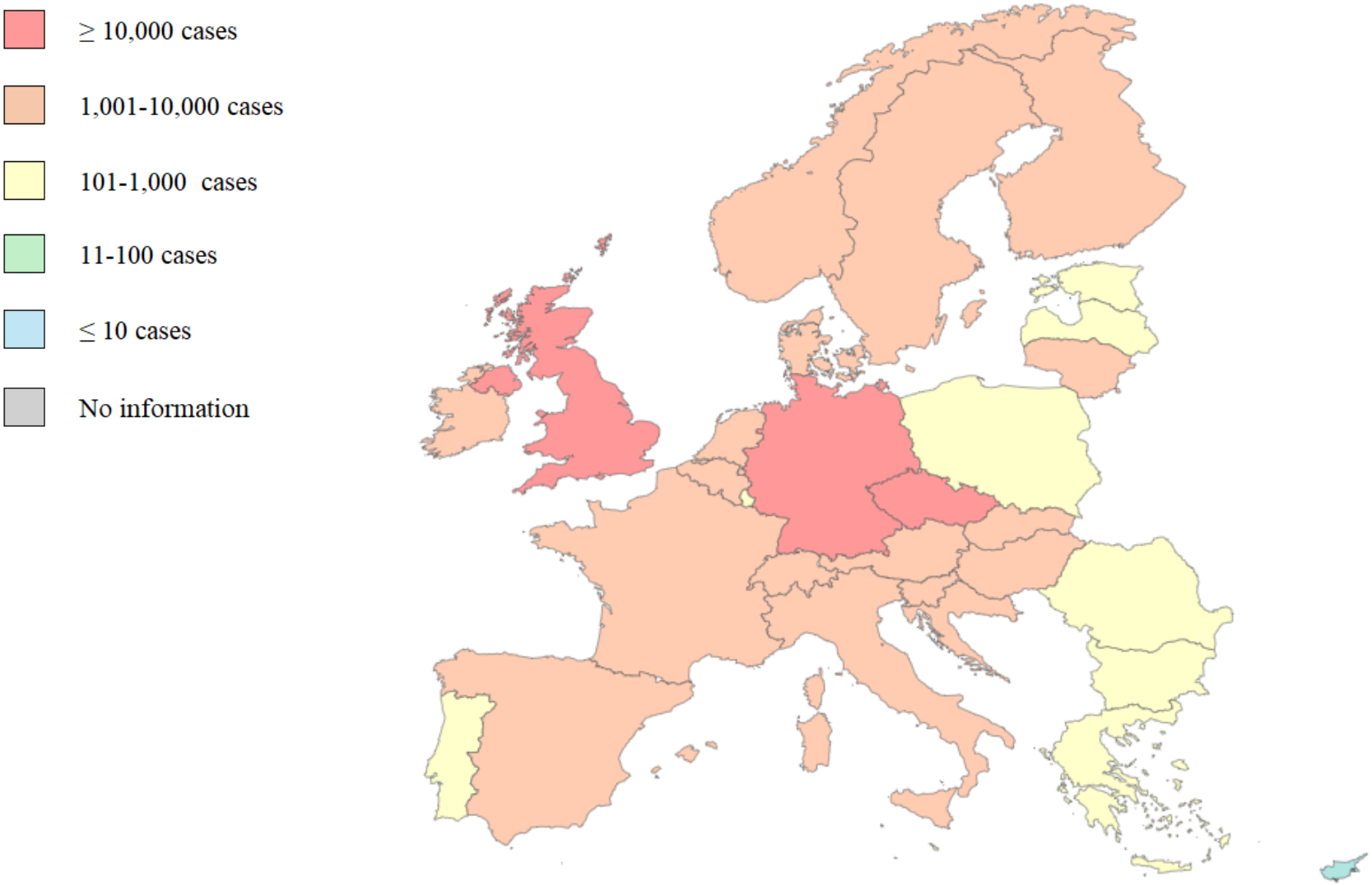

Figure 4. Total number of *Campylobacter* cases across Europe in 2019

CHAPTER I

Additive effect of plasmid-encoded quinolone resistance protein QnrB19 with amino acid substitution in *Salmonella* Typhimurium DNA gyrase

Introduction

Quinolones are widely recognized as the drugs for treating infections caused by NTS. However, the emergence of plasmid-mediated resistance mechanisms poses a significant challenge to the effective treatment of these infections. Among these resistance mechanisms, the plasmid encoded Qnr proteins are particularly notable for their role in reducing quinolone effectiveness. Particularly, previous research has identified QnrB19 as the predominant Qnr variant among *Salmonella* spp. isolates. Despite its prevalence, the specific contribution of QnrB19 to quinolone resistance remains under investigation, especially with coexisting amino acid substitutions in DNA gyrase that significantly facilitates bacterial resistance. To address this gap, Chapter I presents an *in vitro* study that used DNA gyrase assays to examine the impact of QnrB19 on quinolone resistance. This study used recombinant *S*. Typhimurium DNA gyrases, QnrB19 and two commonly used quinolones: CIP and moxifloxacin (MOX) to elucidate the resistant mechanism.

Materials and Methods

Reagents

Relaxed pBR322 DNA was purchased from Inspiralis Ltd., Norwich, United Kingdom. The *E. coli* BL21 (DE3)/pLysS and *E. coli* BL21 (DE3), were purchased from Merck KGaA, Darmstadt, Germany. The reagents and materials used in this study include Luria-Bertani (LB) broth, LB agar, 1 mM isopropyl-β-D-thiogalactopyranoside (IPTG), sodium dodecyl sulfate-polyacrylamide gel electrophoresis (SDS-PAGE), and ethidium bromide, all of which were obtained from Wako Pure Chemical Industries Ltd. Mueller-Hinton broth (MHB) was purchased from Becton (Maryland, United Satates). Millipore 50k Amicon Ultra tubes and complete mini EDTA-free products were purchased from Merck Millipore Ltd, Massachusetts, United States. CIP and ampicillin (AMP) were purchased from LKT Laboratories, Inc., Minnesota, United State and Wako Pure Chemical Industries, Ltd., in Osaka, Japan, respectively. And MOX was purchased Toronto Research Chemical Inc, Ontario, Canada, respectively.

Construction of WT and mutant DNA gyrase expression vectors

Recombinant DNA gyrases with various amino acid substitutions on DNA gyrase including $GyrA^{WT}$, $GyrA^{S83F}$, $GyrA^{D87N}$, and one subunit of GyrB, which was $GyrB^{WT}$ were prepared to assess the antimicrobial effects of the examined compounds. The plasmids carrying the genes encoded for those DNA gyrase subunits were prepared as in previous studies [16,44–47]. Briefly, DNA fragments of genes for *gyrA* and *gyrB* of *S.* Typhimurium NBRC 13245, were amplified using polymerase chain reaction (PCR). For this purpose, primer set for both WT and mutant subunits were employed. The amplification resulted in PCR products of 2.6 kb for *gyrA* and 2.4 kb for *gyrB*. These products were then inserted into a blunt-ended cloning vector and introduced into *E. coli* TOP-10 cells, which were subsequently cultured on LB agar plates supplemented with AMP (100 mg/L) to select the transformed colonies. Following confirmation, the *gyrA* and *gyrB* inserts were excised using *Nde* I and *Xho* I enzymes and ligated into the pET-20b (+) expression vector, prepared with the same restriction sites. This assembly was again transformed into *E. coli* TOP-10 cells as the host for cloning purposes. The resulting recombinant clones, capable of expressing GyrA and GyrB, were identified by their growth on LB agar plates containing AMP (100 mg/L), determining successful cloning and expression plasmid construction. The nucleotide sequence of the DNA gyrase gene located in the plasmid was determined using the BigDye Terminator (version 3.1) Cycle Sequencing Kit, according to the manufacturer's protocol.

Mutant DNA gyrase genes were introduced into the $gyrA^{WT}$ of *S.* Typhimurium NBRC 13245 using pairs of complementary primers included the desired nucleotide substitutions with PCR technique. The modified *gyrA* containing base substitutions was then digested with *Nde* I and *Xho* I enzymes. Subsequently, it was ligated into a $gyrA^{WT}$ expression plasmid that had been similarly digested with these restriction enzymes. The

mutant *gyrA* expression plasmid was transformed into *E. coli* TOP-10 and confirmed the successful cloning as previous.

Expression and purification of recombinant *S.* Typhimurium DNA gyrase subunits

The confirmed plasmids were introduced into *E. coli* as described in the previous studies [16,44–46]. Specifically, *E. coli* BL21 (DE3)/pLysS was transformed by the plasmid carrying the *gyrA* and *E. coli* BL21 (DE3) was transformed by the plasmid carrying *gyrB.* The transformance cells were cultivated in LB broth with AMP (50 mg/L) at 37°C. Expression of GyrA and GyrB proteins was induced by adding 1 mM IPTG when the optical density at 590 nm (OD 590) reached 0.4–0.6, followed by further incubation at 18°C for 16 hours. Post incubation, *E. coli* cells were collected by centrifugation.

The collected cells were then resuspended in a native binding buffer that included a complete mini EDTA-free solution. The suspension underwent sonication using a Sonifier 250 (Branson, Connecticut, United States) for 4 minutes across 10 cycles; each cycle consisting of 40 seconds of sonication followed by 40 seconds of cooling, with a duty cycle set at 30%. To purify the proteins, the supernatants with soluble proteins were passed through a column filled with Ni-NTA agarose resin. The proteins were further concentrated using Millipore 50k Amicon Ultra tubes, mixed with glycerol to achieve a 40% (wt/vol) concentration, and stored in small aliquots at -80°C for the next use. The purity of the proteins was verified through SDS-PAGE analysis.

QnrB19 expression vectors

The synthetic target gene, *qnrB19*, of *S.* Typhimurium (GenBank accession No. NC_012916.1) was obtained in a pUC57 plasmid from Genscript, located in New Jersey, United States. The vector plasmid pET-28b (+) was acquired from Merck KGaA, Darmstadt, Germany, and used to construct the expression plasmid.

Expression and purification of QnrB19

Briefly, *E. coli* BL21 (DE3)/pLysS carrying *qnrB19* in pET20b (+) plasmid vector were cultured in 500 mL of LB broth with ampicillin sodium (50 mg/L) at 37 °C. The expression of QnrB19 was induced by adding 1 mM IPTG when the culture reached an OD_{590} of 0.4-0.6. Thereafter, the bacteria were incubated for 16 hours at 18 °C and harvested by centrifugation. The harvested cell carrying QnrB19 was washed with cold buffer A which consisted of 50 mM Tris-HCl pH 8.0, 200 mM $(NH_4)_2SO_4$, 10% glycerol, and 20 mM imidazole. The cell pellet was then resuspended in the cold buffer A with 1 mg/mL lysozyme and 0.5% Triton X-100 and kept at 4°C overnight after which sonication was performed. Additionally, 0.1 mg/mL DNase was added to the suspension to degrade any remaining DNA. The lysed samples were filtrated and applied to a Ni-NTA agarose resin column and purified using a gradient of imidazole concentrations (30, 40, 50, 100, 200, and 300 mM) in buffer A, containing EDTA-free protease inhibitor cocktail tablets [48]. Millipore 50k Amicon Ultra tubes were used to consolidate the proteins. The

condensed protein in the buffer containing imidazole was transferred to a PD-10 column to remove imidazole and change the buffer to buffer B (20 mM Tris pH 8.0, 10% glycerol, and 50 mM arginine). Thereafter, the purity of the proteins was assessed by SDS-PAGE.

Protective activity of QnrB19 to *S.* Typhimurium DNA gyrase inhibited by quinolones.

DNA gyrase supercoiling assays were conducted to assess the inhibitory effects of quinolones, particularly CIP and MOX with or without QnrB19. Quinolones-inhibiting DNA supercoiling assays were performed using GyrA, GyrB, and 54nM of QnrB19 to evaluate half-maximum inhibitory concentrations (IC_{50}s) of quinolones following protocols described in previous studies [16,44,49]. Briefly, DNA gyrase buffer containing 35 mM Tris-HCl pH 7.5, 24 mM KCl, 4 mM $MgCl_2$, 2 mM DTT, 1.8 mM spermidine, 6.5% glycerol, and 0.1 mg/mL of BSA was mixed with 1 mM ATP, 1.5 nM relaxed pBR322 DNA, 18 nM DNA gyrase subunits, 54 nM of QnrB19, and varying concentrations of quinolones. The concentrations of CIP used against DNA gyrase carrying $GyrA^{WT}$, $GyrA^{S83F}$, and $GyrA^{D87N}$ ranged from 0.02-5.12, 0.08-20.48, and 0.16-40.96 mg/L, respectively. Whereas the concentrations of MOX used against DNA gyrase carrying $GyrA^{WT}$, $GyrA^{S83F}$, $GyrA^{D87N}$ ranged from 0.04-10.24, 0.32-81.92, and 0.64-163.84 mg/L, respectively. The reaction mixtures, totaling 30 µL were incubated at 37°C for 60 min and the reactions were stopped by adding 8 µL of 5×dye mix containing 5% SDS, 25% glycerol, and 0.25 mg/mL of bromophenol blue. Subsequently, the reaction mixtures were mixed with 1xDNA sample buffer containing 0.1% SDS, 10% glycerol, 100 mM Tris-HCl pH 8.0, and 0.05 mg/mL of bromophenol blue to make a 1:3 dilution. Thereafter, 10 µL aliquots of the dilutions were loaded onto a 1% agarose gel in 1x TAE buffer. Electrophoresis was conducted in 1x TAE buffer at 50 mA for 60 min and gel red (1X) was used for staining. IC_{50}s were determined by using the software ImageJ, and a statistical software R version 4.1.3 with the "drc" package was utilized to assess the inhibitory activity of quinolones [50].

To investigate the influence of QnrB19, its impact on supercoiling activity in the presence and absence of quinolones was examined through ATP-dependent DNA supercoiling assays with increasing concentrations of QnrB19. The assays were divided into 2 parts: one without quinolones and the other with quinolones. Briefly, the DNA gyrase buffer was mixed with 1 mM ATP, 1.5 nM relaxed pBR322 DNA, 18 nM DNA gyrase subunits, and serial dilutions of QnrB19 (0 – 4,374 nM). In the reaction with quinolones, the reaction mixtures were prepared as previously described and mixed with the examined drugs at a concentration equal to IC_{80}s. The mixtures were incubated at 37°C for 60 min and terminated by 8 µL of 5x dye mix. Finally, electrophoresis was carried out and IC_{50}s were evaluated, respectively [44].

Quinolone-mediated DNA cleavage assay

DNA cleavage assays with CIP were conducted as described previously [46]. Supercoiled pBR322 DNA was used for the assay. Each 30 µl reaction mixture included 1.5 nM supercoiled pBR322 DNA, 18 nM DNA gyrase subunits, 54nM of QnrB19, and ciprofloxacin hydrochloride in 2-fold serial dilutions. The mixtures were incubated at 37°C for 60 min, followed by treatment with 3 µl of 2% SDS and 3 µl of proteinase K (1 mg/ml) for 30 min at the same temperature. The reactions were terminated using a stop solution. Linearized pBR322 DNA, produced by *Bam* HI digestion, was used as a marker. The assay was performed in triplicate. Both the marker and the reaction mixtures were analyzed on 1% agarose gels, followed by staining as described in earlier experiments. DNA cleavage was quantified using ImageJ software. Dose-response curves were generated using the statistical software R version 4.1.3, employing the "drc" package [50].

Statistical Analysis

Statistical analysis was conducted using R software version 4.1.3 along with "Dplyr", add-on package [51]. Shapiro-Wilk normality test and paired sample t-test were performed, and statistical significance was indicated by a $p < 0.05$.

Results

Expression and purification of recombinant proteins in this study

The WT GyrA ($GyrA^{WT}$), mutant GyrA with amino acid substitutions at position 83 in *gyrA* from serine to phenylalanine ($GyrA^{S83F}$), and aspartic acid to asparagine ($GyrA^{D87N}$), WT GyrB ($GyrB^{WT}$), and QnrB19 were successfully overexpressed by *E. coli* using plasmid vectors and purified through Ni-NTA chromatography following previously established methods (18). The purity and molecular mass of the proteins were assessed by using SDS-PAGE. The results demonstrated protein purities exceeding 95%, and the observed molecular masses were consistent with those reported in a previous study, (18) as shown in Figure 5; GyrA (97kDa), GyrB (89kDa), and QnrB19 (25kDa).

Protective activity of QnrB19 to *S.* Typhimurium DNA gyrase inhibited by quinolones.

Half-maximum inhibitory concentrations (IC_{50}s) were examined using recombinant DNA gyrases, QnrB19, and FQs to investigate the inhibitory effect of quinolones against WT and mutant DNA gyrases in the presence or absence of QnrB19. The results of the DNA supercoiling assay were visualized through gel electrophoresis and dose-response curves were plotted, as shown in Figure 6 to Figure 11. IC_{50}s of CIP and MOX were determined by analyzing the results of the DNA gyrase assay with different concentrations of the drugs. Statistical analysis was performed to demonstrate the significant differences in IC_{50}s, as presented in Table 4 and Figure 12. The amino acid substitutions, specifically $GyrA^{S83F}$ and $GyrA^{D87N}$, in DNA gyrases of *S.* Typhimurium were observed to require a

higher concentration of quinolones to inhibit the normal function of DNA gyrases (Table 4). The IC_{50}s of CIP against $GyrA^{S83F}$ and $GyrA^{D87N}$ were found to be 10- and 26-fold higher than $GyrA^{WT}$, respectively. Likewise, IC_{50}s of MOX against $GyrA^{S83F}$, and $GyrA^{D87N}$ were 16- and 10- fold higher than $GyrA^{WT}$, respectively.

In the presence of QnrB19, IC_{50}s of CIP and MOX against $GyrA^{WT}$ showed a significant difference with an increase of 10-fold and 8-fold respectively, compared to the experiments without QnrB19 as presented in Table 4. Moreover, the IC_{50}s of CIP against $GyrA^{S83F}$ and $GyrA^{D87N}$ were 4- and 13-fold higher respectively, in the presence of QnrB19 than in its absence. Similarly, the IC_{50}s of MOX against $GyrA^{S83F}$, and $GyrA^{D87N}$ were 14- and 10-fold higher respectively, compared to $GyrA^{WT}$. The effects of QnrB19 on supercoiling activity were shown in Figure 13 and 14. In the absence of quinolones, low concentrations of QnrB19 (6-162nM) slightly enhanced the activity of DNA gyrases by approximately 10%. However, high concentrations of QnrB19 (486-4374 nM) inhibited the normal DNA gyrase activity. When quinolones were present, concentrations of QnrB19 ranging from 6-162 nM resulted in greater than 20% of supercoiling activity in both WT and mutant DNA gyrases against CIP and MOX, at concentrations equivalent to their IC_{80}s. Particularly, at concentrations ranging from 18–162 nM, QnrB19 demonstrated a significant recovery of supercoiling activities, exceeding 50%, at the equivalent concentrations of quinolones. However, higher concentrations of QnrB19 (486-4374 nM) in the presence of quinolones, resulted in the inhibition of DNA gyrases. Complete inhibition of supercoiling activity was observed only in experiments involving $GyrA^{S83F}$ and $GyrA^{D87N}$ with CIP, specifically at the QnrB19 concentration of 4374 nM. In contrast, partial inhibition of supercoiling activity was observed in the experiments involving $GyrA^{WT}$ with CIP as well as $GyrA^{WT}$, $GyrA^{S83F}$, and $GyrA^{D87N}$ with moxifloxacin hydrochloride.

Quinolone-mediated DNA cleavage assay

The cleavage assay was performed with both $GyrA^{WT}$ and $GyrA^{S83F}$ DNA gyrases at varying concentrations of CIP to assess the effectiveness of QnrB19 in reducing DNA gyrase complexes and DNA cleavage. The results showed that the presence of 54 nM QnrB19 resulted in decreased DNA cleavage, particularly as the concentrations of CIP increased. This effect was observed in both $GyrA^{WT}$ and $GyrA^{S83F}$ DNA gyrases, as demonstrated in Figure 15 and 16.

Discussion

In this study, I have investigated the mutual impact of mutant DNA gyrases and QnrB19 on quinolones resistance. This was achieved by utilizing recombinant DNA gyrases of *S*. Typhimurium carrying amino acid substitutions, namely, $GyrA^{S83F}$ and $GyrA^{D87N}$ due to their high prevalence and recognized role in conferring quinolones

resistance. The results demonstrated the remarkable capacity of QnrB19 to exert both protective and inhibitory effects on DNA gyrases.

A previous study showed that the R-3 and R-4 moieties of quinolones depicted in Figure 17, could interact with noncatalytic Mg^{2+} and water molecules, leading to the formation of a water-metal ion bridge that facilitates essential interactions between quinolones and DNA gyrase [52,53]. As a result, quinolones gain the ability to interact with serine (codon 83) and aspartic acid (codon 87) resulting in complex formation and permanent DNA breakage [54]. The chemical structure of amino acids reveals that DNA gyrases carrying $GyrA^{S83F}$ or $GyrA^{D87N}$ substitutions lack the hydroxyl group and carboxyl group, respectively [55]. Moreover, the $GyrA^{S83F}$ substitution increases the bulkiness and hydrophobicity, which could physically obstruct the entrance of the quinolone pocket. This obstruction reduces the binding affinity between DNA gyrase and quinolones, potentially leading to quinolones resistance [56,57]. Furthermore, these mutations may also decrease quinolones' ability to stabilize cleavage complexes [29,58]. Consequently, DNA gyrases carrying amino acid substitution have higher IC_{50} than WT DNA gyrase.

This study represents the first attempt to explore the *in vitro* activity of QnrB19 with both WT and mutant DNA gyrases of *S.* Typhimurium against quinolones. Our results indicate that QnrB19 plays a crucial role in conferring quinolones resistance in *S.* Typhimurium. Statistical analysis revealed a significant increase in the IC_{50} values of the tested quinolones in the presence of QnrB19. Notably, the IC_{50} values of ciprofloxacin hydrochloride and moxifloxacin hydrochloride against WT DNA gyrase increased by more than 10-fold and 8-fold, respectively (Table 4 and Figure 12). Considering these findings, I hypothesized that the binding of QnrB19 to DNA gyrase either induces changes in the configuration of the complex involving DNA gyrase, DNA, and quinolones, or directly blocks fluoroquinolone binding to the enzyme. Consequently, the complex might be destabilized, potentially leading to its quinolones release. This could explain the increased amount of quinolones required to inhibit the normal function of DNA gyrase, as demonstrated in Table 4 and Figure 12.

Previous studies have demonstrated that QnrB1, a member of the QnrB family, can interact with GyrB and increase ATP hydrolysis. [21,59] It is, therefore, possible that QnrB19, being a member of the same family, possesses a similar capability to promote ATP hydrolysis, thereby resulting in increased gyrase activity. The presence of QnrB19 led to a slight increase in supercoiling activities in the experiments conducted without the presence of quinolones. At lower concentrations of quinolones, the interaction between QnrB19 and DNA gyrases allows for the maintenance of their normal function. However, as the concentration of quinolones increases, the inhibitory activity of quinolones on DNA gyrase gradually diminishes the supercoiling activities of DNA gyrases. Generally, DNA gyrase plays an essential role ahead replication forks and transcription complexes. Hence,

the activity of DNA gyrase can directly affect the bacterial growth rate. [57,60] Given the finding that QnrB19 can enhance the activity of DNA gyrase, it is plausible to suggest that the presence of QnrB19 may increase the growth rate of the bacteria. Consequently, bacteria carrying *qnrB19* could rapidly spread and outcompete endemic bacteria, leading to the emergence of quinolones resistance.

In reactions conducted without QnrB19, the inhibitory effect of quinolones progressively increased with higher concentrations, ultimately leading to the complete inhibition of supercoiling activities. Although the presence of QnrB19 demonstrated a certain degree of protection against quinolones in our study, complete inhibition at higher concentrations of quinolones was still observed in both WT and mutant DNA. Hence considering our results (Figure 13 and 14) and past studies, it is apparent that the protective ability of QnrB19 has its limitations [61]. It has been previously reported [19,62] that the presence of QnrB19 can protect DNA gyrase function from the inhibition ability of quinolones in a concentration-dependent manner. Consistent with these findings, our study confirmed that the ratio of QnrB19 to DNA gyrase is indeed critical as demonstrated in Figure 14. Specifically, when the ratio was less than 1:1 (18 nM in Figure 14), QnrB19 exhibited the ability to partially restore the function of DNA gyrase. Moreover, at ratios ranging from 1:1 – 9:1, QnrB19 displayed high activity and could restore more than 50% to around 80% of DNA gyrase activity in the presence of the inhibitory levels of quinolones as shown in Figure 14. These findings suggest that the concentration of QnrB19 or the copy number of the plasmid carrying *qnr* may influence the protection level.

Given the observed inhibition of supercoiling activities at the high concentrations of QnrB19, we hypothesize that QnrB19 may competitively bind with DNA gyrase thereby preventing its interaction with DNA as similar as QnrB1 in the previous study [21]. As a result, inhibitory effects on the normal function of DNA gyrase manifest when QnrB19 concentrations reach sufficiently high levels. Our study demonstrated that QnrB19 could efficiently inhibit DNA gyrase with a concentration nearly 100-fold higher than the enzyme concentration. Similarly, previous studies [21] reported that QnrB1 required concentrations over 10,000-fold higher than the enzyme concentration to exert inhibitory effects.

Although IC_{50} values cannot be directly translated to MICs, previous studies [46,63] have demonstrated a positive correlation between these values either in NTS or other bacteria. Furthermore, it has been observed that IC_{50} values tend to be higher than MICs. [46,63] The IC_{50} is determined from *in vitro* tests that access the direct interactions among DNA gyrase, the examined drugs, and QnrB19. In live bacterial cells, factors such as drug accumulation and permeability are crucial for demonstrating inhibitory activity, leading to a high concentration of the drugs inside the cell. [46] Therefore, the high

concentrations of the drugs used in this study were necessary to be included to mimics the accumulation of drugs within bacterial cells.

In a previous study, it was shown that QnrB1 has protective effect on DNA cleavage complexes formed with DNA gyrase in the presence of ciprofloxacin hydrochloride.[21] We have confirmed that QnrB19 exhibits similar activity. Our cleavage assay demonstrated that the amount of linear DNA increases with higher concentrations of the examined drug as shown in Figure 15 and 16. QnrB19 (54 mM) reduced the amount of cleavage DNA for both wild-type and mutant DNA gyrases. In the absence of QnrB19, DNA cleavage was approximately 10% higher compared to when QnrB19 was present, confirming that QnrB19, like QnrB1, protects against ciprofloxacin-induced DNA cleavage.

With the previous finding and the current study, we propose potential interactions involving QnrB19, DNA gyrase, DNA, and quinolones, as depicted in Figure 18, which could occur and protect the normal activity of DNA gyrase [21]. The concentration-dependent activity observed in our study, however, suggests six possible scenarios that can occur in the presence of these components. Firstly, DNA gyrase can function normally without QnrB19 and quinolones interactions. Secondly, quinolones could form a complex with DNA gyrase and DNA resulting in DNA damage. Thirdly, QnrB19 could mimic the T-segment of DNA, and consequently increasing the supercoiling activity. Fourth, mutant DNA gyrase can function normally even with a certain concentration of quinolones. Fifth, high concentration of quinolones could form a complex with mutant DNA gyrase and DNA resulting in DNA damage. Sixth, DNA, QnrB19, and quinolones might be captured by mutant DNA gyrase, thereby forming a complex. The conformation adopted by QnrB19 promotes the release of quinolones, by reducing the affinity between proteins and quinolones. This allows bacteria to maintain their typical chromosomal DNA structures even with high concentration of quinolones. This is the first study showing the additive effect of QnrB19 and amino acid substitutions on the quinolones-resistance in *Salmonella* by molecular level using recombinant proteins.

Conclusions

The interplay between amino acid substitutions in DNA gyrase and the presence of QnrB19 plays a pivotal role in fostering high-level resistance to quinolones. This chapter suggests that QnrB19 may amplify this resistance by inducing a less favorable conformation in mutant DNA gyrases. The simultaneous presence of these resistance mechanisms could enable bacteria to survive in the clinical quinolones' concentration, posing a significant risk to the success of treatment.

Table 4. IC_{50} values of quinolones against WT *Salmonella* DNA gyrase and mutant *Salmonella* DNA gyrases against CIP and MOX

DNA gyrase		IC_{50}s (mg/L)					
		CIP			MOX		
Subunit A	Subunit B	Without QnrB19	With QnrB19	*p* value	Without QnrB19	With QnrB19	*p* value
WT	WT	0.050±0.010*	0.490±0.060*	0.032	0.077±0.020*	0.668±0.169*	0.02
S83F	WT	0.510±0.020*	2.240±0.540*	0.033	0.698±0.130*	9.718±2.141*	0.02
D87N	WT	1.310±0.290*	17.150±5.800*	0.045	0.734±0.008*	7.500±1.300*	0.01

*p <0.05

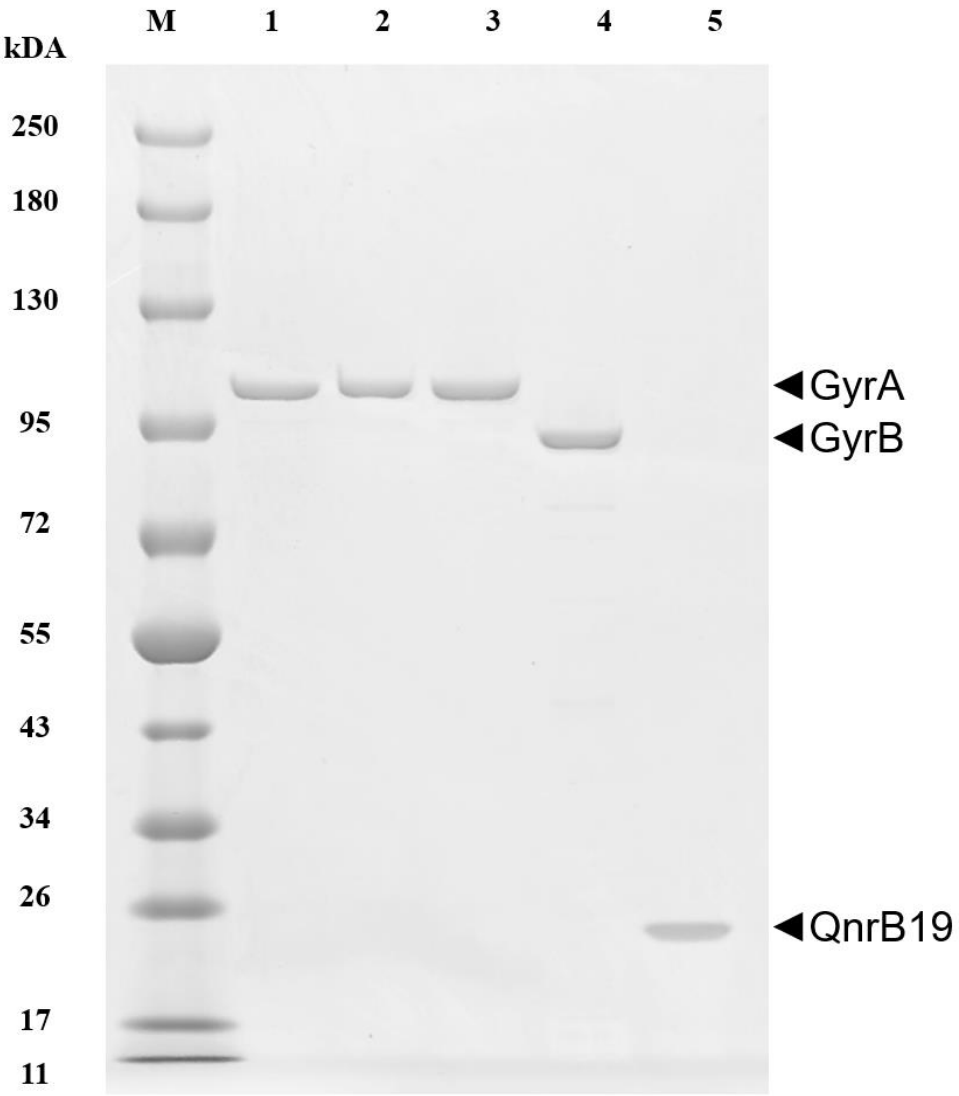

Figure 5. SDS-PAGE analysis of purified GyrA, GyrB and QnrB19.
Protein samples (500 ng) including $GyrA^{WT}$, $GyrA^{S83F}$, $GyrA^{D87N}$, $GyrB^{WT}$, and QnrB19 were loaded onto a 5-20% gradient polyacrylamide gel to the purification of recombinant *S.* Typhimurium DNA gyrases. Lane M represents the protein size marker, while lanes 1-5 correspond to $GyrA^{WT}$, $GyrA^{S83F}$, $GyrA^{D87N}$, $GyrB^{WT}$, and QnrB19 respectively.

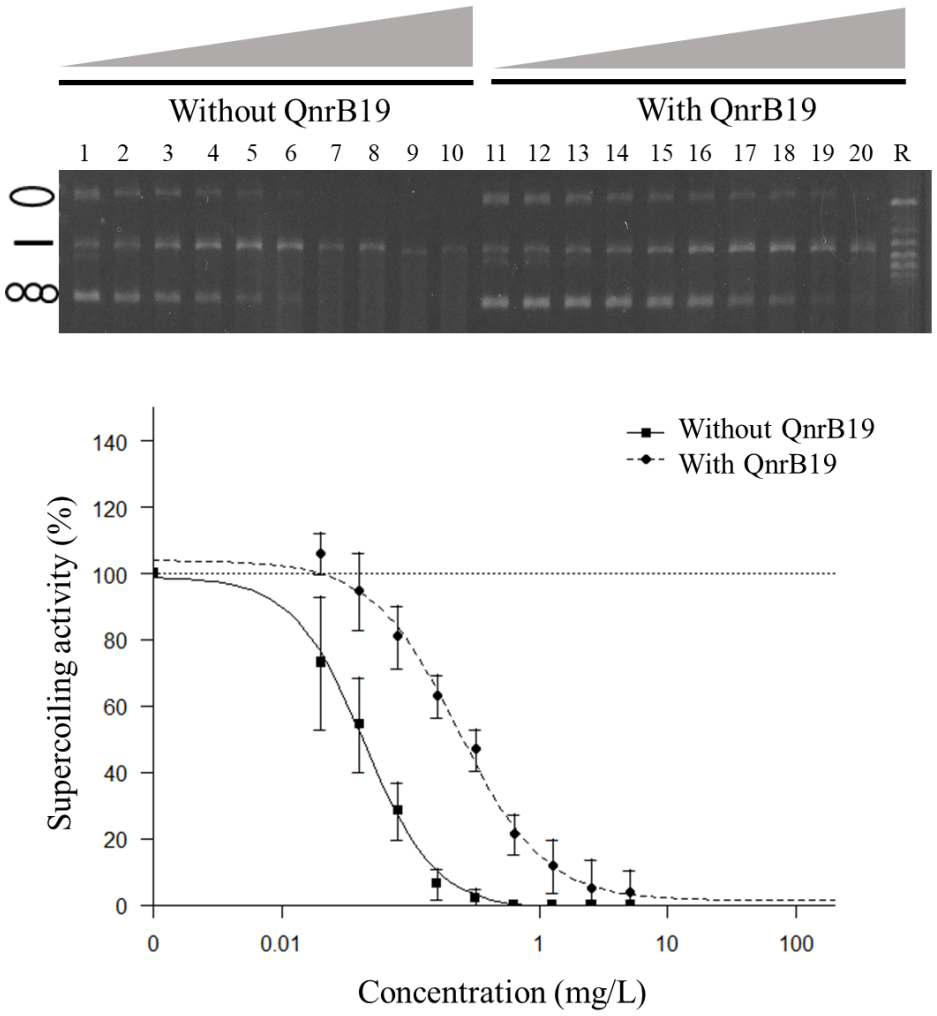

Figure 6. The inhibitory effects of CIP against $GyrA^{WT}$ DNA gyrase in the presence and absence of QnrB19.

The results for DNA gyrases containing $GyrA^{WT}$ with CIP concentrations ranging from 0 to 5.12 mg/L (Lane 1 & 11: 0, Lane 2 & 12: 0.02, Lane 3 & 13: 0.04, Lane 4 & 14: 0.08, Lane 5 & 15: 0.16, Lane 6 & 16: 0.32, Lane 7 & 17: 0.64, Lane 8 and 18: 1.28, Lane 9 & 19: 2.56, Lane 10 & 20: 5.12 mg/L). Gel electrophoresis was employed to visualize the reactions, with Lanes 1-10 showing the reactions involving relaxed DNA, DNA gyrases, and the serial dilutions of quinolones. Lanes 11-20 included these components plus 54 nM of QnrB19. The additional graphs displayed the correlation between supercoiling activity and quinolone concentration, with dotted lines indicating 100% activity. The dose-response curves, in the presence of QnrB19 (dashed lines) and without (solid lines), illustrate the impact of QnrB19 on supercoiling activity.

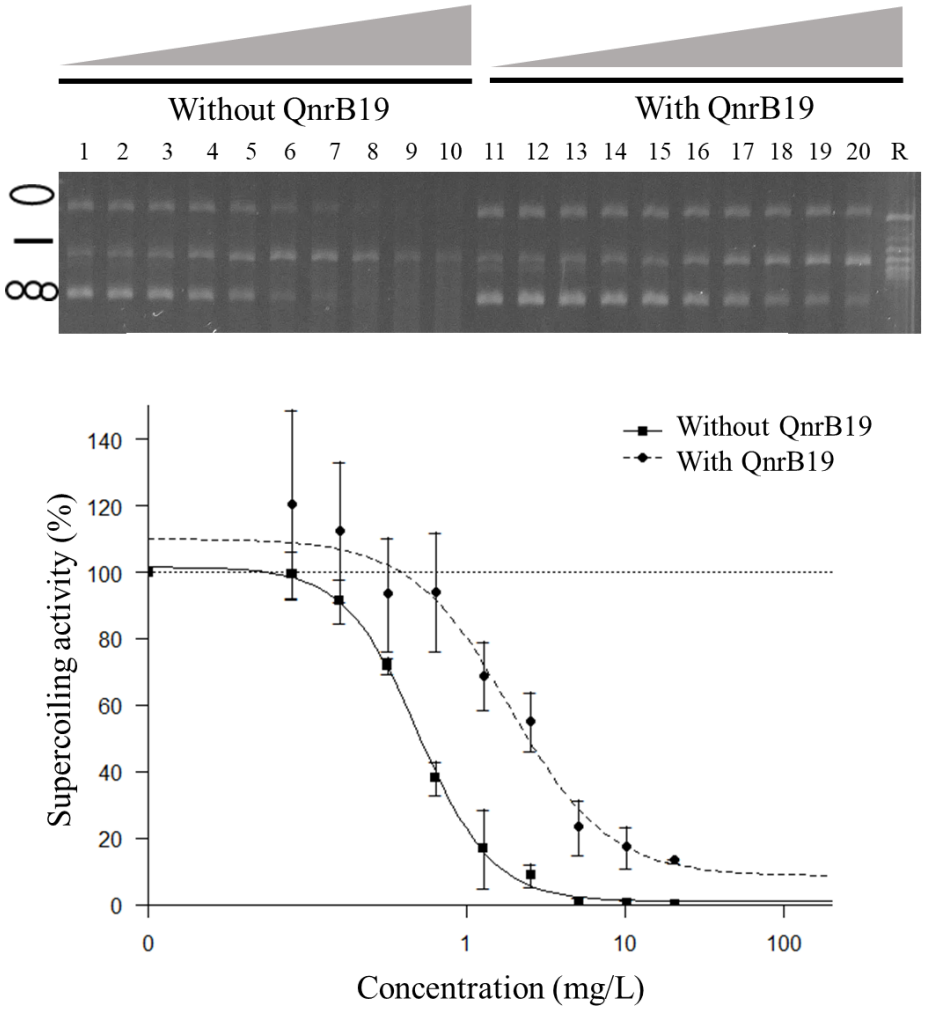

Figure 7. The inhibitory effects of CIP against GyrA^{S83F} DNA gyrase in the presence and absence of QnrB19.
The response of DNA gyrases with the GyrA^{S83F} to CIP, covering a range from 0 to 20.48 mg/L (Lane 1 & 11: 0, Lane 2 & 12: 0.08, Lane 3 & 13: 0.16, Lane 4 & 14: 0.32, Lane 5 & 15: 0.64, Lane 6 & 16: 1.28, Lane 7 & 17: 2.56, Lane 8 and 18: 5.12, Lane 9 & 19: 10.24, Lane 10 & 20: 20.48 mg/L). Gel electrophoresis was employed to visualize the reactions, with Lanes 1-10 showing the reactions involving relaxed DNA, DNA gyrases, and the serial dilutions of quinolones. Lanes 11-20 included these components plus 54 nM of QnrB19. The additional graphs displayed the correlation between supercoiling activity and quinolone concentration, with dotted lines indicating 100% activity. The dose-response curves, in the presence of QnrB19 (dashed lines) and without (solid lines), illustrate the impact of QnrB19 on supercoiling activity.

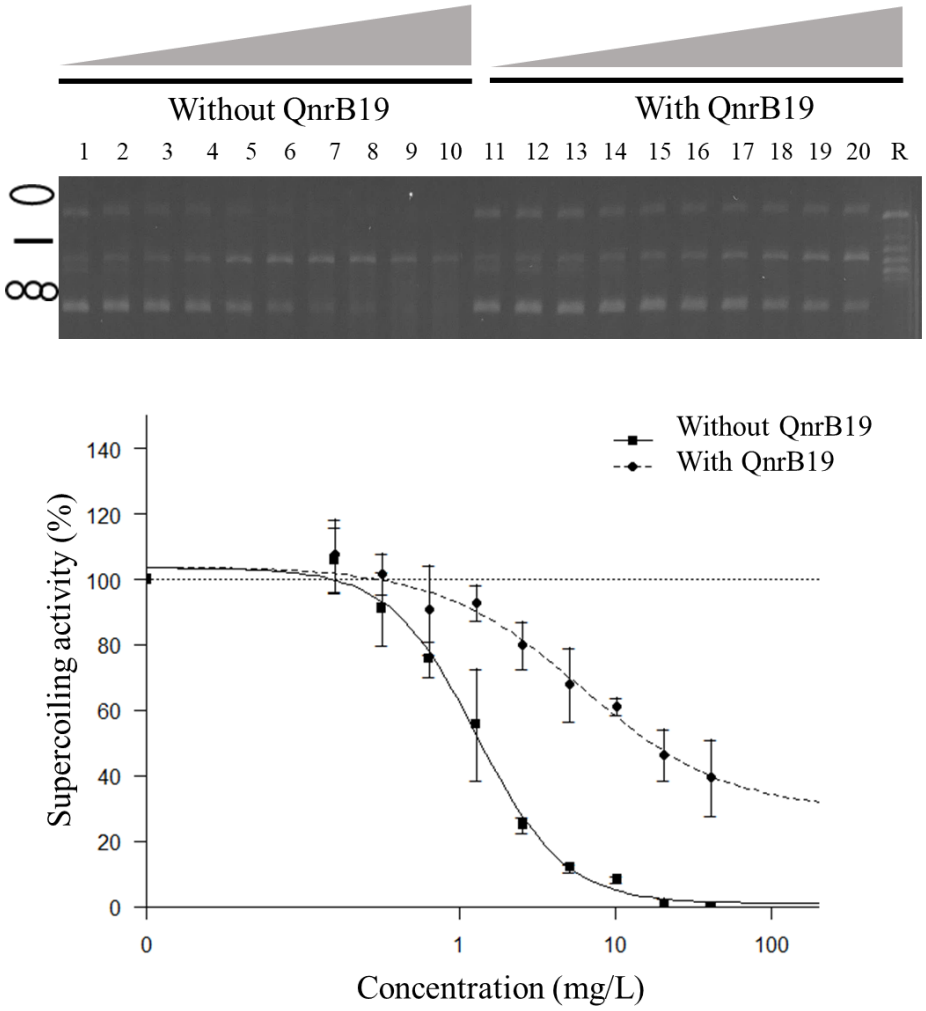

Figure 8. The inhibitory effects of CIP against GyrA^{D87N} DNA gyrase in the presence and absence of QnrB19.
The results for DNA gyrases carrying the GyrA^{D87N} against CIP doses ranging from 0 to 40.96 mg/L (Lane 1 & 11: 0, Lane 2 & 12: 0.16, Lane 3 & 13: 0.32, Lane 4 & 14: 0.64, Lane 5 & 15: 1.28, Lane 6 & 16: 2.56, Lane 7 & 17: 5.12, Lane 8 and 18: 10.24, Lane 9 & 19: 20.48, Lane 10 & 20: 40.96 mg/L). Gel electrophoresis was employed to visualize the reactions, with Lanes 1-10 showing the reactions involving relaxed DNA, DNA gyrases, and the serial dilutions of quinolones. Lanes 11-20 included these components plus 54 nM of QnrB19. The additional graphs displayed the correlation between supercoiling activity and quinolone concentration, with dotted lines indicating 100% activity. The dose-response curves, in the presence of QnrB19 (dashed lines) and without (solid lines), illustrate the impact of QnrB19 on supercoiling activity.

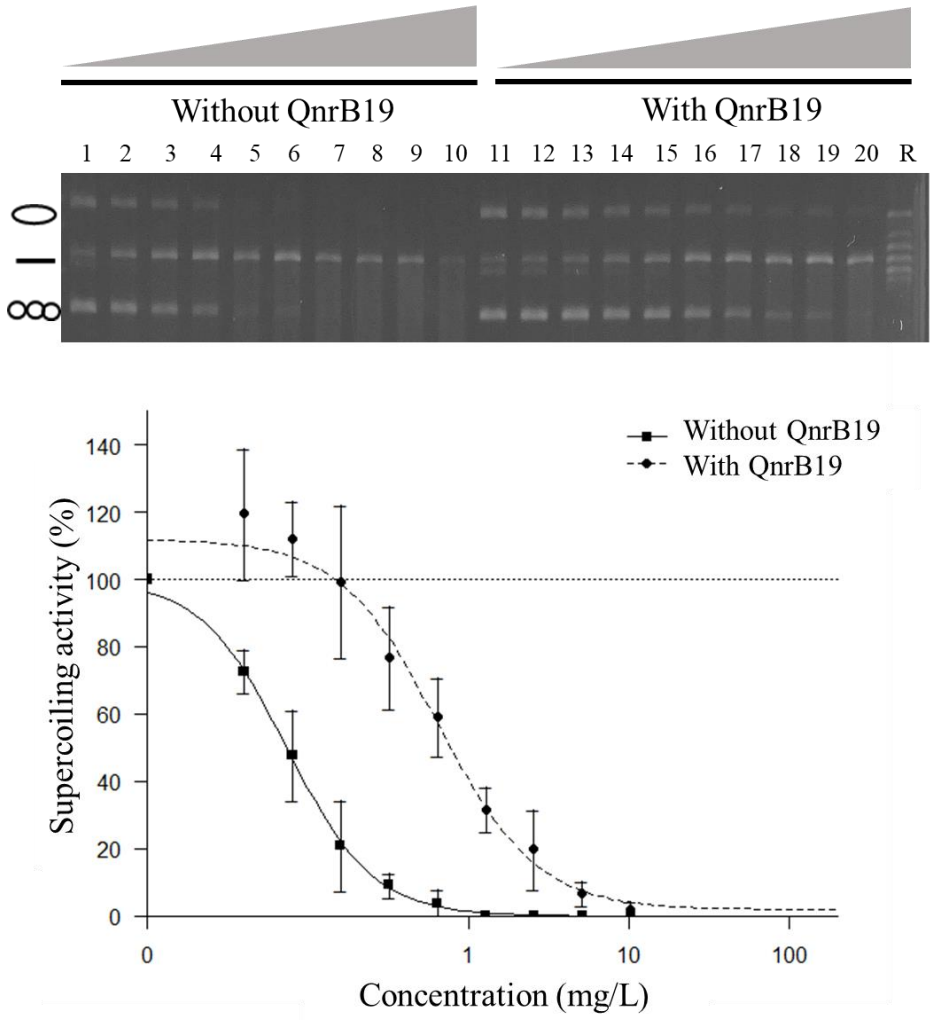

Figure 9. The inhibitory effects of MOX against $GyrA^{WT}$ DNA gyrase in the presence and absence of QnrB19.
The effects of MOX on $GyrA^{WT}$ across a range from 0 to 10.24 mg/L (Lane 1 & 11: 0, Lane 2 & 12: 0.04, Lane 3 & 13: 0.08, Lane 4 & 14: 0.16, Lane 5 & 15: 0.32, Lane 6 & 16: 0.64, Lane 7 & 17: 1.28, Lane 8 and 18: 2.56, Lane 9 & 19: 5.12, Lane 10 & 20: 10.24 mg/L). Gel electrophoresis was employed to visualize the reactions, with Lanes 1-10 showing the reactions involving relaxed DNA, DNA gyrases, and the serial dilutions of quinolones. Lanes 11-20 included these components plus 54 nM of QnrB19. The additional graphs displayed the correlation between supercoiling activity and quinolone concentration, with dotted lines indicating 100% activity. The dose-response curves, in the presence of QnrB19 (dashed lines) and without (solid lines), illustrate the impact of QnrB19 on supercoiling activity.

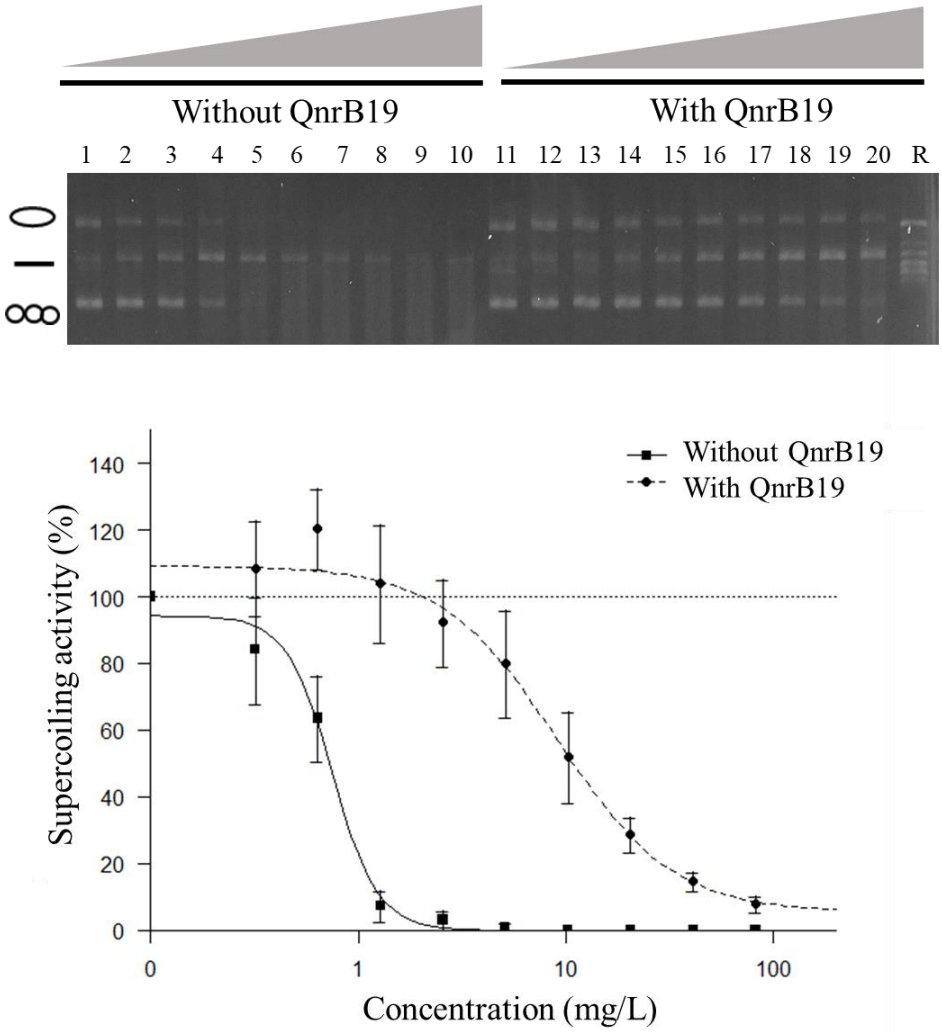

Figure 10. The inhibitory effects of MOX against GyrA^{S83F} DNA gyrase in the presence and absence of QnrB19.
The results for GyrA^{S83F} against MOX, with concentrations extending to 81.92 mg/L (Lane 1 & 11: 0, Lane 2 & 12: 0.32, Lane 3 & 13: 0.64, Lane 4 & 14: 1.28, Lane 5 & 15: 2.56, Lane 6 & 16: 5.12, Lane 7 & 17: 10.24, Lane 8 and 18: 20.48, Lane 9 & 19: 40.96, Lane 10 & 20: 81.92 mg/L). Gel electrophoresis was employed to visualize the reactions, with Lanes 1-10 showing the reactions involving relaxed DNA, DNA gyrases, and the serial dilutions of quinolones. Lanes 11-20 included these components plus 54 nM of QnrB19. The additional graphs displayed the correlation between supercoiling activity and quinolone concentration, with dotted lines indicating 100% activity. The dose-response curves, in the presence of QnrB19 (dashed lines) and without (solid lines), illustrate the impact of QnrB19 on supercoiling activity.

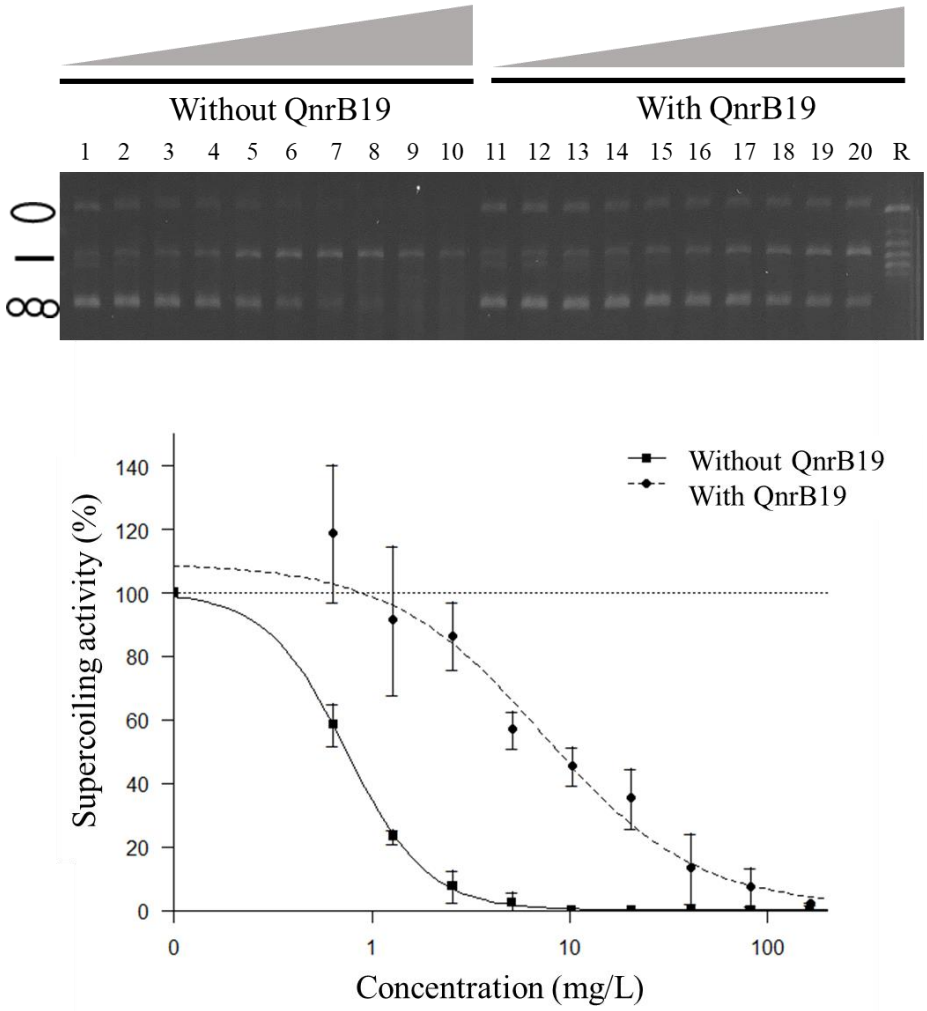

Figure 11. The inhibitory effects of *MOX* against GyrA^{S83F} DNA gyrase in the presence and absence of QnrB19.

The effects of MOX on GyrA^{D87N}, ranging from 0 to 163.84 mg/L (Lane 1 & 11: 0, Lane 2 & 12: 0.64, Lane 3 & 13: 1.28, Lane 4 & 14: 2.56, Lane 5 & 15: 5.12, Lane 6 & 16: 10.24, Lane 7 & 17: 20.48, Lane 8 and 18: 40.96, Lane 9 & 19: 81.92, Lane 10 & 20: 163.84 mg/L). Gel electrophoresis was employed to visualize the reactions, with Lanes 1-10 showing the reactions involving relaxed DNA, DNA gyrases, and the serial dilutions of quinolones. Lanes 11-20 included these components plus 54 nM of QnrB19. The additional graphs displayed the correlation between supercoiling activity and quinolone concentration, with dotted lines indicating 100% activity. The dose-response curves, in the presence of QnrB19 (dashed lines) and without (solid lines), illustrate the impact of QnrB19 on supercoiling activity.

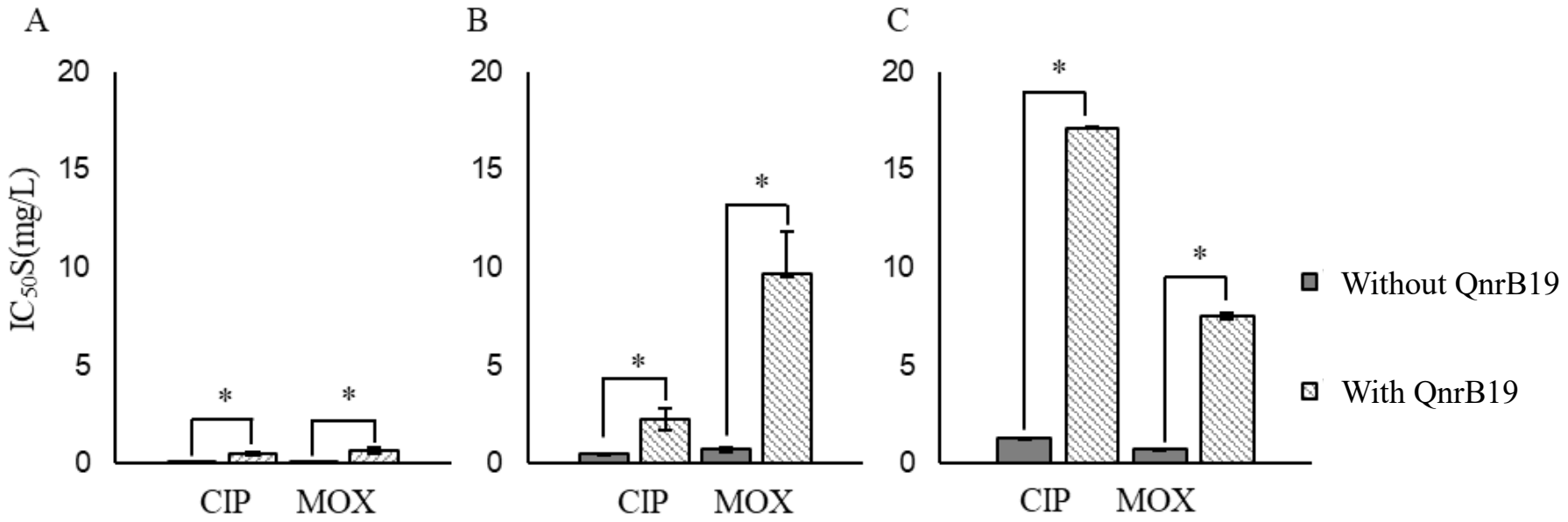

Figure 12. The IC_{50}s of CIP and MOX in the presence and absence of QnrB19.
(A), (B), and (C) show the results for $GyrA^{WT}$, $GyrA^{S83F}$, and $GyrA^{D87N}$, respectively. An asterisk (*) indicates statistical significance at $P<0.05$.

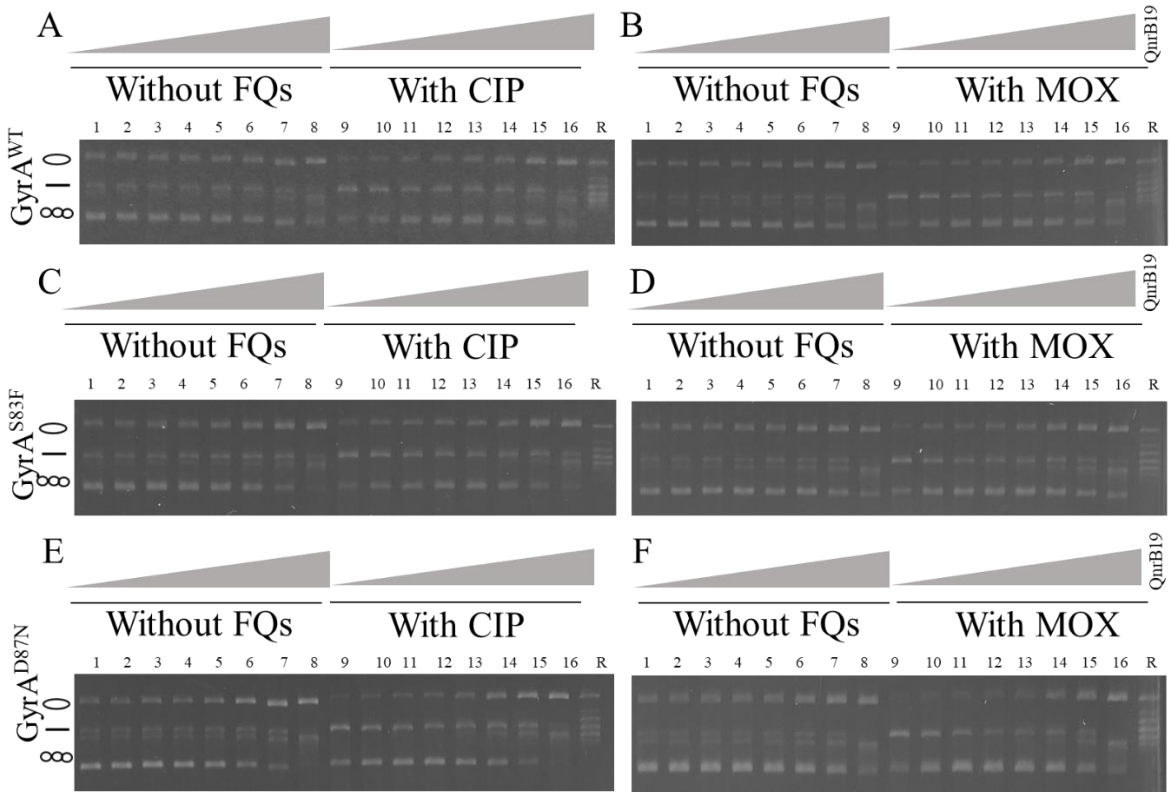

Figure 13. The effects of QnrB19 on supercoiling activity in the absence and presence of quinolones.

(A), and (B) exhibit the results of $GyrA^{WT}$ against IC_{80} of ciprofloxacin hydrochloride (CIP) (0.1 mg/L) and IC_{80} of moxifloxacin hydrochloride (MOX) (0.17 mg/L). (C), and (D) exhibit the results of $GyrA^{S83F}$against $IC_{80}$of CIP (1 mg/L) and IC_{80} of MOX (1 mg/L). (E), and (F) show the results of $GyrA^{D87N}$ against IC_{80} of CIP (3.3 mg/L) and IC_{80} of MOX (1.4 mg/L). Electrophoresis was performed to visualize the effects of QnrB19. Lanes 1-8 show the reactions involving relaxed DNA, DNA gyrases, and serial concentrations of QnrB19 and Lanes 11-20 show reactions involving relaxed DNA, DNA gyrases, quinolones, and serial concentrations of QnrB19 while lane R contains relaxed DNA. The concentrations of QnrB19 for lane 1 & 9, 2 & 10, 3 & 11, 4 & 12, 5 & 13, 6 & 14, 7 & 15, and 8 & 16 were 0, 6, 18, 54, 162, 486, 1458, and 4374 nM, respectively.

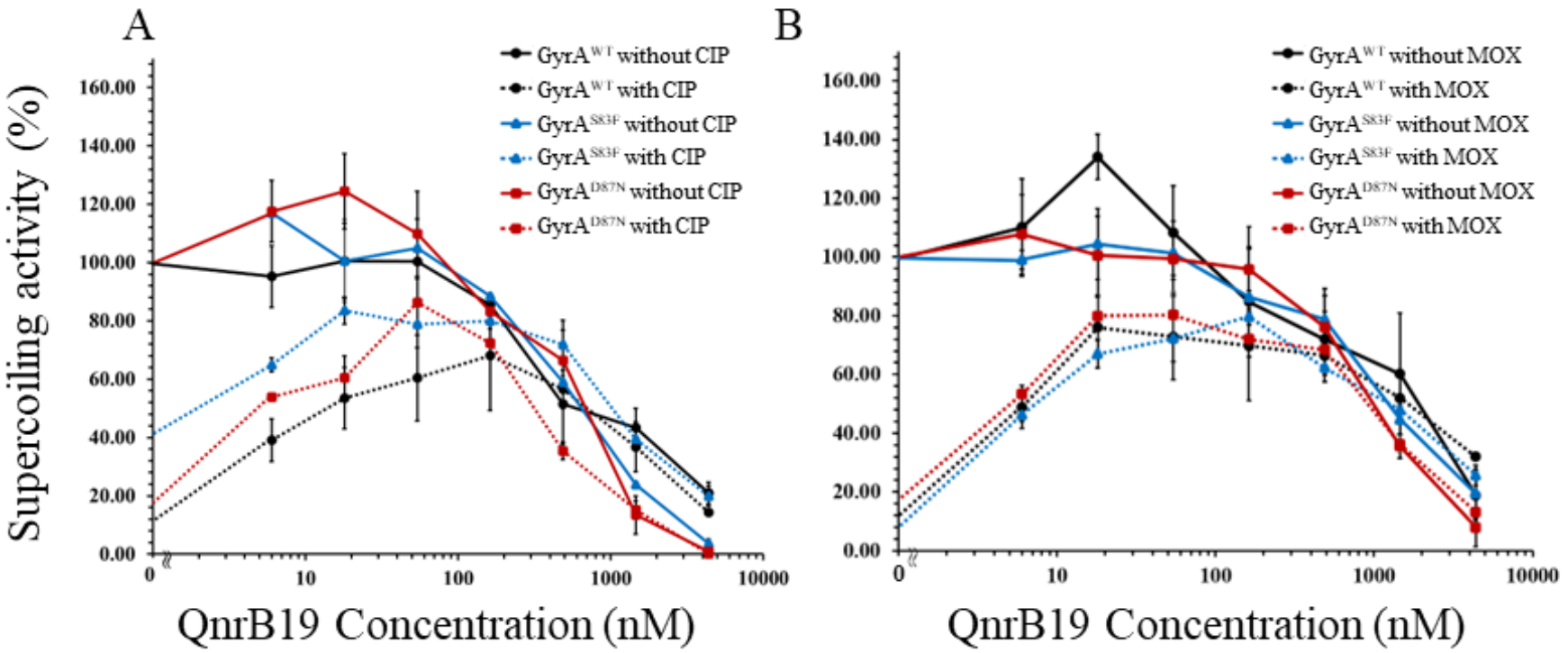

Figure 14. The relationship between supercoiling activity (%) and concentration of QnrB19 (nM)
(A) The relationship between supercoiling activity (%) and concentration of QnrB19 (nM) in the presence of CIP (concentrations equaled to IC_{80}s). (B) The relationship between supercoiling activity (%) and concentration of QnrB19 (nM) in the presence of MOX (concentrations equaled to IC_{80}s).

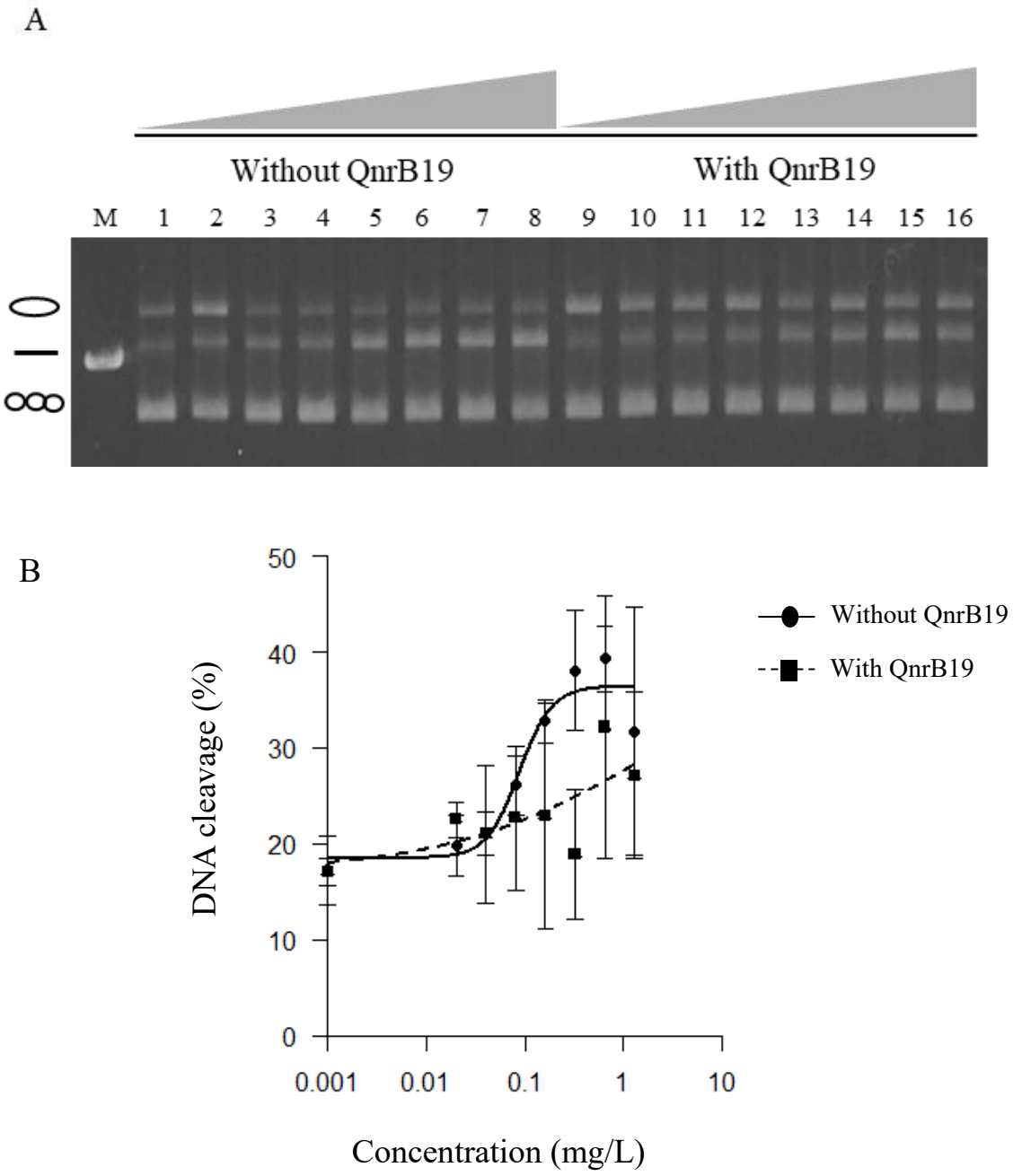

Figure 15. The protective effect of QnrB19 in a quinolone-mediated DNA cleavage assay using $GyrA^{WT}$ against CIP induced cleavage.
(A) Gel electrophoresis of DNA gyrases with $GyrA^{WT}$ exposed to increasing concentrations of CIP ranging from 0 to 1.28 mg/L, comparing conditions without QnrB19 (Lanes 1-8) to those with QnrB19 (Lanes 9-16). (B) Predictive curves, delineating the relationship between CIP concentrations and DNA cleavage levels. Solid line shows the predictive curve of the reaction without QnrB19 and dash line shows the reaction with QnrB19.

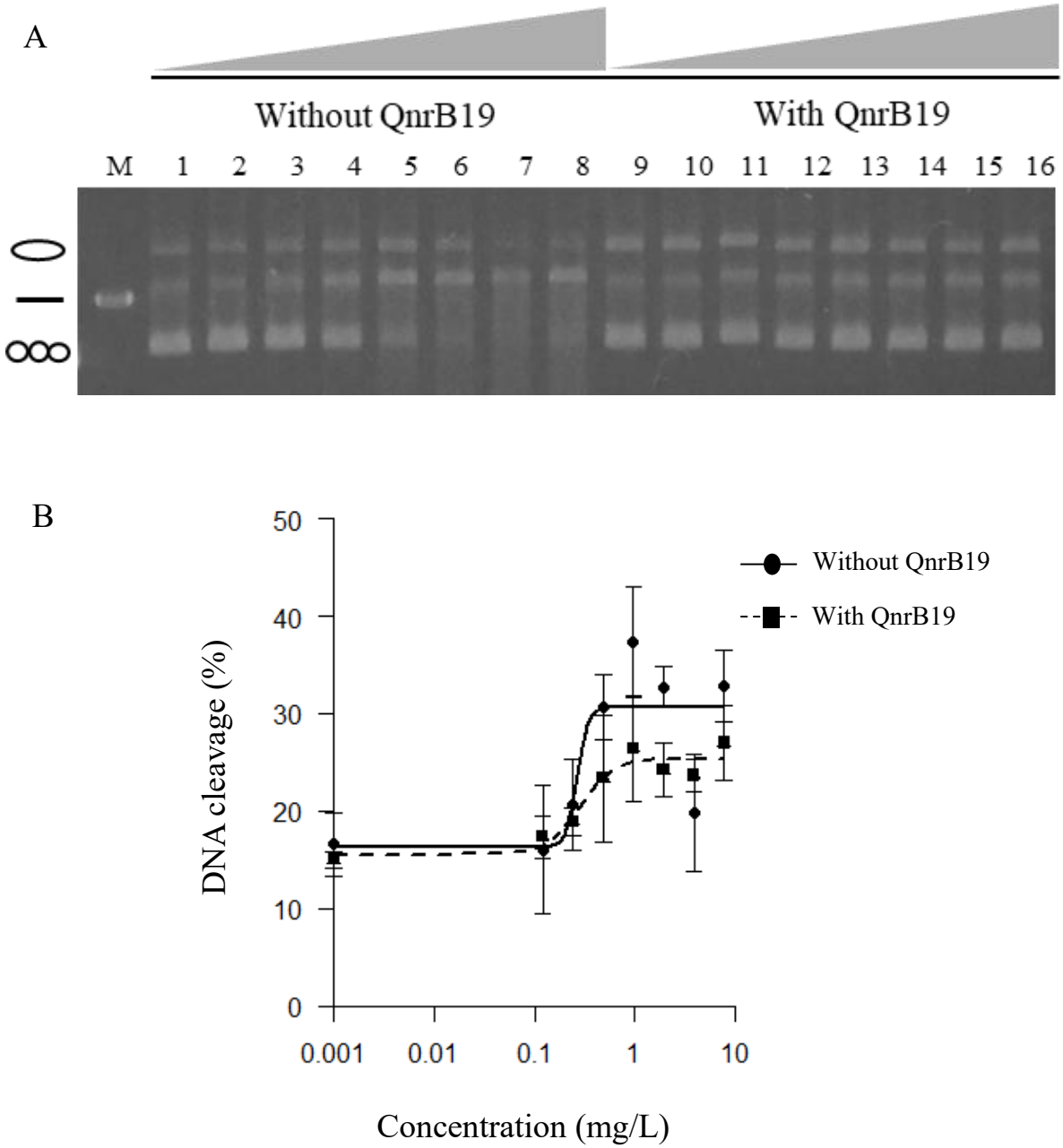

Figure 16. The protective effect of QnrB19 in a quinolone-mediated DNA cleavage assay using GyrA^{S83F} against CIP induced cleavage.
(A) Gel electrophoresis of DNA gyrases with the GyrA^{S83F} mutation exposed to CIP at concentrations ranging from 0 to 7.68 mg/L, comparing assays conducted without QnrB19 (Lanes 1-8) to those with QnrB19 (Lanes 9-16).
(B) The results and a predictive curve from the DNA cleavage assay using DNA gyrases with GyrA^{S83F}, demonstrating the impact of CIP concentration on DNA cleavage. Solid line shows the predictive curve of the reaction without QnrB19 and dash line shows the reaction with QnrB19.

A

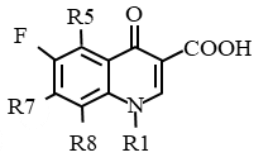

B

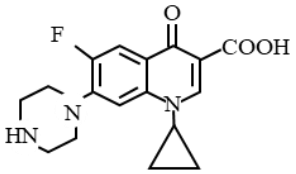

C

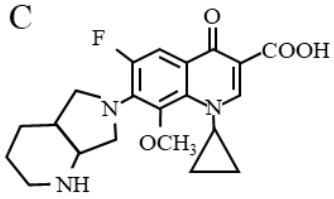

Position	CIP	MOX
R-1	Cyclopropyl	Cyclopropyl
R-6	Fluorine	Fluorine
R-7	Piperazine	Azabicyclic group
R-8	Hydrogen	Methoxy group

Figure 17. Chemical structure of fluoroquinolones
(A) Basic structure, (B) CIP and (C) MOX

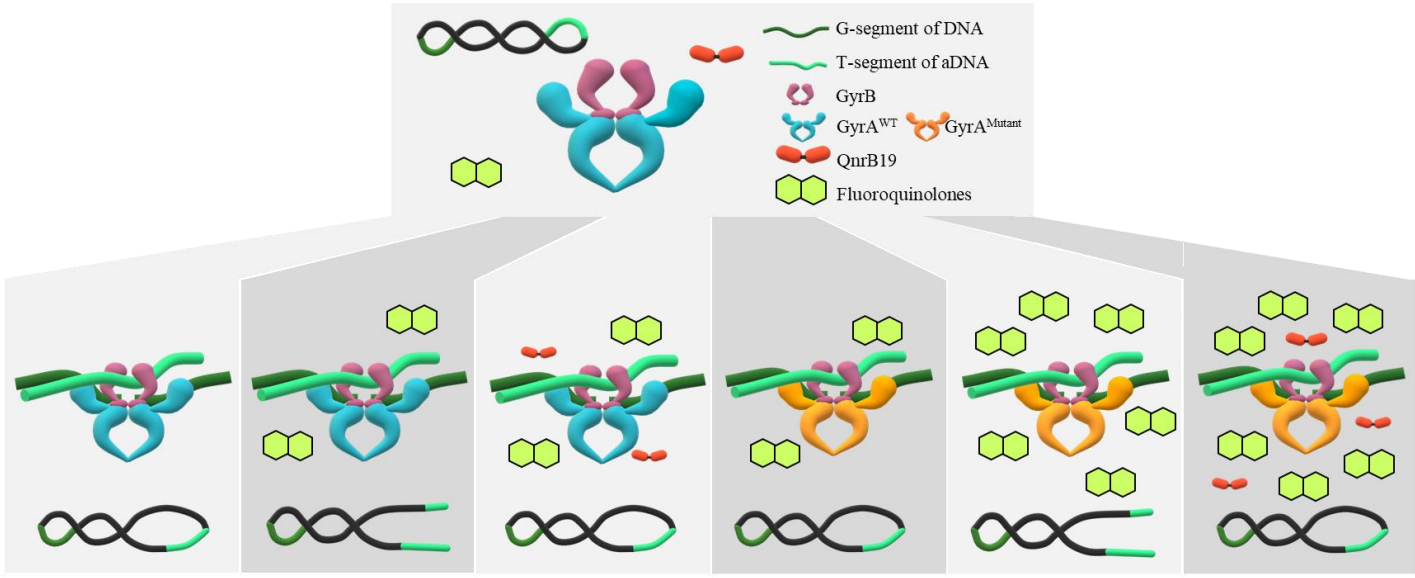

	A	B	C	D	E	F
DNA gyrase	WT	WT	WT	Mutant	Mutant	Mutant
FQs	-	+	+	+	+ (High amount of FQs)	+ (High amount of FQs)
QnrB19	-	-	+	-	-	+
Introduce negative supercoiling	+	-	+	+	-	+
DNA break	-	+	-	-	+	-

Figure 18. The potential interaction of QnrB19 with quinolones.

(A) Depicts the regular functioning of DNA gyrase. (B) Shows the formation of a quinolones-DNA-DNA gyrase complex, leading to DNA damage. (C) Demonstrates QnrB19's ability to safeguard against quinolones. (D) Indicates that a mutant DNA gyrase can operate normally even when quinolones are present. (E) Suggests that high levels of quinolones can cause DNA damage in mutant DNA gyrase. (F) Shows that QnrB19 can protect mutant DNA gyrase under high quinolone concentration.

CHAPTER II

Impact of substitutions at positions 1 and 8 of fluoroquinolones on their activity against mutant DNA gyrase in *Salmonella* Typhimurium

Introduction

WQ-3810, WQ-3334, and WQ-4065 are novel quinolones, belonging to a group known as WQ-compounds. These compounds exhibit unique structural features, particularly at the R-7 position where they all have the 3-isopropylaminoazetizine-1-yl moiety, with further specific modifications occurring at the R1 and R8 positions. Both WQ-3810 and WQ-3334 are modified at R1 with a 6-amino-3,5-difluoropyridine-2-yl group, whereas WQ-4065 is differentiated by its 6-ethylamino-3,5-difluoropyridine-2-yl substitution at the same position. Regarding the R-8 position, WQ-3810 and WQ-4065 incorporate a methyl group, in contrast to WQ-3334, which features a bromine atom. The aim of this study was to assess the antibacterial effectiveness of these novel quinolones against WT and CIP-resistant strains of *Salmonella* DNA gyrase, which is the drug's target. These studies compared the efficacy of WQ-3810, WQ-3334, and WQ-4065 to CIP, the current standard treatment for Salmonellosis.

Materials and Methods

Reagents

The WQ-compounds, WQ-3810, WQ-3334, and WQ-4065 were supplied by Wakunaga Pharmaceutical Co., Ltd., Tokyo, Japan. Enrofloxacin (ENR) was purchased from LKT Laboratories, Inc., Minnesota, United State. The *Salmonella* strains, including *S.* Typhimurium NBRC 13245 and *S.* Enteritidis NBRC 3313, were purchased from the National Institute of Technology and Evaluation in Tokyo, Japan.

Expression and purification of recombinant *S.* Typhimurium DNA gyrase subunits

Recombinant DNA gyrases with various amino acid substitutions on DNA gyrase A subunit including $GyrA^{WT}$, $GyrA^{S83I}$, $GyrA^{S83F}$, $GyrA^{S83Y}$, $GyrA^{D87G}$, $GyrA^{D87N}$, $GyrA^{D87Y}$ and $GyrA^{S83FD87N}$ and one subunit of $GyrB^{WT}$ were expressed, and purified as in chapter I.

Inhibition of *S.* Typhimurium DNA gyrase by quinolones

To investigate the inhibitory effects of the examined compounds on the supercoiling activity of recombinant *S.* Typhimurium DNA gyrase, *in vitro* assays were conducted as described in previous studies [44]. These assays focused on various GyrA mutations, including $GyrA^{WT}$, $GyrA^{S83I}$, $GyrA^{S83F}$, $GyrA^{S83Y}$, $GyrA^{D87G}$, $GyrA^{D87N}$, $GyrA^{D87Y}$ and the double mutant $GyrA^{S83FD87N}$. The assay buffer was prepared with buffer containing 35 mM Tris-HCl (pH 7.5), 24 mM KCl, 4 mM $MgCl_2$, 2 mM DTT, 1.8 mM spermidine, 6.5% glycerol, and 0.1 mg/mL of bovine serum albumin (BSA). To make the reaction mixture, 1 mM ATP, 1.5 nM of the relaxed plasmid pBR322, 18 nM of DNA gyrase subunits, and quinolones including WQ-3810, WQ-3334, WQ-4065 and CIP at various concentrations of quinolones were mixed, resulting in a total of 30 mL of reaction mixture. The reactions were incubated at 37°C for 60 minutes, then terminated with 8 mL of a 5× dye mix (5% SDS, 25% glycerol, and 0.25 mg/mL of bromophenol blue).

Samples of 10 µL from each reaction were subjected to electrophoresis on a 1% agarose gel using 1× TAE buffer for 60 minutes at 50 mA. The gels were stained with ethidium bromide (0.5 mg/mL) to visualize the DNA bands under UV light. The intensity of these bands, indicative of the DNA's supercoiling activity, was quantified using ImageJ software (http://rsbweb.nih.gov/ij). The IC_{50} of the compounds were determined by analyzing the intensity of the supercoiled bands, using an online calculator provided by AAT Bioquest (https://www.aatbio.com/tools/ic50-calculator).

Induction of quinolone resistance in *S.* Typhimurium

To isolate strains with quinolone resistance, *S.* Typhimurium NBRC 13245 was cultured on MH agar using a modified method from a previous study [64]. Firstly, The MICs were measured via the agar dilution method [64]. Aliquots of 200 µL of the inoculum (OD

590 nm = 1) were spread on the MH agar plates supplemented with increasing concentration of CIP (0.01, 0.02, 0.04, 0.08, 0.16, 0.32, 0.64, 1.28, 2.56 and 5.12 mg/L) or ENR (0.01, 0.02, 0.04, 0.08, 0.16, 0.32, 0.64, 1.28, 2.56 and 5.12 mg/L). The plates were incubated at 37ºC overnight and the MICs were determined. Colonies that grew at sub-MIC concentrations were randomly selected and cultured in MH broth at 37°C until reaching an OD 590 of 1. Aliquots of 200 µL were then spread on MH agar supplemented with CIP or ENR at concentrations of 1x, 2x, and 4x the MIC. The growth of colonies was monitored at 18, 24, 32, 48, and 72 hours, and those exhibiting growth were selected for mutation confirmation.

Confirmation of nucleotide sequence alterations

Nucleotide substitutions within the QRDR of the *gyrA* and *parC* were analyzed by PCR and sequencing. The sequences of the forward and reverse primers are shown in Table 5. PCR amplification conditions were as follows: pre-denaturation at 95°C for 1 minute, followed by 30 cycles of denaturation at 95°C for 10 seconds, asnnealing at 47°C for 10 seconds, and extension at 72°C for 30 seconds, with a final extension at 72°C for 5 minutes. The nucleotide sequences of the PCR products were determined using the BigDye Terminator Cycle Sequencing Kit version 3.1 and an ABI Prism 3130xl Gene Analyzer (Thermo Fisher Scientific Inc.). Mutations within the QRDR associated with quinolone resistance were identified by comparing the obtained sequences with the reference genome of *S.* Typhimurium (RefSeq: NC_003197) using MEGA X (https://www.megasoftware.net/).

Antimicrobial susceptibility testing

To determine the MIC of quinolones for *S.* Typhimurium NBRC 13245, *S.* Enteritidis NBRC 3313, and mutant *S*. Typhimurium strains carrying $GyrA^{S83F}$ and $GyrA^{D87Y}$ mutations, microbroth dilution method were employed, aligning with the Clinical and Laboratory Standards Institute (CLSI) guidelines [64,65]. Briefly, the frozen stocks were streaked onto sterile LB agar plates. Subsequently, these colonies were transferred into sterile MHB and incubated until an optical density of 0.5 was reached. The bacterial inoculum was added to a 96-well plate, with each well containing varying concentrations of the quinolones being tested—specifically WQ-3810, WQ-3334, WQ-4065, and CIP and was incubated at 37°C for 18 hours. To ensure accuracy, MICs were measured in duplicate for each bacterial strain.

Statistical Analysis

The statistical analysis of data was conducted with the R software, version 4.1.3, complemented by the "agricolae" package, version 1.3-5 [66]. To compare the efficacy of different compounds, we utilized a one-way analysis of variance (ANOVA). The least significant difference (LSD) test was used to discern which compound groups exhibited

statistically significant differences in their means, adopting a significance threshold of $p < 0.05$.

Results

Expression and purification of recombinant *S.* Typhimurium DNA gyrase

The recombinant DNA gyrases, GyrA and GyrB, of *S.* Typhimurium were successfully expressed and purified with a high level of purity, over 95%. The molecular weights for GyrA were approximately 97 kDa and GyrB was approximately 89 kDa as shown in Figure 19.

Influence of amino acid substitution on DNA gyrase activity of *S.* Typhimurium in response to quinolone

The DNA supercoiling assay results are illustrated by gel electrophoresis in Figure 20 and 21, and drug dose–response curves of all compounds against *S.* Typhimurium DNA gyrases were constructed to reveal the inhibitory activities of quinolones and are given in Figure 22 to 25. In addition, ANOVA calculation was performed followed by LSD multiple range test ($p< 0.05$; Table 6). The calculated IC_{50} demonstrated that there were no significant differences betweenWQ-3810, WQ-3334, CIP, and the WT DNA gyrase; on the contrary, WQ-4065 had significantly higher IC_{50} among the tested quinolones. CIP had higher IC_{50} than WQ-3810 andWQ-3334 against six mutant DNA gyrases, particularly against the D87Y mutant where the IC_{50} of CIP were 20 and 15-fold higher than WQ-3810 and WQ-3334, respectively. WQ-3810 displayed the highest antimicrobial activity, and its activity was higher than other examined quinolones against $GyrA^{S83I}$, and $GyrA^{D87N}$ mutant DNA gyrases.

WQ-4065 showed the lowest antimicrobial activity against DNA gyrases with most mutants, but it exhibited more potent inhibitory activity than CIP against DNA gyrases carrying $GyrA^{D87G}$ and $GyrA^{S83FD87N}$ DNA gyrase. All quinolones had higher IC_{50} against double-mutant than single-mutant DNA gyrases, and the IC_{50} of CIP against double-mutant DNA gyrase was 7,000- fold higher than that against WT DNA gyrase. Although WQ-3810 had the lowest IC_{50} against WT and single amino acid substitutions of DNA gyrases, WQ-3334 demonstrated the most potent inhibitory activity against the double-mutant DNA gyrase in comparison with the other quinolones.

Mutant *S.* Typhimurium strains

MIC results for CIP and ENR against *S.* Typhimurium were 0.04 and 0.08 mg/mL, respectively. These concentrations were subsequently used to induce mutant *S.* Typhimurium strains. Colonies obtained from this induction process were verified by sequencing their

nucleotide sequences in the QRDR of *gyrA* and *parC*. Four mutant strains of *S*. Typhimurium were successfully identified, as detailed in Table 7.

MICs for *S.* Typhimurium and *S.* Enteritidis

The results of antimicrobial susceptibility testing against NTS are detailed in Table 8. A similarity in MICs for both *S*. Typhimurium and *S*. Enteritidis was observed across all drugs. The MIC of CIP was the lowest (0.002 mg/mL), followed by WQ-3810, WQ-3334, and WQ-4065. On the contrary, MICs for mutant *S*. Typhimurium were increasing except MIC of WQ-3810 against *S*. Typhimurium carrying $GyrA^{D87Y}$.

Discussion

This is the first analysis of the impact of substitutions at R1 by difluoropyridine derivatives and R8 by methyl or bromine in quinolones as shown in Figure 26 on antimicrobial activities against mutant DNA gyrases of *S.* Typhimurium. Previous studies proposed the antibacterial activity of WQ-3810 against MDR and quinolones resistance. In clinical isolates, WQ-3810 had remarkable activity even against *A. baumannii*, *E. coli*, *S. pneumoniae*, Methicillin-resistant *S. aureus*, and *N. gonorrhoeae*. The MICs indicated that WQ-3810 could exert potent antibacterial activity against quinolones-resistant bacteria [67]. In the DNA supercoiling assay, WQ-3810 exhibited 4- to 9-fold greater potency than CIP and LEV in *E. coli* DNA gyrase with amino acid substitutions including S83L and D87N in the QRDR of GyrA.[67] In addition, WQ-3334 and WQ-4065 modified from WQ-3810 were compared with their inhibitory effects with WQ-3810 against *M. leprae* and *S*. Typhimurium DNA gyrase in our previous study, and the result showed that WQ-3810 and WQ-3334 had higher antimicrobial activities than WQ-4065 [44,68].

Quinolones could bind to DNA- DNA gyrase complex and directly block DNA replication result in chromosome fragmentation and bacterial cell death [32,33]. This study exhibited the substantial antimicrobial activities of WQ-3810 and WQ-3334 against WT DNA gyrase depending on the substituents in the chemical structure at R1 may contribute to the high affinity for DNA gyrases. The model of quinolones binding pocket in DNA gyrases shows that a change of substituent at R1 confers a different binding affinity to DNA gyrases [69]. The R1 of quinolones can form hydrophobic interaction with drug-receptors, additionally, the substituent at R1 position could specifically interacts with residues in major groove of DNA [70]. CIP, which has a cyclopropyl substituent at R1, exhibits a high potent modification, and has been used as a therapeutic agent of choice against salmonellosis [69,70]. In contrast, a larger substituent at the R1 position in WQ-3180 and WQ-3334 may increase the possibility of letting quinolones get closer to the complex. The unique

structures of these compounds were speculated that the distorted arrangement between R1 and R8 could enhance the antibacterial activity due to steric hindrance against this enzyme [67,71]. Consequently, WQ-3810 and WQ-3334 showed higher effectiveness against WT DNA gyrases than other Quinolones examined in this study. Although, R8 of WQ-3810 and WQ-3334 has methyl group and bromine, respectively, the similar antimicrobial activities were shown against WT DNA gyrase. The findings have revealed that the difference in R-8, including methyl group and bromine in these compounds, may not enhance their antibacterial properties against WT DNA gyrase.

WQ-3810, WQ-3334, and CIP showed high antimicrobial activities against six single amino acid substitution mutant DNA gyrases; particularly, IC_{50}s of WQ-3810 showed the highest antimicrobial activities against six single amino acid substitution mutant DNA gyrase, followed by WQ-3334. In the aspect of mutation in DNA gyrases, the amino acid substitutions in DNA gyrases cause the conformation change of QRDR, resulting in reducing the affinity between quinolones and DNA gyrase [50,69,72]. The study regarding quinolones interactions with gyrase of *E. coli,* which shares 100% similarity in QRDR and 91% identity with whole GyrA of *S.* Typhimurium, suggested that substitutions of Ser83 to Ile and Phe attribute to the loss of the hydroxyl group and result in reducing the Quinolones ability to interact with quinolone binding pocket [73]. Substitution of Ser83 to Tyr may cause interaction of DNA gyrase with quinolones by creating the hydrogen bond, however tyrosine is larger than serine; consequently, quinolones may not be able to enter the pocket and lead to quinolones resistance. Besides, substitutions of Asp87 by Gly, Asn, and Tyr could alter the interaction with the carboxyl group of quinolones, and prevent forming a stabilizing magnesium-water bridge with GyrA which is important for facilitating interaction between quinolones and GyrA at codon 83 and 87 [54]. Taken together, higher concentrations of quinolones are required to inhibit the supercoiling activity of mutant DNA gyrases. The finding emphasized the importance of R1 modification among the novel quinolones since the high bulkiness of the substitution exhibits higher inhibitory activity [50]. This can be referred that the substituent at R1 of WQ-3180 and WQ-3334 could increase the binding affinity to mutant DNA gyrases. Additionally, previous study showed that the distortion of chemical structures led by substitution of the aromatic group at R1 and halogen atom or methyl group at R8, and this strained conformation could be a key factor for the potent antibacterial activity of quinolones [74]. WQ-3810 and WQ-3334 may also have distorted orientation that contribute to the high antimicrobial activity. Although no significant difference was observed between WQ-3810 and WQ-3334 against WT DNA gyrase, WQ-3810 exerted an excellent antimicrobial activity against single amino acid substitution mutant DNA gyrases.

Interestingly in double amino acid substitution, the IC_{50}s of WQ-3810, WQ-3334, WQ-4065, and CIP were 114-, 53-, 110-, and 7,213-fold higher than WT DNA gyrase, respectively. The DNA gyrase with double amino acid mutations could affect the complex's interaction and lead to high quinolones resistance. WQ-3810 gives potent antibacterial activity against WT and single amino acid mutant DNA gyrases; however, WQ-3334 exhibits a more potent inhibitory activity against DNA gyrase's double amino acid substitution. It is thought that the GyrB also has a role in the interaction with Quinolones, particularly at TOPRIM region by stabilizing the DNA in the distorted form while forming the complex and bounding to the quinolone-binding site [71,72]. Recent study found that NH_2 molecule of the R1 group in WQ-3810 and WQ-3334 can interact with GyrB of *M. leprae* in the *in-silico* study and increase the antimicrobial activity [75]. We predicted that the similar mechanism might occur since these compounds maintain their high potency even in the double mutation of DNA gyrase. Accordingly, WQ-3810 and WQ-3334 showed the high inhibitory activities even against DNA gyrase with double amino acid substitution. In addition, the modification of R8 by bromine in WQ-3334 seemed to contribute to the better effect on the double mutation shown as lower IC_{50}. Previous findings regarding the molecular structure of fluoroquinolone also indicated the relationship of structure variation at R1 and R8 of sitafloxacin (SIT) against *S.* Typhimurium DNA gyrases. According to the halogen atom at R8 of SIT, this drug revealed a substantial effect on double amino acid substitution of GyrA among Quinolones [46]. Thus, this can strengthen that the halogen atom substitution at the R8 show an essential role against the double amino acid substitution of GyrA. As a result, WQ-3334 revealed lower IC_{50}s in the experiment of double amino acid substitutions mutant DNA gyrase than WQ-3810.

According to the results of IC_{50}s against mutant DNA gyrase of *S.* Typhimurium, WQ-3810 and WQ-3334 are likely to possess stronger inhibitory activities than the drugs utilized in the current study. However, to produce the high antimicrobial property, Quinolones are required to enter and be accumulated inside the bacterial cell, leading to bacterial death [76]. Therefore, MIC test against *S.* Typhimurium and *S.* Enteritidis with WT DNA gyrase were performed to determine the effectiveness of the drugs. The results indicated that the MIC of CIP was lower than WQ-compounds in both WT *S.* Typhimurium and *S.* Enteritidis because of its high permeability; consequently, CIP can easily enter the bacterial cell and cause intracellular accumulation [50]. Due to the limitation of this study, the MIC values of *Salmonella* mutant DNA gyrases could not be examined. However, the previous study suggested the correlation between the antibacterial activity (MICs) and IC_{50}s of quinolones against *S.* Typhimurium could be used as a screen test to examine novel drugs with promising antibacterial activities [46]. The IC_{50}/MIC ratios for WQ-3810, WQ-3334,

WQ-4065, and CIP in this study were 0.55, 0.38, 0.14, and 3.65, respectively. It is interesting to note that although the ratio of CIP compounds was higher than 1, the ratios of WQ compounds were lower than 1 which can be interpreted that CIP had the higher inhibitory activities against live bacteria than *in vitro* experiments. Accordingly, CIP may have a greater ability to enter and/or accumulate inside the bacterial cell than WQ compounds which means that WQ compounds were inferior in these points. If we consider that WQ-compounds and CIP have similar permeability and/or drug efflux transporter liability, the predicted MICs against mutant *Salmonella* would be lower than CIP, particularly those with strong resistant properties with S83I, and S83FD87N amino acid substitution in GyrA. For example, while more than 1,900 mg/L of CIP speculated to be required for inhibiting the visible growth of *S.* Typhimurium and *S*. Enteritidis with double amino acid substitution in DNA gyrase, only 13.32 and 9.11 mg/L of WQ-3810 and WQ-3334 may be needed. Therefore, further modifications or combination therapy to improve drug accommodation need to be assessed for WQ-3810 and WQ-3334 as effective drugs of quinolones-resistant NTS.

Conclusion

This investigation has revealed that the presence of a 6-amino-3,5-difluoropyridine-2-yl group at the R1 position, along with either a methyl group or bromine at the R8 position, significantly enhances the inhibitory activity of WQ-3810 and WQ-3334 against both WT and mutant forms of DNA gyrase in *S.* Typhimurium, as elucidated through *in vitro* studies. According to these findings, it is proposed that WQ-3810 and WQ-3334 represent promising new quinolones for the treatment of infections caused by quinolones-resistant *Salmonella* species. Further investigations into potential modifications of these compounds, as well as their use in combination with other therapies, are needed to maximize their clinical efficacy.

Table 5. Oligonucleotide sequences of primers used in this study

Primer name	Sequence
Sal-gyrA QRDR Fw	5' – GTTAGATGAGCGACCTTGCG -3'
Sal- gyrA QRDR Rv	5' - GGAATTTTGGTCGGCATGAC -3'
Sal -parC QRDR Fw	5' - CCCTGTTAATGAGCGATATG -3'
Sal -parC QRDR Rv	5' - GCCGTTCAGCAGGATGTTCG -3'

Table 6. IC_{50}s of quinolones including WQ-3810, WQ-3334, WQ-4065, and CIP against WT and mutant *Salmonella* DNA gyrases.

DNA gyrase		IC_{50}s of compounds (mg/L)[a]			
GyrA	**GyrB**	**WQ-3810**	**WQ-3334**	**WQ-4065**	**CIP**
WT[b]	WT[b]	0.033±0.006[#]	0.047±0.007[#]	0.541±0.050*	0.073±0.008[#]
Ser83Ile[c]	WT[b]	1.158±0.129[$]	2.364±0.190[#, $]	39.10±3.860*	5.484±0.182[#]
Ser83Phe[c]	WT[b]	0.052±0.008[$]	0.063±0.010[$]	0.782±0.076*	0.457±0.106[#]
Ser83Tyr[c]	WT[b]	0.414±0.048[#]	0.845±0.130[#]	17.57±1.360*	1.219±0.012[#]
Asp87Gly[c]	WT[b]	0.032±0.001[$]	0.091±0.017[$]	0.464±0.026[#]	0.631±0.065*
Asp87Asn[c]	WT[b]	0.593±0.070[$]	0.649±0.040[#, $]	13.52±1.100*	1.673±0.146[#]
Asp87Tyr[c]	WT[b]	0.033±0.003[#]	0.043±0.003[#]	0.801±0.029*	0.668±0.139*
Ser83Phe-Asp87Asn[c]	WT[b]	3.649±0.270[$]	2.496±0.280[$]	59.71±4.340[*]	523.0±93.000[#]

[a]IC_{50}s, drug concentration required to inhibit the supercoiled activity of DNA gyrase by 50%

[b]WT, Wild-Type

[c]Amino acid substitution

[*, #, $] Significantly different by LSD multiple range test (*p-value* < 0.05)

Table 7. The list of mutant *S*. Typhimurium strains.

No.	Drug inductions	Concentration	DNA gyrase (GyrA)	Topoisomerase IV (ParC)
1.	CIP	1x MIC	Ser83Phe	WT
2.	ENR	1x MIC	Gly81Cys	WT
3.	ENR	2x MIC	Asp87Tyr	WT

Table 8. MICs for *S.* Typhimurium and *S.* Enteritidis

	MIC (mg/L)[a]			
Quinolones	***S.* Typhimurium**			***S.* Enteritidis**
	WT	**Ser83Phe**	**Asp87Tyr**	
WQ-3810	0.060	0.250	0.060	0.060
WQ-3334	0.125	0.250	0.125	0.125
WQ-4065	4.000	4.000	2.000	4.000
CIP	0.020	0.250	0.125	0.020

[a] MIC, Minimum Inhibitory Concentration

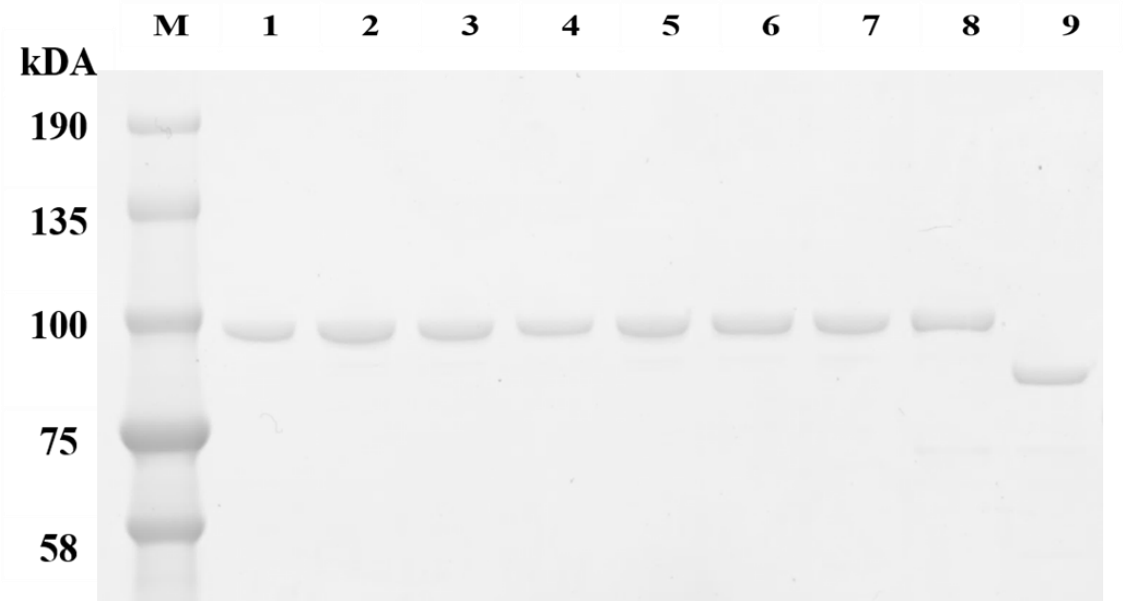

Figure 19. SDS-PAGE analysis of purified GyrA and GyrB.
Recombinant *S.* Typhimurium DNA gyrases including $GyrA^{WT}$, $GyrA^{S83I}$, $GyrA^{S83F}$, $GyrA^{S83Y}$, $GyrA^{D87G}$, $GyrA^{D87N}$, $GyrA^{D87Y}$ and the double mutant $GyrA^{S83FD87N}$ and $GyrB^{WT}$ were illustrated by SDS-PAGE. The protein samples (500 ng) added onto 5–20% gradient polyacrylamide gel. Lane M showed protein size marker, and lanes 1–9 exhibited $GyrA^{WT}$, $GyrA^{S83I}$, $GyrA^{S83F}$, $GyrA^{S83Y}$, $GyrA^{D87G}$, $GyrA^{D87N}$, $GyrA^{D87Y}$ and the double mutant $GyrA^{S83FD87N}$ and $GyrB^{WT}$, respectively.

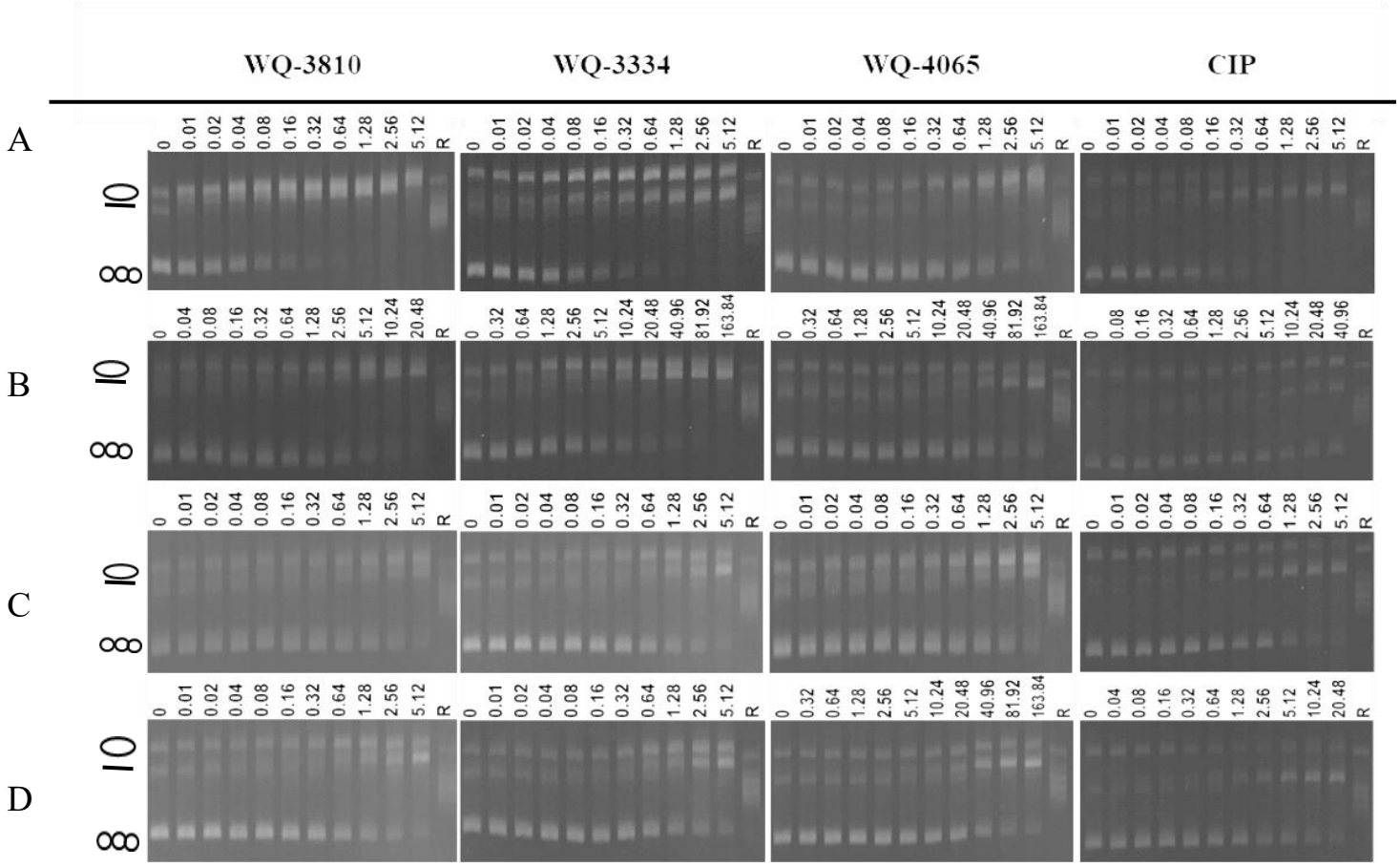

Figure 20. Inhibitory activity of WQ-3810, WQ-3334, WQ-4065 and CIP on the supercoiling activities of *S.* Typhimurium DNA gyrase.

The topologies of the DNA were indicated in front of the gel. and the concentrations of the examined drug are presented on each lane. (A) $GyrA^{WT}$, (B) $GyrA^{S83I}$, (C) $GyrA^{S83F}$ and (D) $GyrA^{S83Y}$.

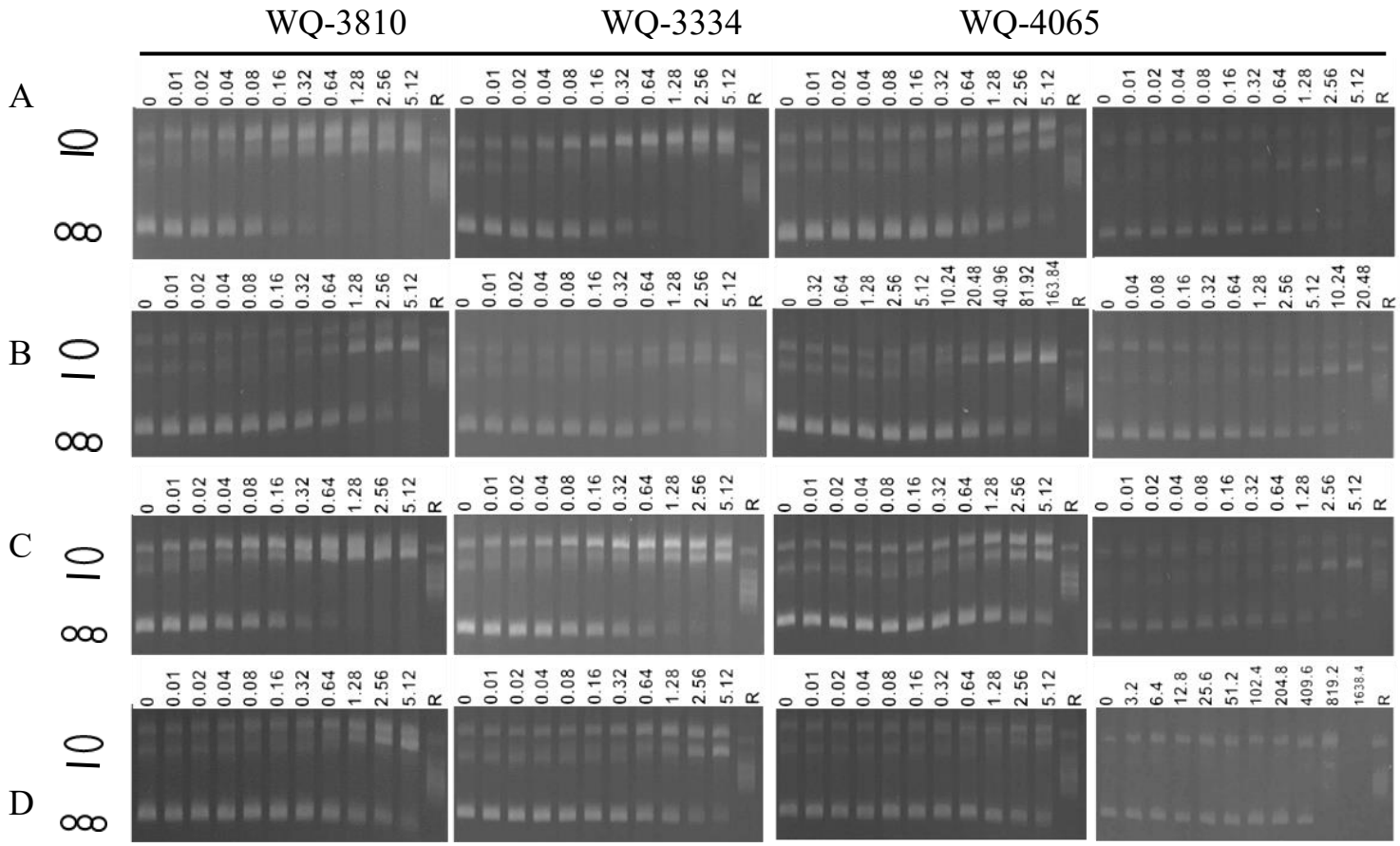

Figure 21. Inhibitory activity of WQ-3810, WQ-3334, WQ-4065 and CIP on the supercoiling activities of *S.* Typhimurium DNA gyrase.

The topologies of the DNA were indicated in front of the gel. and the concentrations of the examined drug are presented on each lane. (A) $GyrA^{D87G}$, (B) $GyrA^{D87N}$, (C) $GyrA^{D87Y}$ and (D) the double mutant $GyrA^{S83FD87N}$.

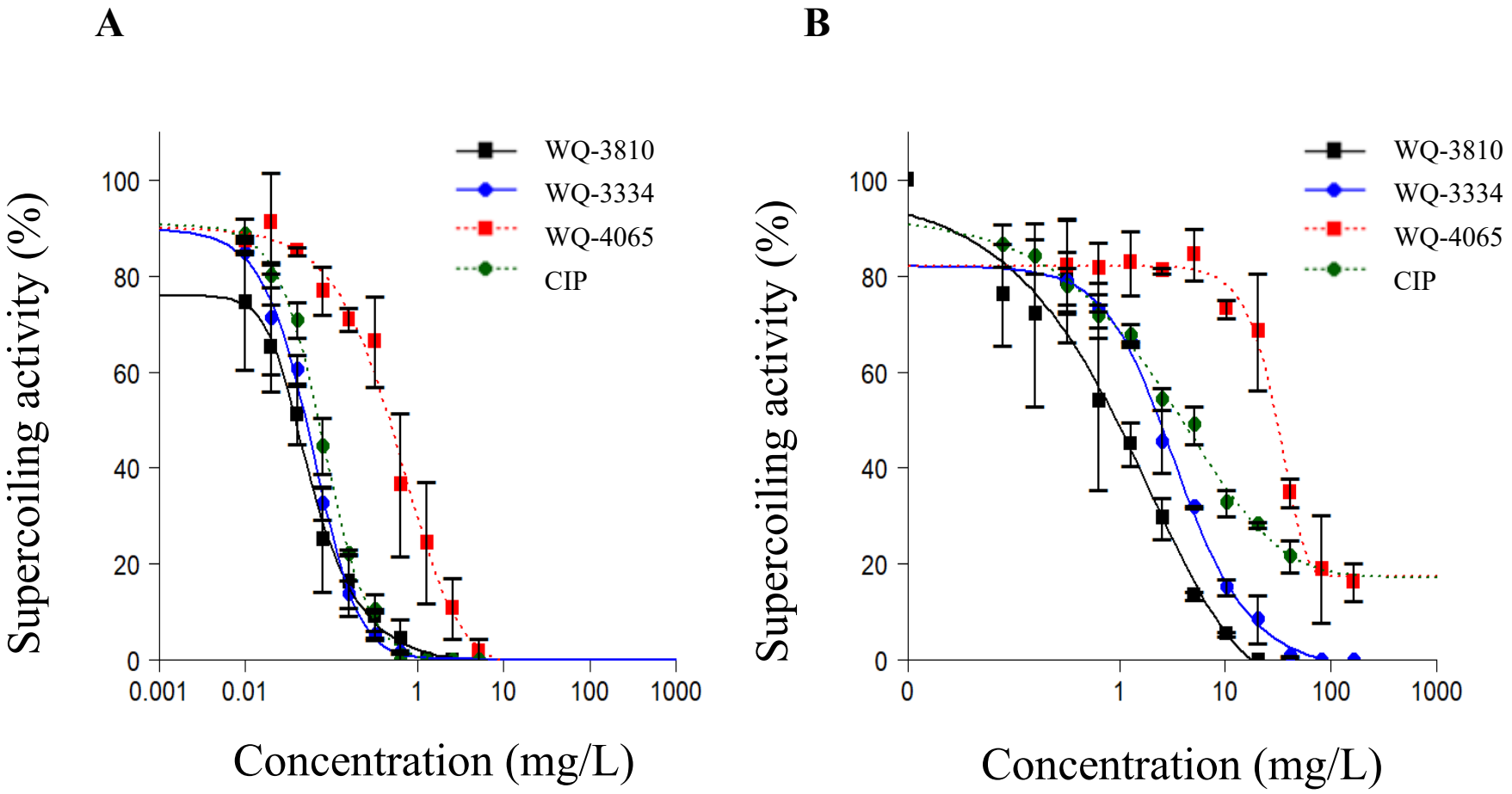

Figure 22. DNA gyrase supercoiling activities against WQ compounds including WQ-3810, WQ-3334, WQ-4065 and CIP. The inhibitory activity of the examined drugs against (A) $GyrA^{WT}$ and (B) $GyrA^{S83I}$.

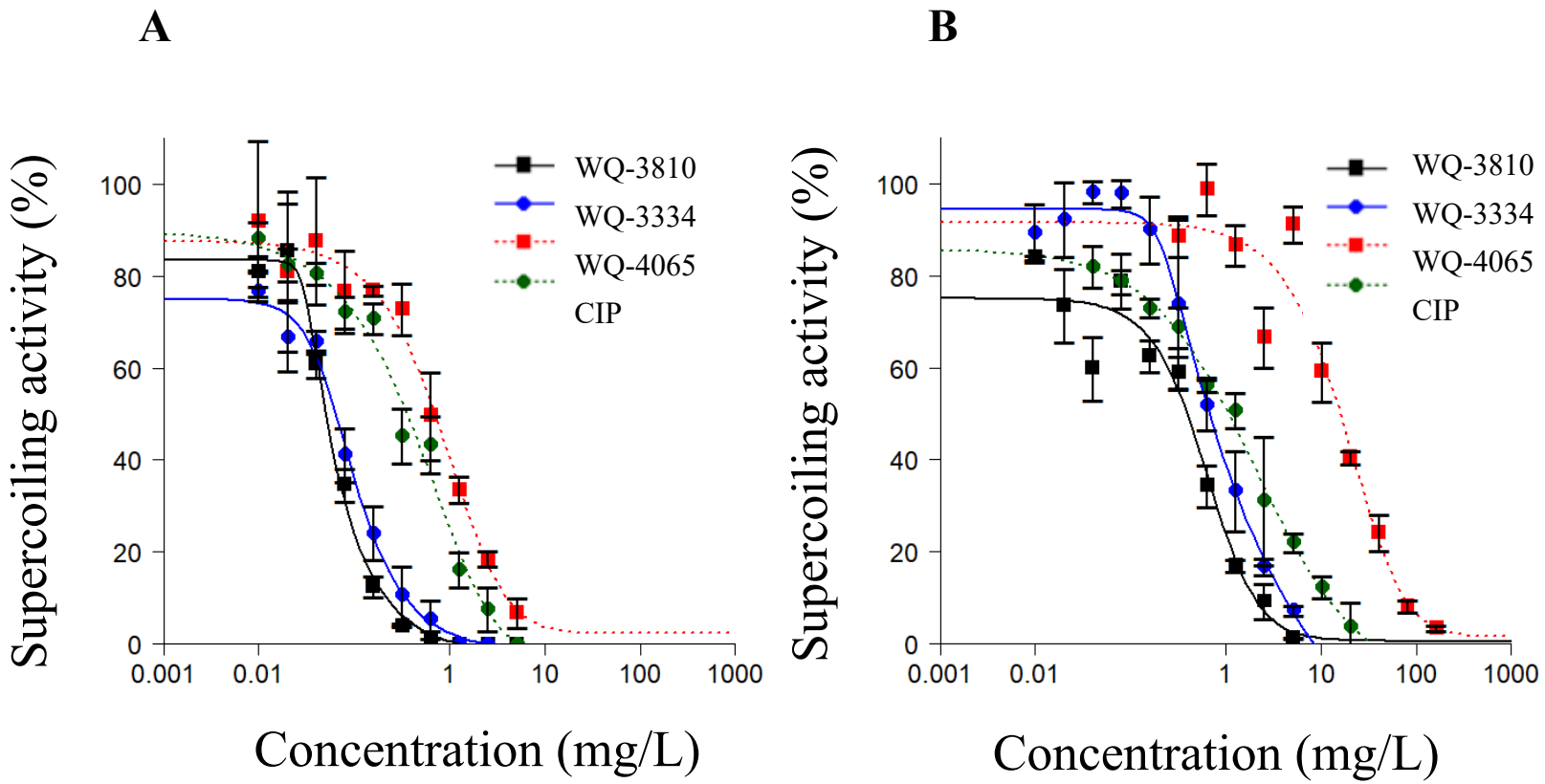

Figure 23. DNA gyrase supercoiling activities against WQ compounds including WQ-3810, WQ-3334, WQ-4065 and CIP. The inhibitory activity of the examined drugs against (A) $GyrA^{S83F}$ and (B) $GyrA^{S83Y}$.

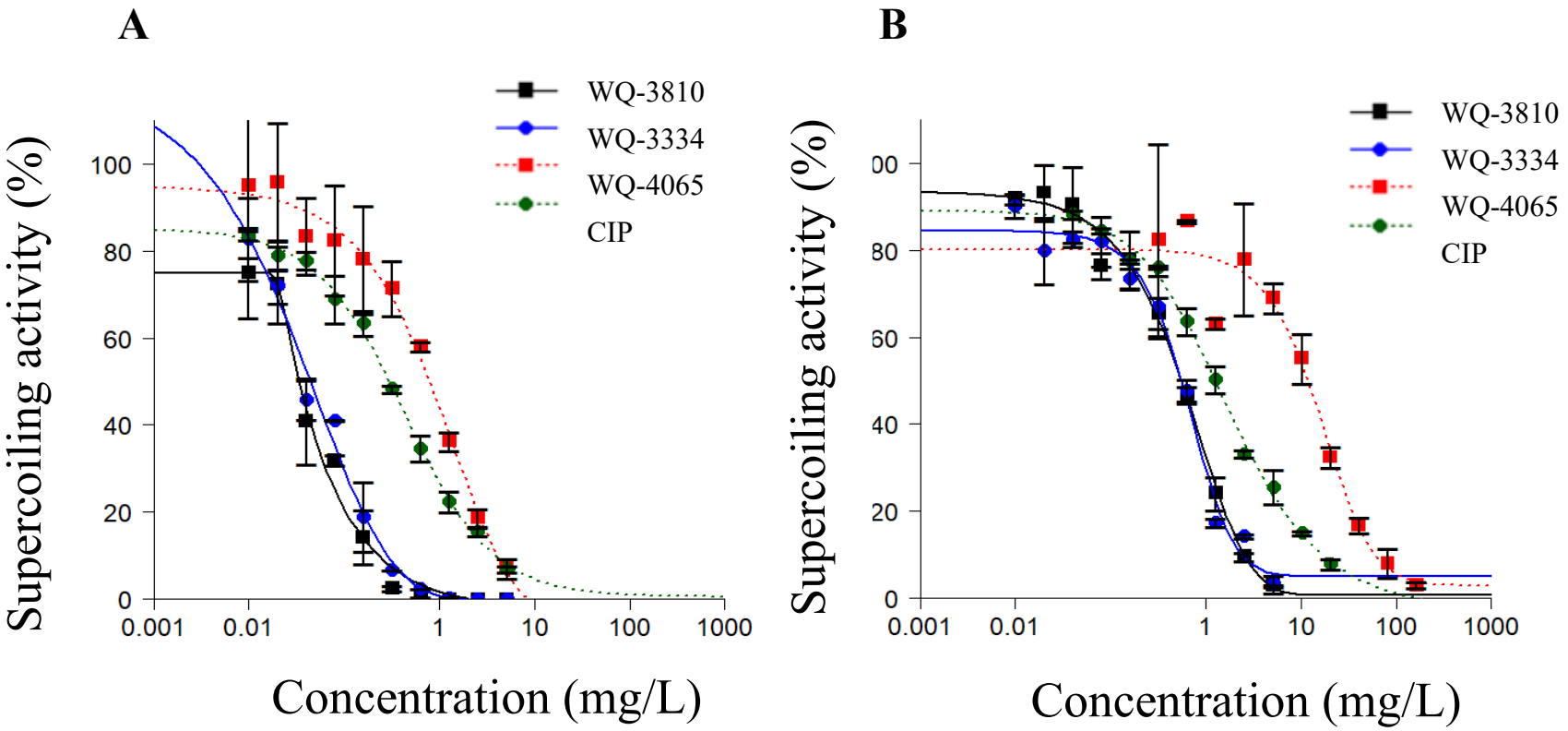

Figure 24. DNA gyrase supercoiling activities against WQ compounds including WQ-3810, WQ-3334, WQ-4065 and CIP. The inhibitory activity of the examined drugs against (A) $GyrA^{D87G}$ and (B) $GyrA^{D87N}$.

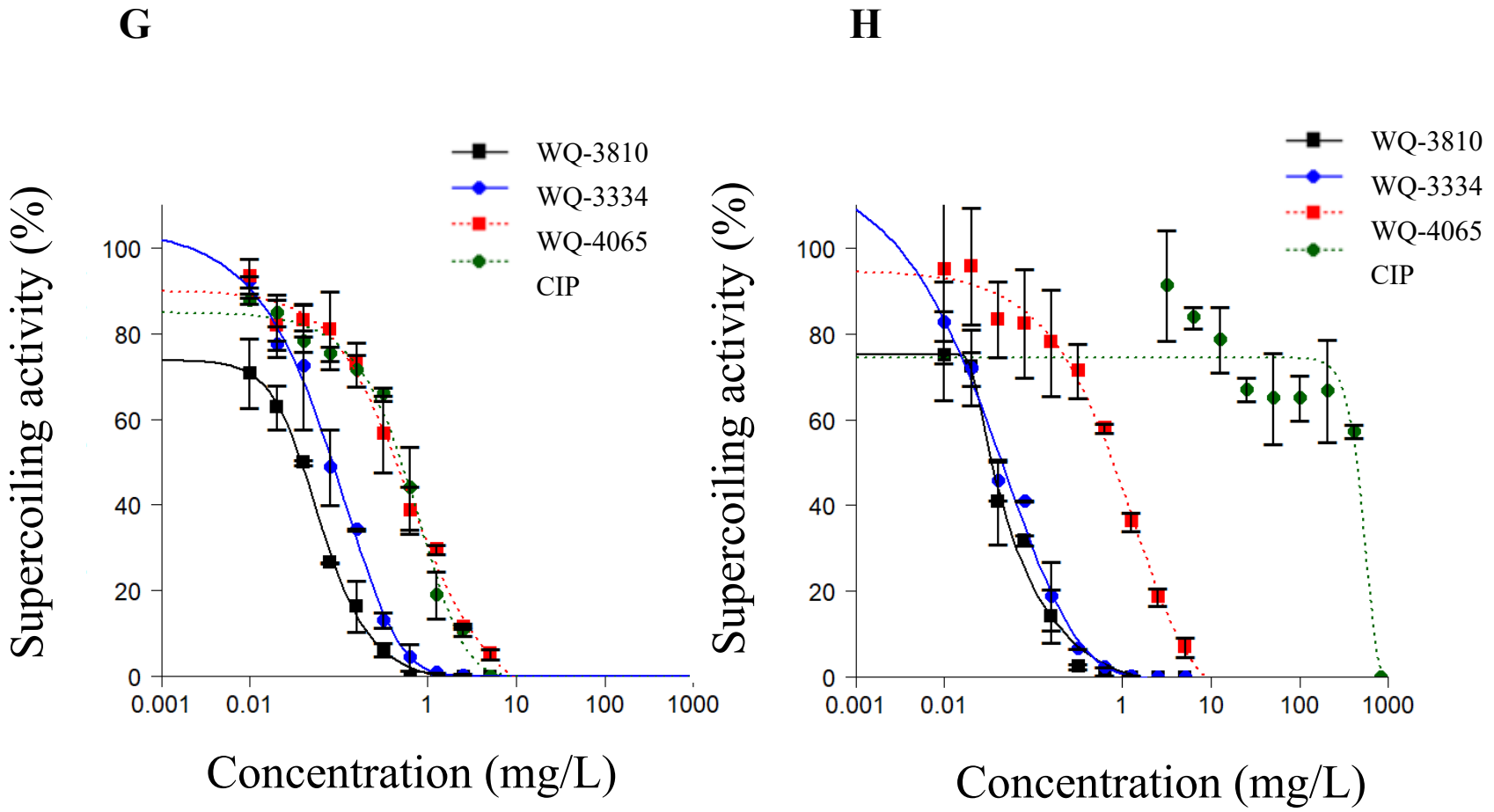

Figure 25. DNA gyrase supercoiling activities against WQ compounds including WQ-3810, WQ-3334, WQ-4065 and CIP. The inhibitory activity of the examined drugs against (A) $GyrA^{D87Y}$ and (B) the double mutant $GyrA^{S83FD87N}$.

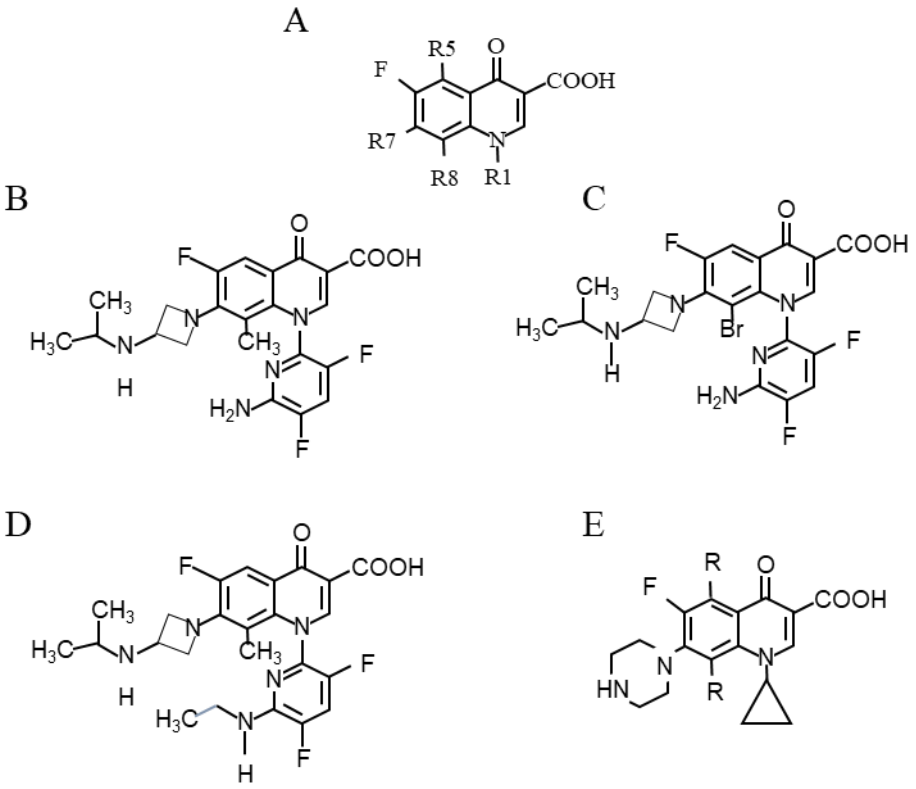

Position	WQ-3810	WQ-3334	WQ-4065	CIP
R1	6-amino-3,5-difluoropyridine-2-yl	6-amino-3,5-difluoropyridine-2-yl	6-ethylamino-3,5-difluoropyridine-2-yl	Cyclo-propyl
R6	Fluorine	Fluorine	Fluorine	Fluorine
R7	3-isopropyl-aminoazetizine-1-yl	3-isopropyl-aminoazetizine-1-yl	3-isopropyl-aminoazetizine-1-yl	Piperazine
R8	Methyl group	Bromine	Methyl group	Hydrogen

Figure 26. Structure of quinolones in this chapter.
(A) Basic structure, (B) WQ-3810, (C) WQ-3334, (D) WQ-4065 and (E) CIP.

CHAPTER III

Effect of WQ-3334 on *C. jejuni* carrying a DNA gyrase with dominant amino acid substitutions conferring quinolone resistance.

Introduction

WQ compounds have been demonstrated to have a potent inhibitory activity against *S*. Typhimurium. In this chapter, I extended the investigation to assess the activity of WQ-3334, WQ-4064, and WQ-4065 against both WT and mutant *C. jejuni* DNA gyrase, the primary target of these drugs. The objective of this study was to evaluate the effectiveness of these novel quinolones through both *in vitro* and *in silico* assays. This approach aimed to provide a comprehensive evaluation of their inhibitory potential against resistant strains of *C. jejuni.*

Materials and Methods

Reagents

The reagents used in Chapter III were obtained from Chapter I and II. NAL was purchased from FUJIFILM Wako Pure Chemical Corporation (Osaka, Japan), respectively.

Construction of WT and mutant *C. jejuni* DNA gyrases expression vectors

WT and mutant DNA gyrases expression vectors used in the present work were prepared in the previous study [77]. Briefly, DNA was extracted from *C. jejuni* ATCC33560 and the vector plasmid pET-20b (+) DNA was used to construct expression plasmids for *gyrA* and the *B* subunit of *C. jejuni* DNA gyrase.

Expression and purification of recombinant *C. jejuni* DNA gyrase subunits

Recombinant DNA gyrase subunits were expressed and purified as described in a previous study [77]. Briefly, expression vectors carrying the *gyrA* and *gyrB* genes of *C. jejuni* were transformed into *E. coli* BL21(DE3)/*pLysS*. Transformants were grown in LB medium with 100 mg/L of AMP, and the expression of GyrA and GyrB was induced by the addition of 1 mM of IPTG and incubated at 18°C for 16 hours. Harvested *E. coli* was sonicated by using Branson Sonifier 250 and purified by column chromatography using Ni-NTA agarose resin.

The purity of recombinant DNA gyrase subunits of *C. jejuni* used in this study were examined by SDS-PAGE with Blue stained Protein Standard, Broad Range (11-250 kDa). Recombinant proteins (300 ng) were loaded on a SuperSep^{TM} Ace 5-20% gradient gel.

Inhibition of *C. jejuni* DNA gyrase by quinolones

To determine IC_{50} of WQ compounds, supercoiling inhibitory assay was performed as previously described [72] with modifications. The reaction mixture consisted of DNA gyrase assay solution, 0.13 μg of relaxed pBR322 DNA, and 36 nM of GyrA and GyrB in a total volume of 30 μL. Reactions were run at 37ºC for 45 min and stopped by the addition of 8 μL of 5x Dye mix. Reaction mixtures were subjected to electrophoresis in 1.2% agarose gel in TAE buffer and stained with ethidium bromide (0.5 mg/L). To assess the inhibitory effects of WQ compounds on DNA gyrases, IC_{50} were determined using the intensity of supercoiled DNA accessed by ImageJ software. (http://rsbweb.nih.gov/ij) and calculated by IC_{50} calculator, available at AAT Bioquest (https://www.aatbio.com/tools/ic50-calculator) [49,75,79].

In silico docking simulation

Docking simulations of WQ-3334 and DNA gyrases were done as in *silico* analysis. The crystal structure of the *E. coli* DNA gyrase (PDB ID: 6RKS), which showed 82.50%

homology to QRDR of GyrA subunit in amino acid sequence of *C. jejuni*, was used for this docking simulation as there was no crystal structure of *C. jejuni* DNA gyrase available [80]. Amino acid substitution was reproduced using the Crystallographic Object-Oriented Tool kit (WinCoot-0.9.8.92; Paul Emsley). The Ser83 of *E. coli* GyrA was changed to Thr, which corresponds to the Thr86 of *C. jejuni* GyrA, and this structure was used for docking simulations as WT model. A model in which Thr83 of GyrA in the WT model was replaced by Ile (T83I model) also was used for the docking simulation. The docking simulation was done by Molecular Operating Environment (MOE; 2022.02 Chemical computing group ULC, Montreal, Canada). Simulation analysis was done by using WinCoot and distance between objects were calculated. Figures were constructed by PyMOL v2.5 (Schrödinger, USA). Affinity of WQ-3334 against DNA gyrases was estimated by this simulation.

Induction of quinolone resistance in *C. jejuni*

In this study, I utilized ten strains of *C. jejuni*. Five of these strains, both quinolone-susceptible and resistant, were isolated from chicken meat. Additionally, four quinolone-resistant strains were obtained by inducing resistance in a type strain *C. jejuni* ATCC 33560, which is recognized as a quality control strain for antimicrobial susceptibility testing [81]. Briefly, *C. jejuni* ATCC 33560 was cultured on MHA plates supplemented with varying concentrations of CIP (0.1, 0.3, 1, 3, 10, and 100 mg/L) and NAL (10, 50, 100, and 300 mg/L) to isolate quinolone resistant strains. Incubation was carried out at 37°C under microaerophilic conditions (N_2: 85%, CO_2: 10%, and O_2: 5%).

The obtained colonies were confirmed by the nucleotide substitution in the QRDR of *gyrA* by PCR and sequencing. The forward and reverse primers were 5'-AGAGATGGTTTAAAGCCTGTTC-3' and 5'-ACGCCCTGTGCGATAAGCTTC-3' at nucleotide position 120-142 and 700-720, respectively. The amplification was performed as followed conditions: initial pre-denaturation at 95°C for 1 minute; 30 cycles of denaturation at 95°C for 10 seconds; annealing at 47°C for 10 seconds and extension at 72°C for 30 seconds; and a final extension at 72°C for 5 minutes. The nucleotide sequences of the PCR products were determined by using BigDye™ Terminator cycle sequencing kit version 3.1 and ABI Prism 3130xl Gene Analyzer.

Specific genomic mutations in the QRDR associated with quinolone resistance were identified by comparing obtained sequences with the reference genome of *C. jejuni* (RefSeq: NC_002163.1, ATCC 700819) using MEGA X (https://www.megasoftware.net/). Mutants *C. jejuni* strains carrying T86I and D90N DNA gyrases were used in this study.

MICs for WT and mutant *C. jejuni* strains

To compare the susceptibility of *C. jejuni* to the examined compounds with CIP, MIC tests were conducted using a method adapted from the guidelines established by the

Clinical and Laboratory Standards Institute (CLSI) M45 [82]. Specifically, the bacterial stocks were streaked out on MHA plate for 48 h under microaerobic condition (85% N_2, 10% CO_2, 5% O_2) at 37°C. Colonies were suspended into MHB and turbidity was adjusted to 0.5 McFarland. And the solution was diluted 100 times to obtain 10^6 CFU/mL. Bacterial solution and serial concentrations of WQ compounds (0–64 mg/L) were mixed and incubated 48 hours under micro- aerobic condition at 37°C. Results were observed optically. The MICs and IC_{50} of each examined drugs were converted to log10 and assessed by estimating a linear regression to show their relationships. The relationships were quantified by the R-square valves [46].

Statistical Analysis

The statistical analysis using R software version 4.1.3 with the package "agricolae" version 1.3-5 was performed with one-way ANOVA. Additionally, I applied the LSD test to pinpoint groups with statistically distinct means (significance denoted by $p < 0.05$) [66].

Results

Recombinant DNA gyrases

Recombinant *C. jejuni* DNA gyrases including GyrA ^{WT}, GyrA^{T86I} and GyrA^{D90N} subunit and GyrB^{WT} subunit were successfully expressed and purified. The high purity of proteins, exceeding 95% was confirmed by SDS-PAGE as shown in Figure 27.

Induction of mutant *C. jejuni* strains

The quinolones-resistant strains induced by CIP or NAL selection were found to have DNA gyrase carrying GyrA^{T86I} and GyrA^{D90N}, respectively.

Inhibitory activities of WQ-3334, WQ-4064 and WQ-4065 against *C. jejuni* recombinant DNA Gyrases

The results of supercoiling inhibitory assays, conducted with varying concentrations of WQ compounds, are presented in Figure 28. The calculated IC_{50}s are summarized in Table 9 and Figure 29. Notably, DNA gyrases with GyrA^{T86I} displayed the highest resistance to the WQ compounds examined in this study. WQ-3334 exhibited the most potent inhibitory activity against all DNA gyrases.

Docking simulations of WQ-3334 and DNA gyrases

The results of the docking simulations are shown in Figure 30, where the R7 group of WQ-3334 interacted with Thr83 (2.83 Å), Tyr86 (2.17 Å), and Ala118 (2.70 Å) of GyrA in the WT model. Furthermore, the R1 group of WQ-3334 interacted with GyrA Asp82 in the WT model (3.25 Å). In contrast, in the T83I model, only the interaction between GyrA

Asp87 and WQ-3334 was observed (2.37 Å), and no interaction between the T83I model and the R1 group of WQ-3334 was observed.

MICs for WT and mutant *C. jejuni*

The MICs of WQ compounds against WT and mutant strains carrying $GyrA^{T86I}$ and $GyrA^{D90N}$ were examined. MICs of each WQ compound and CIP against *C. jejuni* strains with DNA gyrases with $GyrA^{WT}$, $GyrA^{T86I}$ and $GyrA^{D90N}$ ranged from 0.00375 to 64 mg/L (Table 10). WQ-3334 was found to be the most effective drug against WT strains. Strong correlations between the MICs and IC_{50} of WQ-3334, WQ-4064 and WQ-4065 against WT and mutants DNA gyrase were found with R-squared of 1, 0.95 and 0.93, respectively, as shown in Figure 31.

Discussion

WQ-3334 has been shown as a strong inhibitory activity against several quinolones-resistant pathogens [49,75]. However, its antimicrobial activity against *C. jejuni* remains unknown. To elucidate this, I investigated the structure-activity relationships of WQ-3334, alongside WQ-4064 and WQ-4065, utilizing supercoiling assay, MICs test and *in silico* docking simulation. The chemical structures of the examined compounds in this study were exhibited in Figure 32. Previous studies suggest that the amino acids substitutions at Thr86 and Asp90 in DNA gyrase *C. jejuni* within GyrA play pivotal roles in binding of quinolone to DNA gyrase [27,30,36,83,84]. To assess the impact of these amino acid substitutions, I used recombinant DNA gyrases harboring $GyrA^{T86I}$ and $GyrA^{D90N}$ substitutions due to their prevalences and their contributions to quinolone resistance. The investigation showed that WQ-3334 exhibited potent efficacy against mutant DNA gyrases, whereas WQ-4064 and WQ-4065 displayed less effectiveness, as indicated by their IC_{50} and MICs. Specifically, the IC_{50} of WQ-4064 and WQ-4065 against WT DNA gyrase were 1.64-fold and 5-fold higher than that of WQ-3334, respectively. This trend persisted when using DNA gyrases carrying $GyrA^{T86I}$ and $GyrA^{D90N}$, the IC_{50}s of WQ-4064 and WQ-4065 against DNA gyrase with $GyrA^{T86I}$ were 5.4-fold and 5.2-fold higher than WQ-3334, respectively. Similarly, the IC_{50} of WQ-4064 and WQ-4065 against DNA gyrase with $GyrA^{D90N}$ were 2.1-fold and 3.5-fold higher than WQ-3334, respectively.

The observed phenomenon can be explained by the structure-activity relationship of quinolones which shows that a change of substituent at R1 confers different binding affinities to DNA gyrases as in Chapter II [69]. Briefly, the R1 of quinolones can form hydrophobic interaction with the drug-binding site of DNA gyrases and can further specifically interact with residues in the major groove of DNA. The modification at R1 of

quinolones with a small structure can enhance the drug activity against WT and mutant DNA gyrases as shown in the previous studies and in this study [49,75]. Therefore, WQ-3334 with the structure of 6-amino-3,5-difluoropyridine-2-yl at R1 conferred a stronger inhibitory effect than WQ-4064 and WQ-4065 which have 6-methylamino-3,5-difluoropyridine-2-yl and 6-ethylamino-3,5-difluoropyridine-2-yl, respectively (Figure 32). In contrast, the increasing bulkiness of the substituent at R1 may reduce the drug activity due to physical obstruction of the interaction with DNA gyrase, resulting in the high IC_{50} of WQ-4064 and WQ-4065 against both WT and mutant DNA gyrases as shown in Table 9 and in previous studies [49,75].

Currently, there are hypotheses for the mechanism of quinolones in inhibiting DNA gyrase, although it is well known that both GyrA and GyrB are involved in this complex [54,85]. One of proposed model suggested that the strong interaction between quinolones and DNA gyrase is predicted to primarily rely on a water-metal ion bridge associated with GyrA [54,86]. Consequently, amino acid substitutions within GyrA that lead to conformational changes can reduce the capability of quinolones to interact with DNA gyrase through the water-metal ion bridge [50]. Particularly, a hydroxyl group is removed in case of DNA gyrase carrying $GyrA^{T86I}$, preventing quinolones from establishing the bridge with DNA gyrase. Similarly, a substitution at $GyrA^{D90N}$ can disrupt DNA gyrase's interaction with quinolones by losing carboxyl group, hindering the formation of the bridge with GyrA that facilitates interactions between the drug and GyrA. Consequently, higher concentrations of quinolones are required to inhibit the supercoiling activity of mutant DNA gyrases across all tested drugs.

In mutant DNA gyrases, quinolones lose their capacity to establish a strong bond with GyrA, which typically relies on the water-metal ion bridge [71,87]. However, these quinolones still seem to effectively interact with GyrB especially WQ-3334 that may have a stronger interaction with GyrB compared to WQ-4064 and WQ-4065. The IC_{50} of WQ-3334 against DNA gyrases carrying $GyrA^{T86I}$ and $GyrA^{D90N}$ were 11.0 ± 0.7 and 1.60 ± 0.28 mg/L, respectively. On the other hand, those of WQ-4064 against DNA gyrases carrying $GyrA^{T86I}$ and $GyrA^{D90N}$ were 60.4 ± 2.1 and 3.39 ± 0.70 mg/L, representing 5.49-fold and 2.12-fold increases compared to WQ-3334, respectively. In addition, IC_{50} of WQ-4065 against DNA gyrases harboring $GyrA^{T86I}$ and $GyrA^{D90N}$ were 57.8 ± 1.7 and 5.62 ± 0.4 mg/L, showing 2.1-fold and 3.5-fold increases compared to WQ-3334, respectively. These findings suggest a strong inhibitory activity of WQ-3334 against mutant DNA gyrases, regardless of amino acid substitutions. This observation aligns with former studies indicating that modifications at the R1 position of quinolones with 6-amino-3,5-difluoropyridin-2-yl are more favorable when associated with GyrB compared to bulkier

substituents of WQ-4064 and WQ-4065 [49,86]. Additionally, the modification of the R8 position with a halogen atom (bromine) in WQ-3334 led to an increased inhibitory effect in the previous studies [31,49]. In contrast, WQ-4064 and WQ-4065, which had methyl group modifications at the same R8 position showed less inhibitory effects, particularly against mutant DNA gyrases. Therefore, the bromine at R8 can also contribute significantly to its effectiveness, emphasizing that WQ-3334 has a strong antimicrobial activity against mutant DNA gyrases.

Another model is that quinolone could directly interact with DNA gyrase [88,89]. In this study, to thoroughly determine the effectiveness of WQ-3334 against WT and mutant DNA gyrases, I employed *in silico* molecular docking simulations using modified *E. coli* DNA gyrase structures, where the 83rd amino acid of *E. coli* GyrA corresponds to the 86th amino acid of *C. jejuni* GyrA, to examine the effect of amino acid substitutions in *C. jejuni* on the interaction with WQ-3334. Without water molecules, I confirmed that WQ-3334 can still interact with both WT and mutant DNA gyrase, showing its inhibitory activity. It was suggested that the R1 group of WQ-3334 could interact with Asp85 in GyrA of *C. jejuni* (Asp82 in the WT model). On the other hand, it was indicated that the interaction between the R1 group of WQ-3334 and GyrA may have been lost, when Thr86 was mutated to Ile. The S score of WQ-3334 was -7.3046 for the WT model and -7.1345 for the T83I model, indicating a higher binding strength for WT than GyrA^{T86I} DNA gyrase. This strengthens the fact that a higher concentration of quinolones is required to inhibit the activity of GyrA^{T86I} DNA gyrase due to the less affinity of quinolones.

To comprehensively assess drug effectiveness, I conducted MICs tests to consider the other factors that contribute to the antimicrobial activity such as influx into the bacteria and efflux from the bacteria. WQ-3334 showed a stronger inhibitory activity than WQ-4064 and WQ-4065 against seven strains with quinolones-resistant mutations. Therefore, WQ-3334 was found to be an effective drug against WT and quinolones-resistant *C. jejuni* harboring GyrA^{T86I} and GyrA^{D90N} mutations even when assessed in live bacterial conditions. I further calculated the correlation between MICs and IC_{50} using linear regression. The IC_{50} of examined drugs against *C. jejuni* DNA gyrases showed strong correlations with MICs as shown in Figure 31, confirming their ability to inhibit the growth of the bacteria. However, the MICs and IC_{50} were not directly proportional. For example, MICs of WQ-3334 against WT DNA gyrase was approximately 30-fold higher than IC_{50}, however, MICs of WQ-3334 against GyrA^{D90N} DNA gyrase was approximately 10-fold higher than IC_{50}. The discrepancy of the ratio between MICs and IC_{50} has been observed in previous studies, suggesting differences in bacterial properties such as cell-permeability properties and influx or efflux pump activity which can lead to drug accumulation within bacterial cell [46,90]. While

bacterial properties may influence MICs and prevent direct translation of IC_{50} to MICs, IC_{50} determined by the supercoiling assay can serve as a rapid screening technique for novel candidate drugs with promising antibacterial activities. The previous study and this study suggest that quinolones with low IC_{50} can potentially be effective drug as they would exhibit low MICs [46]. In contrast, quinolones with high IC_{50} in the assay may not be suitable candidates for further evaluation as antibacterial drugs, as they are likely to result in high MICs [46]. This highlights the promise of WQ-3334 as a candidate drug for the treatment of quinolone-resistant *C. jejuni*.

Conclusion

This study showed the effectiveness of WQ-3334 as a novel quinolone with high inhibitory activity against both WT and mutant DNA gyrases of *C. jejuni*. The presence of 6-amino-3,5-difluoropyridine-2-yl at R1 in WQ-3334 making it a compelling candidate for treating campylobacteriosis caused by quinolones-resistant *C. jejuni* strains. This study paves the way for the development of effective treatments in the ongoing battle against antibiotic-resistant pathogens.

Table 9. IC_{50} of WQ compounds for DNA gyrases in WT and mutants.

GyrA	GyrB	**IC_{50}s of compounds (mg/L)***		
		WQ-3334	WQ-4064	WQ-4065
WT	WT	$0.188 \pm 0.039^{a, c}$	$0.309 \pm 0.074^{a, b}$	$0.956 \pm 0.074^{b, c}$
T86I	WT	$11.0 \pm 0.7^{d, f}$	$60.4 \pm 2.1^{d, e}$	$57.8 \pm 1.7^{e, f}$
D90N	WT	$1.60 \pm 0.28^{g, i}$	$3.39 \pm 0.70^{g, h}$	$5.62 \pm 0.4^{h, i}$

*IC_{50}: WQ compound concentration for 50% of inhibitory activity against DNA gyrase.

^{a}-^{i} Significantly different by LSD multiple range test (*p-value* < 0.05)

Table 10. MICs (mg/L) of WQ compounds for WT and mutants DNA gyrases in *C. jejuni* isolates. (Ciprofloxacin: CIP, Nalidixic acid: NAL)

GyrA	Isolates	WQ-3334	WQ-4064	WQ-4065	CIP
WT	ATCC 33560	0.015	0.03	0.06	0.25
WT	Chicken meat isolate1	0.00375	0.0075	0.0075	0.125
WT	Chicken meat isolate2	0.0075	0.015	0.03	0.125
WT	Chicken meat isolate3	0.06	0.12	0.24	0.5
T86I	Selected mutation by CIP	2	4	8	64
T86I	Selected mutation by CIP	2	4	8	64
T86I	Chicken meat isolate4	0.5	1	2	16
T86I	Chicken meat isolate5	0.5	1	2	16
D90N	Selected mutation by NAL	0.25	0.5	1	4
D90N	Selected mutation by NAL	0.5	1	2	4

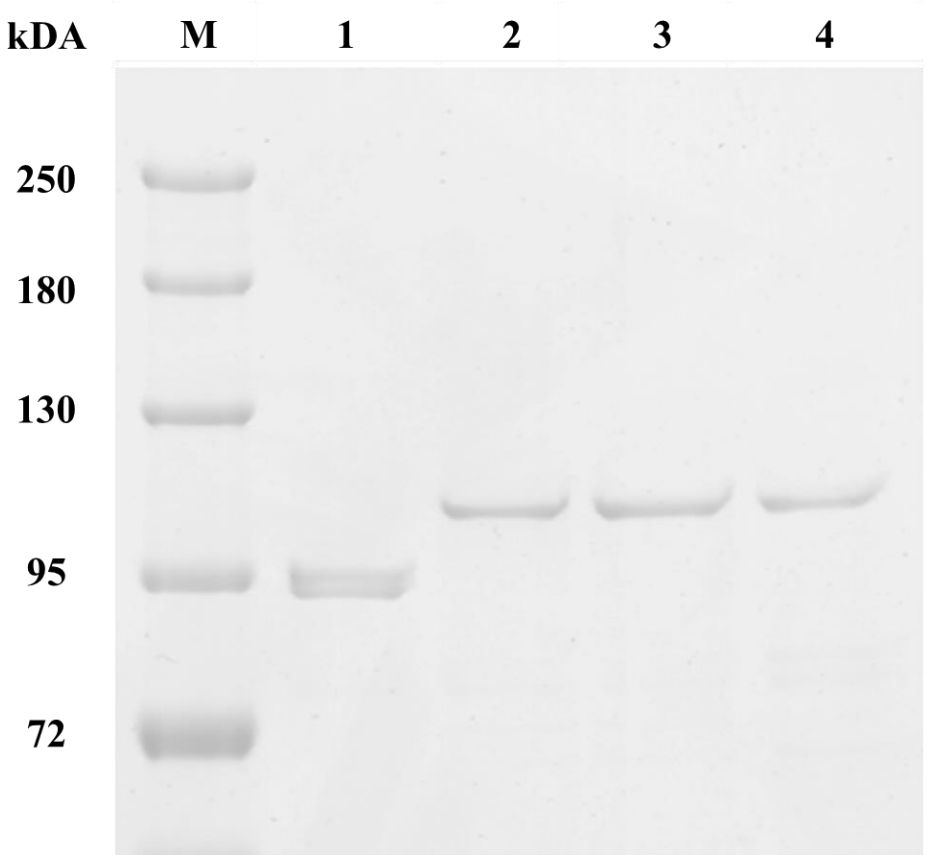

Figure 27. SDS-PAGE analysis of purified GyrA and GyrB.
Recombinant *C. jejuni* DNA gyrase including $GyrB^{WT}$, $GyrA^{WT}$, $GyrA^{T86I}$ and $GyrA^{D90N}$ and were illustrated by SDS-PAGE. The protein samples (300 ng/well) added onto 5-20% gradient polyacrylamide gel. Lane M showed protein size marker, and lanes 1-4 exhibited $GyrB^{WT}$, $GyrA^{WT}$, $GyrA^{T86I}$ and $GyrA^{D90N}$, respectively.

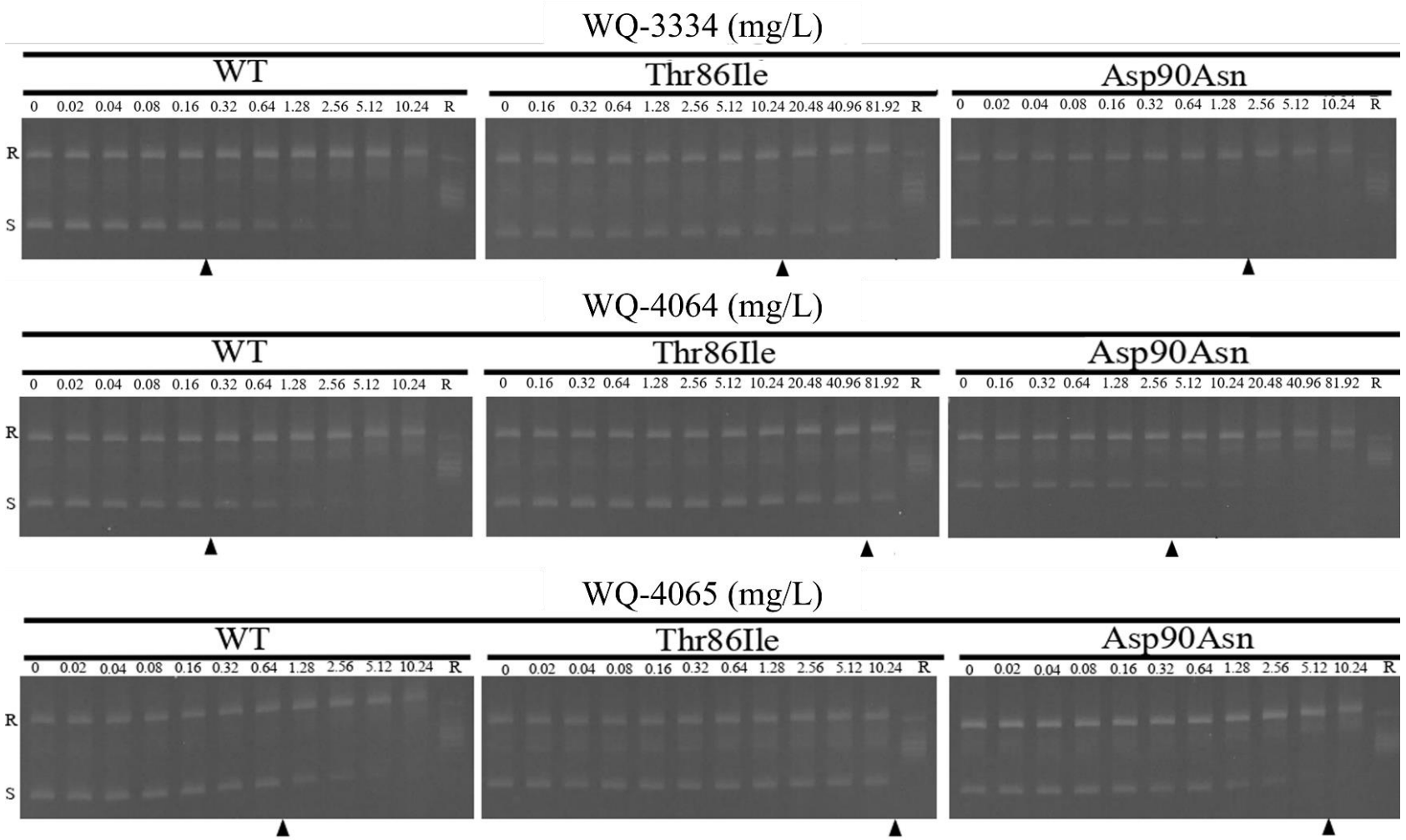

Figure 28. WQ compounds inhibited DNA supercoiling assay.

Relaxed DNA (pBR322) was mixed and incubated with ATP, GyrA, GyrB and WQ compounds at the described concentrations. Each WQ compound was examined for its inhibitory activity against WT DNA gyrase and mutant DNA Gyrases. R and S denote that the relaxed and supercoiled DNA, respectively. (▲: IC_{50})

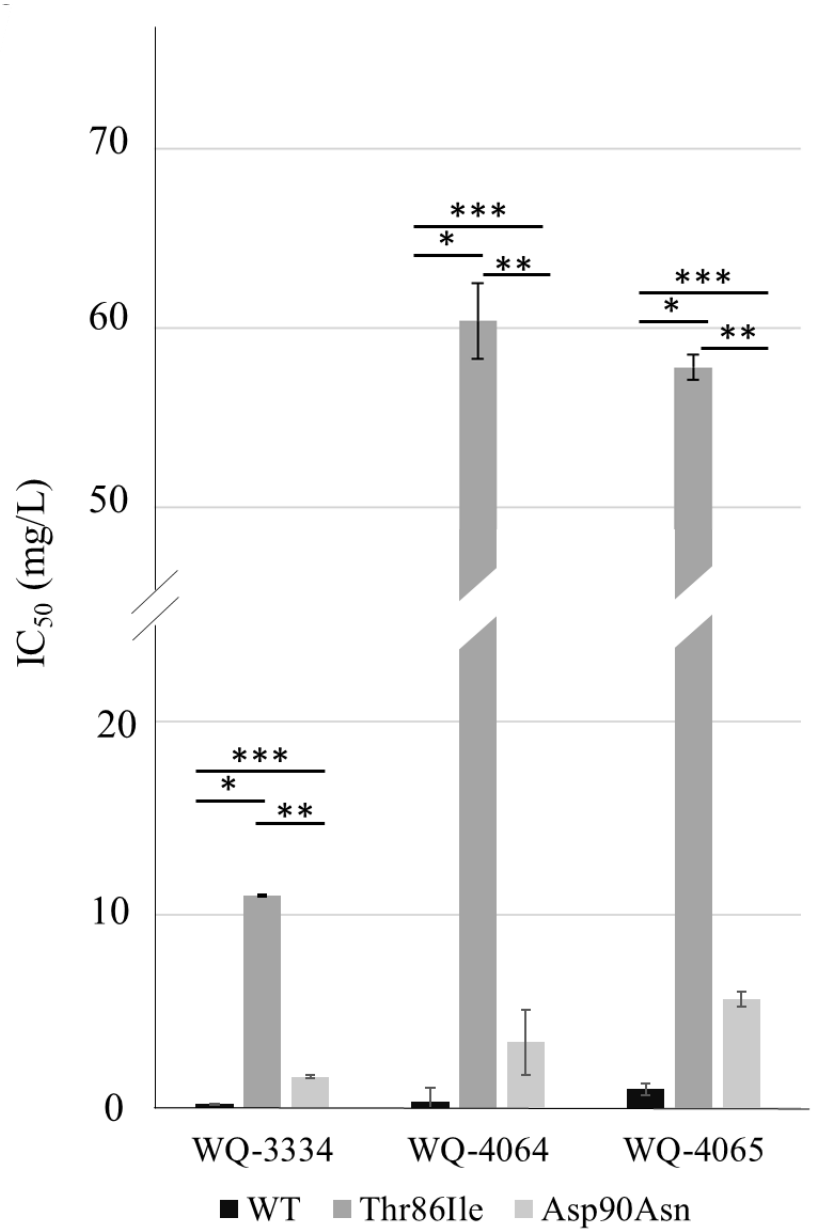

Figure 29. The inhibitory activity of WQ-compounds.
The IC_{50} of WQ-3334, WQ-4064 and WQ-4065 against $GyrA^{WT}$ DNA gyrase (black), $GyrA^{T86I}$ DNA gyrase (gray), and $GyrA^{D90N}$ DNA gyrase (light grey) were shown (* indicated $P<0.05$)

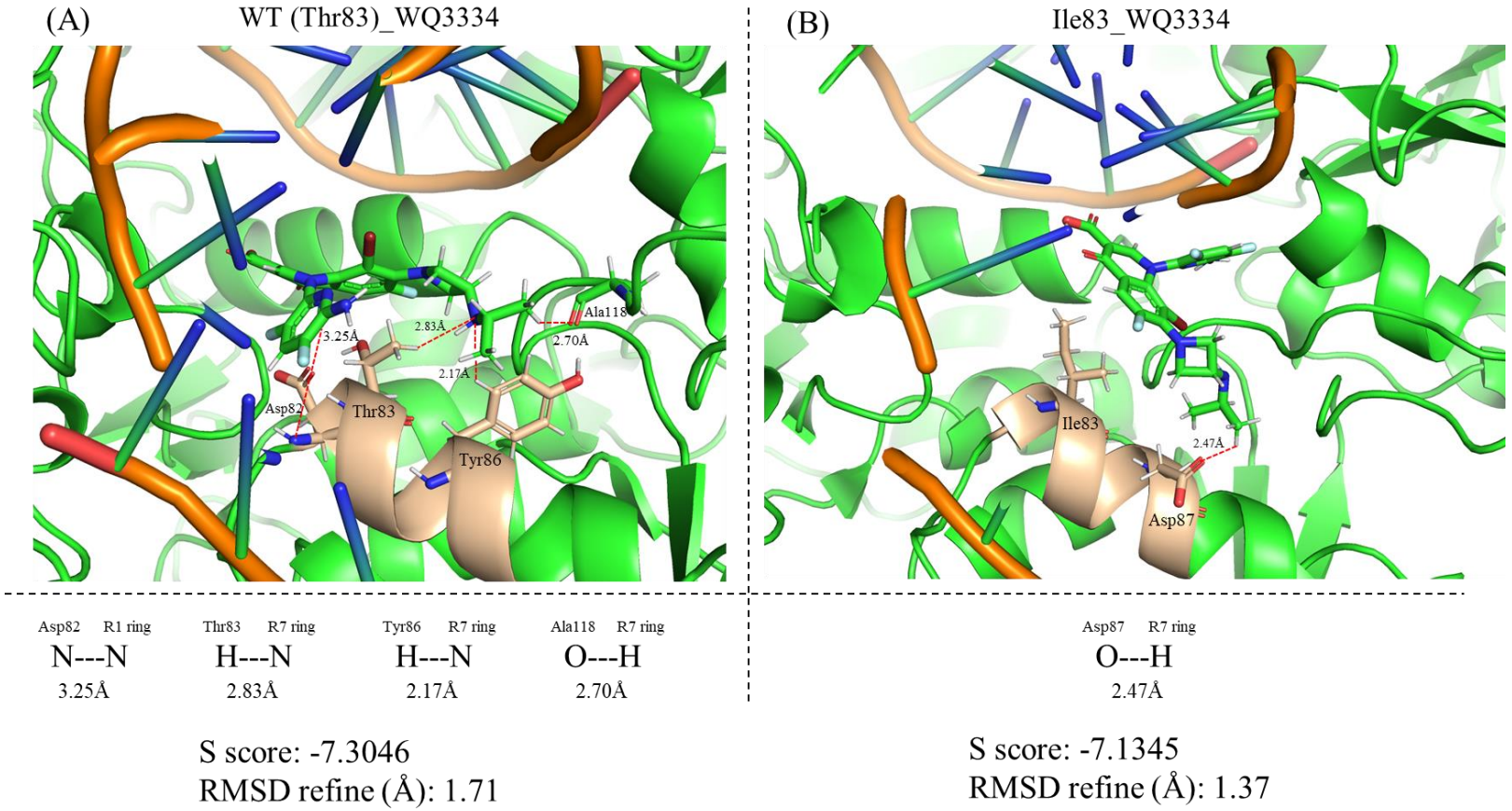

Figure 30. Molecular interaction between the modified *E. coli* DNA gyrases and WQ-3334.
The amino acid at position 83 in *E. coli* GyrA corresponds to the amino acid at position 86 in *C. jejuni* GyrA. (A) Indicates the result of docking simulation between WQ-3334 and the WT model. Asp at position 82, Thr at position 83, Tyr at position 86 and Ala at position 118 interact with WQ-3334. (B) Results of docking simulation between WQ-3334 and the T83I model, showing that only Asp at position 87 interacts with WQ-3334.

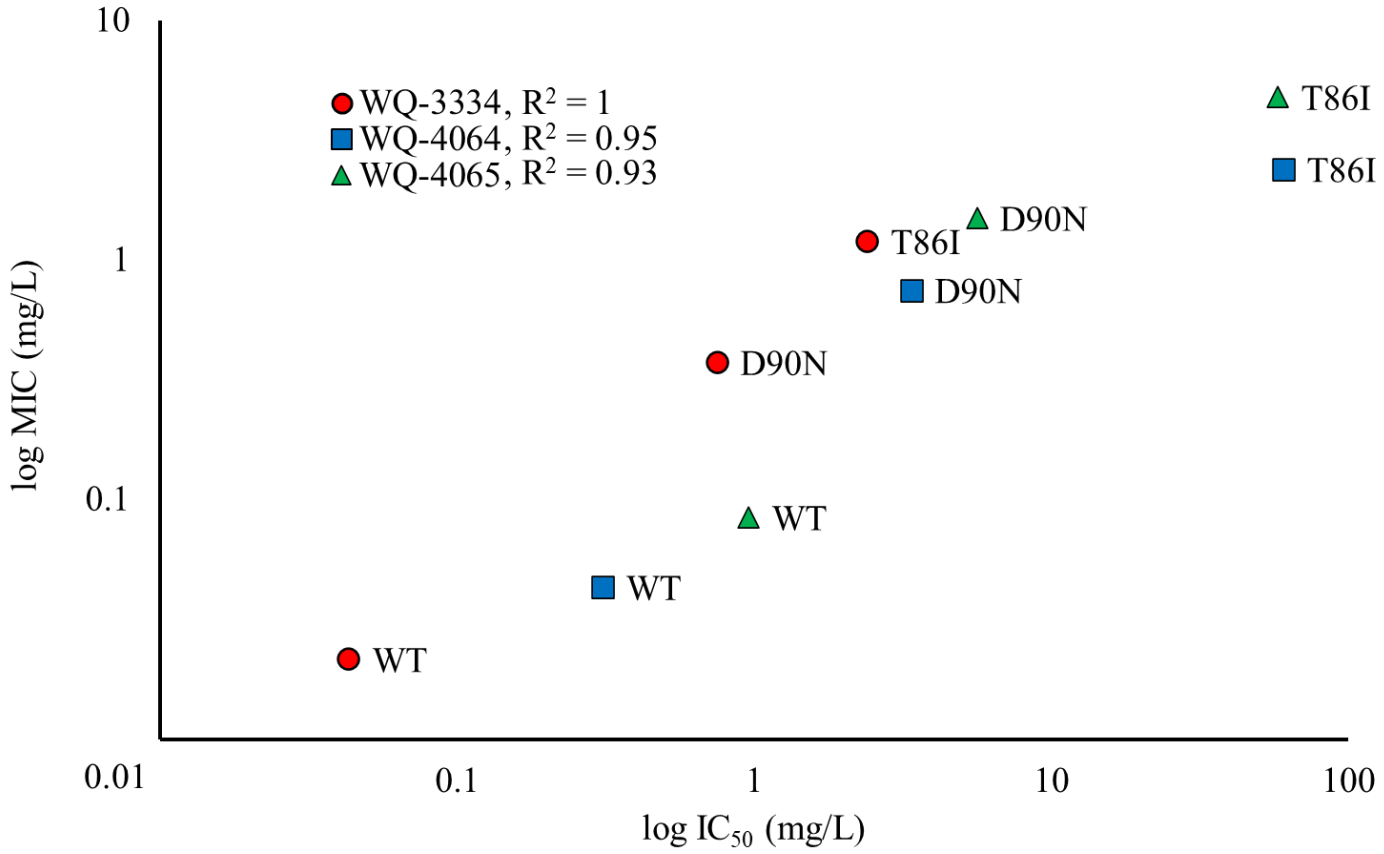

Figure 31. Correlation between MICs and IC50 of the examined drugs against WT and mutant DNA gyrases

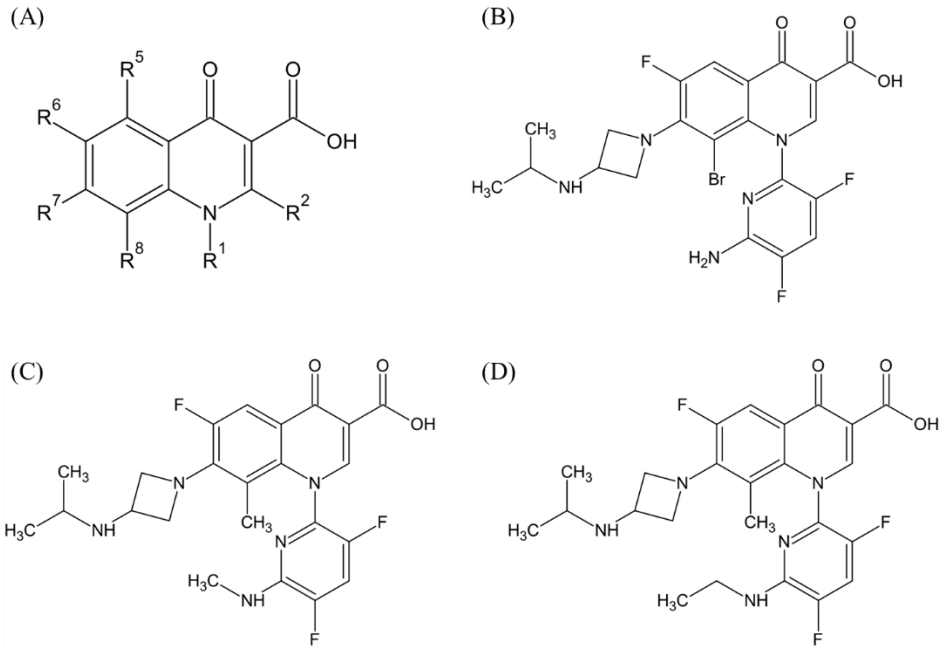

Position	WQ-3334	WQ-4064	WQ-4065	CIP
R1	6-amino-3,5-difluoropyridine-2-yl	6-methylamino-3,5-difluoropyridine-2-yl	6-ethylamino-3,5-difluoropyridine-2-yl	Cyclo-propyl
R6	Fluorine	Fluorine	Fluorine	Fluorine
R7	3-isopropyl-aminoazetizine-1-yl	3-isopropyl-aminoazetizine-1-yl	3-isopropyl-aminoazetizine-1-yl	Piperazine
R8	Bromine	Bromine	Methyl group	Hydrogen

Figure 32. Structure of quinolones in this chapter
Figure 21(A) Basic structure, Figure 21 (B) WQ-3334, Figure 21 (C) WQ-4064 and Figure 21 (D) WQ-4065.

GENERAL CONCLUSION

The escalating risk of health caused by quinolone-resistant *Salmonella* and *Campylobacter* highlights critical challenges in managing bacterial infections effectively. This thesis presented a comprehensive analysis of the quinolone-resistant mechanisms, focusing on the roles of amino acid substitutions in DNA gyrase and the impact of PMQR genes particularly QnrB19 and exploring the potential candidate drugs for the treatment of quinolone resistant bacterial infection.

Chapter I highlighted the complexity of resistance mechanisms where genetic mutations in the QRDR of DNA gyrase significantly reduce the efficacy of quinolones, one of the drugs of treatments for NTS infections using the *in vitro* assay. These mutations may decrease the binding affinity of quinolones, thereby hindering quinolones' ability to inhibit DNA gyrase. Moreover, the presence of QnrB19 further complicates the resistance by protecting DNA gyrase against quinolone inhibition. This additive effect of these resistant mechanisms not only challenges the effectiveness of existing antimicrobial drugs but also highlights the adaptability of bacterial pathogens to pharmacological pressures.

Chapter II presented the investigation of novel quinolone derivatives using the *in vitro* assay including supercoiling assay and MIC test, specifically the WQ-compounds, revealed promising possibilities for overcoming the resistant bacteria. These compounds, targeting DNA gyrase, exhibited high inhibitory activity against both WT and resistant *Salmonella* strains, suggesting that WQ-3810 and WQ-3334 could be candidate drugs for the treatment of quinolones-resistant NTS.

Chapter III extended this investigation to *Campylobacter* spp., exploring the effects of WQ-3334, WQ-4064, and WQ-4065 on both WT and mutant strains. Through a combination of supercoiling assays, MIC tests, and *in silico* docking simulations, this chapter not only deepened our understanding of the structural-activity relationships of these compounds but also highlighted their therapeutic potential against quinolone-resistant *Campylobacter*. The findings suggest that WQ-3334 could play a crucial role in managing the infection of quinolone resistant *Campylobacter* spp.

Although I have demonstrated the effectiveness of the WQ-compound with a 6-amino-3,5-difluoropyridine-2-yl group at the R1 position against mutant strains of *Salmonella* and *Campylobacter*, the impact of these compounds in the presence of both amino acid substitutions in GyrA subunit and Qnr, particularly QnrB19, remains unexplored. Future research is necessary to investigate these interactions and assess the potential of these compounds against quinolones resistant bacteria.

The additive effect on the co-existing quinolone resistance mechanisms, including amino acid substitutions in DNA gyrase and the presence of QnrB19 was shown in Chapter

I. The presence of QnrB19 could increase the IC_{50}s of CIP and MOX against $GyrA^{WT}$ to 10-fold and 8-fold, respectively. Similarly, in the presence of QnrB19, the IC_{50} of CIP for $GyrA^{S83F}$ and $GyrA^{D87N}$ increased further, by 4- and 13-fold, while MOX IC_{50}s increased by 14- and 10-fold, illustrating the additive effect of QnrB19 on drug resistance. Therefore, further study on the development of inhibitory compounds against this phenomenon is necessary. In Chapter II and III, I explored the impact of WQ-compounds which is the novel quinolones against *S.* Typhimurium and *C. jejuni.* The modification at R1 by 6-amino-3,5-difluoropyridine-2-yl group resulted in strong inhibitory activities against these resistant bacteria as exhibited by the low IC_{50} and MICs. In conclusion, this thesis emphasizes the necessity for continuous research and identifies candidate drugs against the emergence of drug resistant NTS and *C. jejuni*. The findings in this thesis advocate for a multi-faceted approach that includes developing new drugs and understanding resistance mechanisms in depth, to manage and mitigate the impact of AMR effectively.

ACKNOWLEDGEMENTS

I am profoundly grateful to Professor Yasuhiko Suzuki of the Division of Bioresources at the International Institute for Zoonosis Control, Hokkaido University, for his invaluable advice, inspiration, and the stimulating discussions that have significantly shaped my academic journey. His support and patience in teaching me throughout my studies have been instrumental in my growth. My deep appreciation also extends to Professor Chie Nakajima, from the same division, for her generous support and insightful counsel that has enriched my research experience.

I owe a debt of gratitude to Professor Norikazu Isoda, Professors Hideaki Higashi, Professor Satoru Konnai and Associate Professor Toyotaka Sato whose roles on my thesis committee were important. Their precious feedback and suggestions have greatly contributed to the enhancement of my work.

Further, I wish to express my gratitude to Professor Motohiro Horiuchi and Assistant Professor Siriporn Kongsoi, alongside Michael Henshaw, Lecturer of English for Academic Purposes, for their constant encouragement and support in pushing me to explore and recognize my true potential.

My sincere thanks to the WISE office and Hokkaido University Dx Doctoral Fellowship for providing me the opportunity to conduct my research at Hokkaido University and to broaden my horizons through international exposure. I am also grateful to the WPI Nano Life Science Institute, Kanazawa University for offering invaluable resources and support throughout my research endeavor.

I extend my heartfelt thanks to all members of the Division of Bioresources and the laboratory staff. Your warm, friendly, and constructive research environment has been a cornerstone of my academic progression. Special thanks are due to Nami Ajiam-Miura, for her generous support and for sharing insights that have been beneficial not only to my academic endeavors but also to my personal journey in Japan.

Lastly, I cannot express enough gratitude to my boyfriend and friends. Your unwavering support and the lively spirit have been my greatest encouragement. This dissertation is a result of the contributions of everyone acknowledged, extending to those not mentioned.

And I have been fortunate to receive it at every step of this significant journey.

REFERENCES

[1] Majowicz SE, Musto J, Scallan E, Angulo FJ, Kirk M, O'Brien SJ, *et al*. The global burden of nontyphoidal *Salmonella* gastroenteritis. Clin Infect Dis 2010;50:882–9. https://doi.org/10.1086/650733.

[2] World Health Organization. Antimicrobial resistance. World Heal Organ 2023. https://www.who.int/news-room/fact-sheets/detail/antimicrobial-resistance#:~:text=AMR is a natural process,in humans%2C animals and plants. (accessed February 27, 2024).

[3] Murray CJ, Ikuta KS, Sharara F, Swetschinski L, Robles Aguilar G, Gray A, *et al*. Global burden of bacterial antimicrobial resistance in 2019: a systematic analysis. Lancet 2022;399:629–55. https://doi.org/10.1016/S0140-6736(21)02724-0.

[4] World Health Organization. WHO estimates of the global burden of foodborne diseases: executive summary. World Heal Organ 2015:225. https://iris.who.int/handle/10665/200046 (accessed December 20, 2023).

[5] World Health Organization. Prioritization of pathogens to guide discovery, research and development of new antibiotics for drug-resistant bacterial infections, including tuberculosis. vol. 6. Geneva: World Health Organization; 2017 (WHO/EMP/IAU/2017.12); 2017.

[6] World Health Organization. WHO Bacterial Priority Pathogens List, 2024: bacterial pathogens of public health importance to guide research, development and strategies to prevent and control antimicrobial resistance. Geneva: World Health Organization; 2024 (CC BY-NC-SA 3.0 IGO); 2024.

[7] Jajere SM. A review of Salmonella enterica with particular focus on the pathogenicity and virulence factors, host specificity and adaptation and antimicrobial resistance including multidrug resistance. Vet World 2019;12:504–21. https://doi.org/10.14202/vetworld.2019.504-521.

[8] Freitas Neto OC de PFRB, A BJ. Sources of human non-typhoid salmonellosis: A review. Brazilian J Poult Sci 2010;12:1–11. https://doi.org/10.1590/s1516-635x2010000100001.

[9] Li Q. Mechanisms for the Invasion and Dissemination of Salmonella. Can J Infect Dis Med Microbiol 2022;2022. https://doi.org/10.1155/2022/2655801.

[10] Varma JK, Mølbak K, Barrett TJ, Beebe JL, Jones TF, Rabatsky-Ehr T, *et al.* Antimicrobial-resistant nontyphoidal Salmonella is associated with excess bloodstream infections and hospitalizations. J Infect Dis 2005;191:554–61. https://doi.org/10.1086/427263.

[11] Stanaway JD, Parisi A, Sarkar K, Blacker BF, Reiner RC, Hay SI, *et al*. The global burden of non-typhoidal salmonella invasive disease: a systematic analysis for the Global Burden of Disease Study 2017. Lancet Infect Dis 2019;19:1312–24. https://doi.org/10.1016/S1473-3099(19)30418-9.

[12] Hopkins KL, Davies RH, Threlfall EJ. Mechanisms of quinolone resistance in *Escherichia coli* and *Salmonella*: recent developments. Int J Antimicrob Agents 2005;25(5):358–373. https://doi.org/10.1016/j.ijantimicag.2005.02.006.

[13] Shaheen A, Tariq A, Iqbal M, Mirza O, Haque A, Walz T, et al. Mutational Diversity in the Quinolone Resistance-Determining Regions of Type-II Topoisomerases of *Salmonella* Serovars. Antibiotics 2021;10:1–26. https://doi.org/10.3390/antibiotics10121455.

[14] Yoshida H, Bogaki M, Mika N, Yamanaka LM, Nakamura S. Quinolone resistance-determining region in the DNA gyrase *gyrB* gene of *Escherichia coli*. Antimicrob Agents Chemother 1991;35(8):1647–1650. https://doi.org/10.1128/AAC.35.8.1647.

[15] Pham TDM, Ziora ZM, Blaskovich MAT. Quinolone antibiotics. Medchemcomm 2019;10:1719–39. https://doi.org/10.1039/c9md00120d.

[16] Koide K, San LL, Pachanon R, Park J-H, Ouchi Y, Kongsoi S, et al. Amino Acid Substitution Ser83Ile in GyrA of DNA Gyrases Confers High-Level Quinolone Resistance to Nontyphoidal *Salmonella* Without Loss of Supercoiling Activity. Microb Drug Resist 2021;27(10):1397–1404. https://doi.org/10.1089/mdr.2020.0437.

[17] Rodríguez-Martínez JM, Cano ME, Velasco C, Martínez-Martínez L, Pascual Á. Plasmid-mediated quinolone resistance: An update. J Infect Chemother 2011;17:149–82. https://doi.org/10.1007/s10156-010-0120-2.

[18] Rodríguez-Martínez JM, Machuca J, Cano ME, Calvo J, Martínez-Martínez L, Pascual A. Plasmid-mediated quinolone resistance: Two decades on. Drug Resist Updat 2016;29:13–29. https://doi.org/10.1016/j.drup.2016.09.001.

[19] Pachanon R, Koide K, Kongsoi S, Nakajima C, Kapalamula TF, Suthienkul O, *et al*. Interaction of the plasmid-encoded quinolone resistance protein QnrB19 with Salmonella Typhimurium DNA gyrase. J Infect Chemother 2020;26:1139–45. https://doi.org/10.1016/j.jiac.2020.06.002.

[20] Vetting MW, Hegde SS, Wang M, Jacoby GA, Hooper DC, Blanchard JS. Structure of QnrB1, a plasmid-mediated fluoroquinolone resistance factor. J Biol Chem 2011;286:25265–73. https://doi.org/10.1074/jbc.M111.226936.

[21] Mazurek Ł, Ghilarov D, Michalczyk E, Pakosz Z, Metelev M, Czyszczoń W, *et al*. Pentapeptide repeat protein QnrB1 requires ATP hydrolysis to rejuvenate poisoned gyrase complexes. Nucleic Acids Res 2021;49:1581–96. https://doi.org/10.1093/nar/gkaa1266.

[22] Vetting MW, Hegde SS, Zhang Y, Blanchard JS. Pentapeptide-repeat proteins that act as topoisomerase poison resistance factors have a common dimer interface. Acta Crystallogr Sect F Struct Biol Cryst Commun 2011;67:296–302. https://doi.org/10.1107/S1744309110053315.

[23] Pachanon R, Koide K, Kongsoi S, Nakajima C, Kapalamula TF, Suthienkul O, *et al.* Interaction of the plasmid-encoded quinolone resistance protein QnrB19 with

Salmonella Typhimurium DNA gyrase. J Infect Chemother 2020;26:1139–45. https://doi.org/10.1016/j.jiac.2020.06.002.

[24] Allos BM. *Campylobacter jejuni* infections: Update on emerging issues and trends. Clin Infect Dis 2001;32:1201–6. https://doi.org/10.1086/319760.

[25] Food E, Authority S. The European Union One Health 2019 Zoonoses Report. EFSA J 2021;19. https://doi.org/10.2903/j.efsa.2021.6406.

[26] Liu F, Lee SA, Xue J, Riordan SM, Zhang L. Global epidemiology of campylobacteriosis and the impact of COVID-19. Front Cell Infect Microbiol 2022;12. https://doi.org/10.3389/fcimb.2022.979055.

[27] Wieczorek K, Osek J. Antimicrobial resistance mechanisms among campylobacter. Biomed Res Int 2013;2013:34060. https://doi.org/10.1155/2013/340605.

[28] Redgrave LS, Sutton SB, Webber MA, Piddock LJV. Fluoroquinolone resistance: Mechanisms, impact on bacteria, and role in evolutionary success. Trends Microbiol 2014;22:438–45. https://doi.org/10.1016/j.tim.2014.04.007.

[29] Aldred KJ, Kerns RJ, Osheroff N. Mechanism of quinolones action and resistance. Biochemistry 2014:52–3. https://doi.org/10.1021/bi5000564.

[30] Payot S, Bolla JM, Corcoran D, Fanning S, Mégraud F, Zhang Q. Mechanisms of fluoroquinolone and macrolide resistance in *Campylobacter* spp. Microbes Infect 2006;8:1967–71. https://doi.org/10.1016/j.micinf.2005.12.032.

[31] Kongsoi S, Changkwanyeun R, Yokoyama K, Nakajima C, Changkaew K, Suthienkul O, *et al*. Amino acid substitutions in GyrA affect quinolone susceptibility in *Salmonella* typhimurium. Drug Test Anal 2016;8(10):1065–1070. https://doi.org/10.1002/dta.1910.

[32] Hooper DC, Jacoby GA. Topoisomerase Inhibitors: Fluoroquinolone Mechanisms of Action and Resistance. Cold Spring Harb Perspect Med 2016;6(9):a0253:1–21. https://doi.org/10.1101/cshperspect.a025320.

[33] Bush NG, Diez-Santos I, Abbott LR, Maxwell A. Quinolones: Mechanism, lethality and their contributions to antibiotic resistance. Molecules 2020;25. https://doi.org/10.3390/molecules25235662.

[34] Correia S, Poeta P, Hébraud M, Capelo JL, Igrejas G. Mechanisms of quinolone action and resistance: where do we stand? J Med Microbiol 2017;66:551–9. https://doi.org/10.1099/jmm.0.000475.

[35] WHO Global Priority List of Antibiotic Resistant Bacteria n.d. https://www.who.int/medicines/publications/WHO-PPL-Short_Summary_25Feb-ET_NM_WHO.pdf (accessed December 24, 2021).

[36] Daichi K, Aoi H, Sugimoto K, Ueshima T, Amano H, Itoh K, *et al*. In vitro activity of WQ-3810, a novel fluoroquinolone, against multidrug-resistant and fluoroquinolone-resistant pathogens. Int J Antimicrob Agents 2014;44:443–9. https://doi.org/10.1016/j.ijantimicag.2014.07.017.

[37] Chen Q, Gong X, Zheng F, Ji P, Yuan Z, Liu Y, et al. Prevalence and characteristics of quinolone resistance in *Salmonella* isolated from retail foods in Lanzhou, China. J Food Prot 2019;82:1591–7. https://doi.org/10.4315/0362-028X.JFP-19-001.

[38] Ehud E, Hong SL, Lim S, Hayer SS, Boxrud D, Taylor AJ, et al. Circulation of Plasmids Harboring Resistance Genes to Quinolones and / or Extended-Spectrum Cephalosporins in. Antimicrob Agents Chemother 2019;63:1–15. https://doi.org/https://doi.org/10.1128/aac.02602-18.

[39] Soares FB, Camargo CH, Cunha MPV, de Almeida EA, Bertani AM de J, de Carvalho E, et al. Subtyping of plasmid-mediated quinolone resistance among Salmonella serotypes by whole genome sequencing. Diagn Microbiol Infect Dis 2019;94:403–6. https://doi.org/10.1016/j.diagmicrobio.2019.02.015.

[40] Monte DF, Lincopan N, Berman H, Cerdeira L, Keelara S, Thakur S, et al. Genomic Features of High-Priority Salmonella enterica Serovars Circulating in the Food Production Chain, Brazil, 2000–2016. Sci Rep 2019;9:1–12. https://doi.org/10.1038/s41598-019-45838-0.

[41] Cui M, Zhang P, Li J, Sun C, Song L, Zhang C, et al. Prevalence and characterization of fluoroquinolone resistant *Salmonella* isolated from an integrated broiler chicken supply chain. Front Microbiol 2019;10:1–8. https://doi.org/10.3389/fmicb.2019.01865.

[42] Mąka Ł, Maćkiw E, Stasiak M, Wołkowicz T, Kowalska J, Postupolski J, *et al.* Ciprofloxacin and nalidixic acid resistance of Salmonella spp. isolated from retail food in Poland. Int J Food Microbiol 2018;276:1–4. https://doi.org/10.1016/j.ijfoodmicro.2018.03.012.

[43] Kuang D, Zhang J, Xu X, Shi W, Chen S, Yang X, et al. Emerging high-level ciprofloxacin resistance and molecular basis of resistance in *Salmonella enterica* from humans, food and animals. Int J Food Microbiol 2018;280:1–9. https://doi.org/10.1016/j.ijfoodmicro.2018.05.001.

[44] Pachanon R, Koide K, Kongsoi S, Nakajima C, Ajima N, Kapalamula TF, *et al.* Effectiveness of Fluoroquinolones with Difluoropyridine Derivatives as R1 Groups on the *Salmonella* DNA Gyrase in the Presence and Absence of Plasmid-Encoded Quinolone Resistance Protein QnrB19. Microb Drug Resist 2021;27:1412–9. https://doi.org/10.1089/mdr.2020.0455.

[45] Pachanon R, Koide K, Kongsoi S, Nakajima C, Kapalamula TF, Suthienkul O, *et al*. Interaction of the plasmid-encoded quinolone resistance protein QnrB19 with *Salmonella* Typhimurium DNA gyrase. J Infect Chemother 2020;26:1139–45. https://doi.org/10.1016/j.jiac.2020.06.002.

[46] Kongsoi S, Yokoyama K, Suprasert A, Utrarachkij F, Nakajima C, Suthienkul O, *et al*. Characterization of *Salmonella* Typhimurium DNA gyrase as a target of quinolones. Drug Test Anal 2015;7(8):714–720. https://doi.org/10.1002/dta.1744.

[47] Kongsoi S, Changkwanyeun R, Yokoyama K, Nakajima C, Changkaew K,

Suthienkul O, *et al*. Amino acid substitutions in GyrA affect quinolone susceptibility in *Salmonella* typhimurium. Drug Test Anal 2016;8:1065–70. https://doi.org/10.1002/dta.1910.

[48] Tavío MM, Jacoby GA, Hooper DC. QnrS1 structure-activity relationships. J Antimicrob Chemother 2014;69:2102–9. https://doi.org/10.1093/jac/dku102.

[49] Suwanthada P, Kongsoi S, Miura N, Belotindos L, Piantham C, Toyting J, *et al*. Impact of substitutions at 1 and 8 position of fluoroquinolones on the activity against mutant DNA gyrases of *Salmonella* Typhimurium. Microb Drug Resist 2023;29:552–60. https://doi.org/10.1089/mdr.2023.0014.

[50] Koide K, Kongsoi S, Nakajima C, Suzuki Y. WQ-3810 exerts high inhibitory effect on quinolone-resistant DNA gyrase of *Salmonella* Typhimurium. Biosci Biotechnol Biochem 2019;83(12):2249–2256. https://doi.org/10.1080/09168451.2019.1650634.

[51] Wickham H, François R, Henry L, Müller K, Vaughan D. dplyr: A Grammar of Data Manipulation. R Packag Version 114 2023. https://github.com/tidyverse/dplyr (accessed April 20, 2022).

[52] Aldred KJ, McPherson SA, Turnbough CL, Kerns RJ, Osheroff N. Topoisomerase IV-quinolone interactions are mediated through a water-metal ion bridge: Mechanistic basis of quinolone resistance. Nucleic Acids Res 2013;41:4628–39. https://doi.org/10.1093/nar/gkt124.

[53] Andersson MI, MacGowan AP. Development of the quinolones. J Antimicrob Chemother 2003;51:1–11. https://doi.org/10.1093/jac/dkg212.

[54] Aldred KJ, Breland EJ, Vlčková V, Strub MP, Neuman KC, Kerns RJ, *et al*. Role of the water-metal ion bridge in mediating interactions between quinolones and Escherichia coli topoisomerase IV. Biochemistry 2014;53:5558–67. https://doi.org/10.1021/bi500682e.

[55] Ginguay A, Cynober LA. Amino acids: Amino acid metabolism. Encycl Biol Chem Third Ed 2021;1:2–9. https://bio.libretexts.org/Courses/University_of_California_Davis/BIS_2A%3A_Introductory_Biology_(Easlon)/Readings/04.3%3A_Amino_Acids (accessed April 25, 2024).

[56] Yonezawa M, Takahata M, Banzawa N, Matsubara N, Watanabe Y, Narita H. Analysis of the NH2-Terminal83 rd Amino Acid of *Escherichia coli* GyrA in Quinolone-Resistance 1995;39:243–7. https://doi.org/10.1111/j.1348-0421.1995.tb02196.x.

[57] Vashist J, Vishvanath, Kapoor R, Kapil A, Yennamalli R, Subbarao N, *et al*. Interaction of nalidixic acid and ciprofloxacin with wild type and mutated quinolone-resistance-determining region of DNA gyrase a. Indian J Biochem Biophys 2009;46:147–53. https://doi.org/10.1002/cbic.200800041.

[58] Drlica K, Hiasa H, Kerns R, Malik M, Mustaev A, Zhao X. Quinolones: Action and Resistance Updated. Curr Top Med Chem 2009;9:981–98.

https://doi.org/10.2174/156802609789630947.

[59] Kim ES, Chen C, Braun M, Kim HY, Okumura R, Wang Y, *et al*. Interactions between QnrB, QnrB mutants, and DNA gyrase. Antimicrob Agents Chemother 2015;59:5413–9. https://doi.org/10.1128/AAC.00771-15.

[60] Rovinskiy NS, Agbleke AA, Chesnokova ON, Patrick Higgins N. Supercoil levels in e. Coli and *salmonella* chromosomes are regulated by the c-terminal 35–38 amino acids of gyra. Microorganisms 2019;7. https://doi.org/10.3390/microorganisms7030081.

[61] Mérens A, Matrat S, Aubry A, Lascols C, Jarlier V, Soussy CJ, *et al*. The pentapeptide repeat proteins MfpAMt and QnrB4 exhibit opposite effects on DNA gyrase catalytic reactions and on the Ternary gyrase-DNA-quinolone complex. J Bacteriol 2009;191:1587–94. https://doi.org/10.1128/JB.01205-08.

[62] Hegde SS, Vetting MW, Roderick SL, Mitchenall LA, Maxwell A, Takiff HE, et al. Biochemistry: A fluoroquinolone resistance protein from *Mycobacterium tuberculosis* that mimics DNA. Science (80-) 2005;308:1480–3. https://doi.org/10.1126/science.1110699.

[63] Miura-Ajima N, Suwanthada P, Kongsoi S, Kim H, Pachanon R, Koide K, et al. Effect of WQ-3334 on *Campylobacter jejuni* carrying a DNA gyrase with dominant amino acid substitutions conferring quinolone resistance. J Infect Chemother 2024. https://doi.org/10.1016/j.jiac.2024.04.002.

[64] Randall LP, Cooles SW, Piddock LJV, Woodward MJ. Mutant prevention concentrations of ciprofloxacin and enrofloxacin for *Salmonella enterica*. J Antimicrob Chemother 2004;54:688–91. https://doi.org/10.1093/jac/dkh360.

[65] CLSI. CLSI M100-ED29: 2021 Performance Standards for Antimicrobial Susceptibility Testing, 30th Edition. vol. 40. 2020.

[66] Felipe de M, Muhammad Y. agricolae: Statistical Procedures for Agricultural Research.R package version 1.4.0 2020. https://myaseen208.github.io/agricolae/https://cran.r-project.org/package=agricolae. (accessed December 20, 2021).

[67] Kazamori D, Aoi H, Sugimoto K *et al.* In vitro activity of WQ-3810, a novel fluoroquinolone, against multidrug-resistant and fluoroquinolone-resistant pathogens. Int J Antimicrob Agents 2014;44(5):443–449. https://doi.org/10.1016/j.ijantimicag.2014.07.017.

[68] Park JH, Yamaguchi T, Ouchi Y *et al*. Interaction of Quinolones Carrying New R1 Group with *Mycobacterium leprae* DNA Gyrase. Microb Drug Resist 2021;27(12):1616–1623. https://doi.org/10.1089/mdr.2020.0408.

[69] Lee S, Park T, Lee Y. Structure-activity relationship of fluoroquinolone in *Escherichia coli*. Arch Pharm Res 1998;21:106–12. https://doi.org/10.1007/BF02974013.

[70] Llorente B, Leclerc F, Cedergren R. Using SAR and QSAR analysis to model the

activity and structure of the Quinolone-DNA complex. Bioorganic Med Chem 1996;4:61–71. https://doi.org/10.1016/0968-0896(96)83749-7.

[71] Heddle J, Maxwell A. Quinolone-binding pocket of DNA gyrase: Role of GyrB. Antimicrob Agents Chemother 2002;46:1805–15. https://doi.org/10.1128/AAC.46.6.1805-1815.2002.

[72] Peterson LR. Quinolone molecular structure-activity relationships: What we have learned about improving antimicrobial activity. Clin Infect Dis 2001;33. https://doi.org/10.1086/321846.

[73] Duprey A, Groisman EA. DNA supercoiling differences in bacteria result from disparate DNA gyrase activation by polyamines. PLoS Genet 2020;16:1–20. https://doi.org/10.1371/journal.pgen.1009085.

[74] Kuramoto Y, Ohshita Y, Yoshida J, Yazaki A, Shiro M, Koike T. A novel antibacterial 8-chloroquinolone with a distorted orientation of the N1-(5-amino-2,4-difluorophenyl) group. J Med Chem 2003;46:1905–17. https://doi.org/10.1021/jm0205090.

[75] Park J-H, Yamaguchi T, Ouchi Y, Koide K, Mori S, Kim H, *et al*. WQ-3810 inhibits DNA gyrase activity in ofloxacin-resistant *Mycobacterium leprae*. J Infect Chemother n.d.;26(4):335–42. https://doi.org/10.1016/j.jiac.2019.10.013.

[76] Vergalli J, Atzori A, Pajovic J, Dumont E, Malloci G, Masi M, *et al*. in flux versus bacterial efflux n.d.:1–12. https://doi.org/10.1038/s42003-020-0929-x.

[77] Changkwanyeun R, Usui M, Kongsoi S, Yokoyama K, Kim H, Suthienkul O, *et al.* Characterization of *Campylobacter jejuni* DNA gyrase as the target of quinolones. J Infect Chemother 2015;21:604–9. https://doi.org/10.1016/j.jiac.2015.05.003.

[78] Changkwanyeun R, Usui M, Kongsoi S, Yokoyama K, Kim H, Suthienkul O, *et al.* Characterization of *Campylobacter jejuni* DNA gyrase as the target of quinolones. J Infect Chemother 2015;21:604–9. https://doi.org/10.1016/j.jiac.2015.05.003.

[79] Ouchi Y, Mukai T, Koide K, Yamaguchi T, Park J-H, Kim H, *et al.* WQ-3810: A new fluoroquinolone with a high potential against fluoroquinolone-resistant *Mycobacterium tuberculosis*. Tuberculosis 2020;120, 10189. https://doi.org/10.1016/j.tube.2019.101891.

[80] Vanden Broeck A, Lotz C, Ortiz J, Lamour V. Cryo-EM structure of the complete *E. coli* DNA gyrase nucleoprotein complex. Nat Commun 2019;10:1–12. https://doi.org/10.1038/s41467-019-12914-y.

[81] Tang Y, Sahin O, Pavlovic N, Lejeune J, Carlson J, Wu Z, *et al.* Rising fluoroquinolone resistance in *Campylobacter* isolated from feedlot cattle in the United States. Sci Rep 2017;7:1–8. https://doi.org/10.1038/s41598-017-00584-z.

[82] Clinical and Laboratory Standards Institute (CLSI). M45-Methods for Antimicrobial Dilution and Disk Susceptibility Testing of Infrequently Isolated or Fastidious Bacteria. vol. 35. 2015.

[83] Smith JL, Fratamico PM. Fluoroquinolone resistance in *Campylobacter*. J Food Prot 2010;73:1141–52. https://doi.org/10.4315/0362-028X-73.6.1141.

[84] Wang Y, Wai Mun Huang, Taylor DE. Cloning and nucleotide sequence of the *Campylobacter jejuni* gyrA gene and characterization of quinolone resistance mutations. Antimicrob Agents Chemother 1993;37:457–63. https://doi.org/10.1128/AAC.37.3.457.

[85] Yan M, Sahin O, Lin J, Zhang Q. Role of the CmeABC efflux pump in the emergence of fluoroquinolone-resistant *Campylobacter* under selection pressure. J Antimicrob Chemother 2006;58:1154–9. https://doi.org/10.1093/jac/dkl412.

[86] Park J-H, Yamaguchi T, Ouchi Y, Koide K, Pachanon R, Chizimu JY, et al. Interaction of Quinolones Carrying New R1 Group with *Mycobacterium leprae* DNA Gyrase. Microb Drug Resist 2021;00:1–8. https://doi.org/10.1089/mdr.2020.0408.

[87] Schoeffler AJ, May AP, Berger JM. A domain insertion in *Escherichia coli* GyrB adopts a novel fold that plays a critical role in gyrase function. Nucleic Acids Res 2010;38:7830–44. https://doi.org/10.1093/nar/gkq665.

[88] Barnard FM, Maxwell A. Interaction between DNA gyrase and quinolones: Effects of alanine mutations at GyrA subunit residues Ser83 and Asp87. Antimicrob Agents Chemother 2001;45:1994–2000. https://doi.org/10.1128/AAC.45.7.1994-2000.2001.

[89] Hooper DC. Mechanisms of action of antimicrobials: Focus on fluoroquinolones. Clin Infect Dis 2001;32:9–15. https://doi.org/10.1086/319370.

[90] Walton L, Elwell LP. *In vitro* cleavable-complex assay to monitor antimicrobial potency of quinolones. Antimicrob Agents Chemother 1988;32:1086–9. https://doi.org/10.1128/AAC.32.7.1086.